Development and applications of a smartphone-based mobile electroencephalography (EEG) system

Anthony David Bateson BEng (Hons), FHEA

Thesis submitted for the degree of Doctor of Philosophy

University of Hull and the University of York

Hull York Medical School

September 2018

Abstract

Electroencephalography (EEG) is a clinical and research technique used to non-invasively acquire brain activity. EEG is performed using static systems in specialist laboratories where participant mobility is constrained. It is desirable to have EEG systems which enable acquisition of brain activity outside such settings. Mobile systems seek to reduce the constraining factors of EEG device and participant mobility to enable recordings in various environments but have had limited success due to various factors including low system specification. The main aim of this thesis was to design, build, test and validate a novel smartphone-based mobile EEG system.

A literature review found that the term 'mobile EEG' has an ambiguous meaning as researchers have used it to describe many differing degrees of participant and device mobility. A novel categorisation of mobile EEG (CoME) scheme was derived from thirty published EEG studies which defined scores for participant and device mobilities, and system specifications. The CoME scheme was subsequently applied to generate a specification for the proposed mobile EEG system which had 24 channels, sampled at 24 bit at a rate of 250 Hz. Unique aspects of the EEG system were the introduction of a smartphone into the specification, along with the use of Wi-Fi for communications. The smartphone's processing power was used to remotely control the EEG device so as to enable EEG data capture and storage as well as electrode impedance checking via the app. This was achieved by using the Unity game engine to code an app which provided the flexibility for future development possibilities with its multi-platform support.

The prototype smartphone-based waist-mounted mobile EEG system (termed 'io:bio') was validated against a commercial FDA clinically approved mobile system (Micromed). The power spectral frequency, amplitude and area of alpha frequency waves were determined in participants with their eyes closed in various postures: lying, sitting, standing and standing with arms raised. Since a correlation analysis to compare two

systems has interpretability problems, Bland and Altman plots were utilised with a priori justified limits of agreement to statistically assess the agreement between the two EEG systems. Overall, the results found similar agreements between the io:bio and Micromed systems indicating that the systems could be used interchangeably. Utilising the io:bio and Micromed systems in a walking configuration, led to contamination of EEG channels with artifacts thought to arise from movement and muscle-related sources, and electrode displacement.

To enable an event related potential (ERP) capability of the EEG system, additional coding of the smartphone app was undertaken to provide stimulus delivery and associated data marking. Using the waist-mounted io:bio system, an auditory oddball paradigm was also coded into the app, and delivery of auditory tones (standard and deviant) to the participant (sitting posture) achieved via headphones connected to the smartphone. N100, N200 and P300 ERP components were recorded in participants sitting, and larger amplitudes were found for the deviant tones compared to the standard ones. In addition, when the paradigm was tested in individual participants during walking, movement-related artifacts impacted negatively upon the quality of the ERP components, although components were discernible in the grand mean ERP.

The io:bio system was redesigned into a head-mounted configuration in an attempt to reduce EEG artifacts during participant walking. The initial approach taken to redesign the system involved using electronic components populated onto a flexible PCB proved to be non-robust. Instead, the rigid PCB form of the circuitry was taken from the io:bio waist-mounted system and placed onto the rear head section of the electrode cap via a bespoke cradle. Using this head-mounted system, in a preliminary auditory oddball paradigm study, ERP responses were obtained in participants whilst walking. Initial results indicate that artifacts are reduced in this head-mounted configuration, and N100, N200 and P300 components are clearly identifiable in some channels

Table of Contents

List of Figures

List of Tables

Abbreviations

AR	Augmented Reality
AUC	Area Under Curve
BCI	Brain-Computer Interfacing
CAD	Computer Aided Design
CoME	Categorisation of Mobile EEG
CI	Confidence Interval
CLI	Command Line Interface
dB	Decibel
EDF	European Data Format
ECG	Electrocardiogram
EEG	Electroencephalogram
EMG	Electromyogram
EOG	Electrooculogram (EOG)
ERP	Event Related Potentials
FDA	Food and Drug Administration
FMCG	Fast Moving Consumer Goods
fNIRS	Functional Near Infra-Red Spectroscopy
Hz	Hertz
IC	Integrated Circuit
ICP	In-Circuit Programming

ICC	Intra-individual Correlation Coefficient
IFCN	International Federation of Clinical Neurophysiology
LAN	Local Area Network
MC	Motor Cortex
MTBI	Mild Traumatic Brain Injury
PCB	Printed Circuit Board
PFC	Prefrontal Cortex
PSD	Power Spectral Density
RTOS	Real Time Operating System
SD Card	Secure Digital Card
SD	Standard Deviation
SEM	Standard Error of the Mean
SPI	Serial Peripheral Interface
SSVEP	Steady State Visual Evoked Potentials
UI	User Interface
USB	Universal Serial Bus
VR	Virtual Reality

Acknowledgements

Firstly, I would like to express my sincere gratitude to my advisor Dr Aziz Asghar for his continuous support of my PhD study and my related personal development. His patience, motivation, and knowledge have been invaluable to me. His guidance helped me in the research and writing of this thesis. I could not have imagined having a better advisor and mentor for my PhD study. This was especially important since I am an engineer within a medical environment and therefore a 'fish out of water'. Furthermore, I believe he has helped me to evolve from a teacher into a researcher; this is particularly important for my career development and my future.

Besides my main supervisor, I would like to thank the rest of my thesis advisory panel: Dr Heidi Baseler, Dr Kevin Paulson and Dr Fayyaz Ahmed for their insightful comments and encouragement, but also for the hard questions which encouraged me to critically question my research from various perspectives.

I would never have been able to undertake the highly competitive PhD scholarship post within HYMS if it was not for Professor S. Kelly (Dean of Faculty of Science at the time) allowing me to take unpaid leave from my duties as a lecturer in the School of Engineering at the University of Hull. It was this opportunity that allowed (hopefully) the step change in my career development.

My sincere thanks also go to Mr Nathan Brown (my current academic manager) for his words of encouragement and subsequent support in my research endeavours. I would also like to thank my close personal friend and colleague, Peter Lobo-Kazinczi for his help and advice regarding hardware aspects of the PhD. He also provided a good sounding board for my engineering ideas and how they could be materialised physically.

My wife has not only supported me financially throughout my PhD journey but has also continuously provided me with emotional and writing support and therefore deserves not only my continuing love but also special acknowledgement for her beyond the call support. Last but not the least, I would like to thank my Mum, Margaret, and my two sons Tomas and Luke for supporting me throughout this process and my life in general. Hopefully my endeavours will provide encouragement to my sons to be the best they can be!

Author's publication list

Anthony D. Bateson, Heidi A. Baseler, Kevin S. Paulson, Fayyaz Ahmed, and Aziz U. R. Asghar, (2017).

"Categorisation of Mobile EEG: A Researcher's Perspective".

Special issue entitled: Portable and Wearable Brain Technologies for Neuroenhancement and Neurorehabilitation.

BioMed Research International, vol. 2017, Article ID 5496196, 15 pages.

https://doi.org/10.1155/2017/5496196

Author's Declaration: I confirm that this work is original and that if any passage(s) or diagram(s) have been copied from academic papers, books, the internet or any other sources these are clearly identified by the use of quotation marks and the reference(s) is fully cited. I certify that, other than where indicated, this is my own work and does not breach the regulations of HYMS, the University of Hull or the University of York regarding plagiarism or academic conduct in examinations. I have read the HYMS Code of Practice on Academic Misconduct, and state that this piece of work is my own and does not contain any unacknowledged work from any other sources.

Chapter 1: General Introduction

1.1 Electroencephalogram

Electroencephalography (EEG) is the measurement of the electrical activity of the brain at the scalp surface. It is used clinically to diagnose numerous conditions, including epilepsy [1], sleep disorders [2], coma [3], investigation of stroke [4] and brain death [5]. EEG is also used in an event related potential (ERP) configuration to acquire time-locked responses to the presentation of sounds [6-8] or visual stimuli [9-11]. As a clinical and research tool EEG is relatively inexpensive, is wearable [12,13] and has high temporal resolution. Owing to the extremely small amplitude of EEG signals (10 to 100 μV), and their vulnerability to distortion by artifacts, research utilising EEG has concentrated on using static systems under restricted laboratory conditions to reduce artifacts relating to movement [14]. This research approach has provided a wealth of knowledge about how the brain functions within a constrained environment, but does not answer the question of how the brain functions outside of the laboratory constraints.

Although static EEG systems have generated a plethora of useful clinical and research data, mobile EEG offers the advantages of being undertaken outside of traditional specialist laboratory environments and in natural environments. This enables observation of brain activity in mobile EEG settings. Although it is still in its infancy, it is optimised for mobility and therefore is better suited for measurement and analysis of brain function in real world environments. Electronics developments relating to microcontrollers and analogue to digital convertors have concentrated on miniaturisation and reduction of power consumption. Both of these aspects are beneficial to mobile EEG. Mobile smartphones are also benefiting from such advances and are now capable of processing and storing large amounts of data. If all of these advances were included in a mobile EEG system progress in trying to produce a small, lightweight system capable of producing research data could be realised.

The overall objective of this thesis is to develop, build, validate and utilise a novel smartphone-based mobile electroencephalography (EEG) monitoring system in human participants. In Chapter 1 of the thesis a review is undertaken of the general background literature and history related to EEG. Chapter 2 discusses the definition problem of 'mobile EEG' and a novel scoring system is derived and developed from a detailed review of the mobile EEG literature. In Chapter 3, a prototype smartphone-based waist-mounted mobile EEG system is designed, tested and an associated smartphone app coded. This is followed by Chapter 4 where the novel mobile EEG waist-mounted system is validated in participants. Extension of the capabilities of the smartphone app to include stimulus delivery and associated data marking to enable ERP EEG capability is in Chapter 5. In Chapter 6, the prototype mobile EEG system is further adapted by transposing the mounting position from waist-mounted to head-mounted in a preliminary study. Finally, Chapter 7 is a general discussion which highlights the advantages, limitations and current/future research directions of the smartphone-based mobile EEG system.

1.1.1 History of electroencephalography

A historical perspective helps to demonstrate that advances in research understanding have quite often been facilitated by new tool developments. A brief history of EEG follows, focussing on the key technological developments that have enabled advances in EEG research. There are a number of studies and reviews that focus on the history of EEG and provide further detail [15-18].

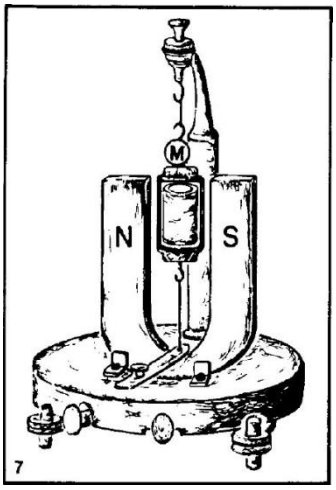

Figure 1.1 Mirror galvanometer used by Caton. Taken from Collura *et al*. [16].

Caton is regarded as making the first key step in the evolution of modern day EEG systems in the late nineteenth century [16]. His work on recording electrical activity from the exposed brains of rabbits and monkeys using a mirror galvanometer (Figure 1.1) was the first reported measurement of electroencephalographic activity. For this work to be improved upon, a better way of measuring the electrical activity was required. By applying the use of an instrument with greater accuracy, or some other quantifiable benefit, new research could be undertaken.

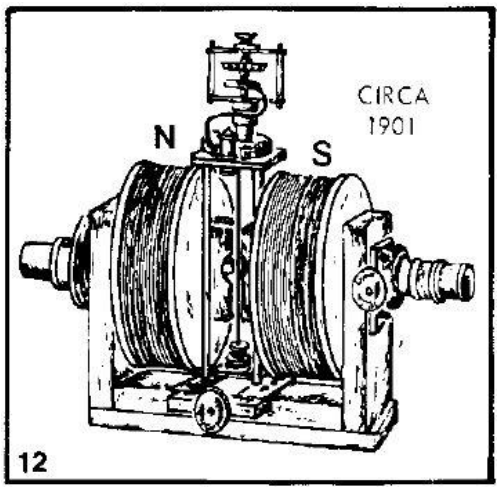

Figure 1.2 Einthoven string galvanometer used by Beck. Taken from Collura *et al*. [16].

Adolf Beck (1863–1939) moved to using an Einthoven string galvanometer after his earlier work (Figure 1.2). His motivation for changing his instrument was to improve the quality of his data recordings. The Einthoven string galvanometer was the first device capable of recording physiological potentials without distortion. The instrument was developed by Wilhelm Einthoven and earned him a Nobel Prize in 1924 [16]. It became the effective replacement for the mirror galvanometer as it provided greater accuracy (sensitivity of 1 mV/cm and a frequency response to 200 Hz). It enabled Beck to advance his research by being able to study relationships between the cerebral cortex and cerebellum.

It was the work of Dr Hans Berger, who became interested in the electrical activity of the brain in 1902, that again advanced the field by changing to a new instrument. All of his early recordings were made with a Lippmann capillary electrometer, but for his later work he used a string galvanometer with photographic capability. With this he managed to make permanent recording of 1-3minutes in length. In 1924 he began his work with humans (Figure 1.3), and in 1924 he was able to observe EEG from a 17-year-old participant. He published on the scalp recording of human EEG for which he coined the term 'Elektenkephalogram.'

Figure 1.3 Dr Berger's first attempts to record EEG in 1924. Taken from Collura *et al*. [16].

He also recorded a partial complex seizure in 1933, but only briefly mentioned these observations in passing. He used the terms “alpha” and “beta” essentially as they are used today. In addition, he also established the use of the 30mm/s paper speed, which subsequently became a standard for EEG recordings.

Later in 1934 Adrian and Matthews published the paper verifying the concept of “human brain waves” and identified regular oscillations around 10 to 12 Hertz (Hz) which they termed “alpha rhythm” [19]. Although Adrian was an electrophysiologist, Matthews was an electrical engineer who designed and constructed instrumentation suitable for EEG. Matthews developed an oscillograph with a high frequency cut-off of 955 Hz that recorded on moving bromide paper. He also developed an ink writing oscillograph with a high frequency cut off of 64 Hz which was used for most of the work with Adrian.

Matthews introduced the use of differential input amplifiers (amplifiers that amplify the difference between two input voltages). By using differential input amplifiers to record electrophysiology Adrian was able to set up a three channel system [16], which improved upon the single used previously by being able to record three channels simultaneously. The success of Adrian and Matthews largely resulted from their inter-disciplinary approach to solving their research problems. Together they had the ability to find appropriate new technologies, engineer new tools, and apply their use in research [15].

1.1.2 EEG frequencies

The human brain is made up of billions of brain cells called neurons. The combination of millions of neurons sending signals at once produces electrical activity in the brain, which can be detected using sensitive medical equipment (such as an EEG), measuring electricity levels over areas of the scalp.

An EEG is recorded using electrodes attached to a person's scalp, or via the implantation of needle-like electrodes directly into various portions of the brain. The waveforms recorded from the brain are largely oscillatory in nature and occur over a range of frequencies. Brainwaves are produced by synchronised electrical activity from masses of neurons communicating with each other.

EEG recordings can be categorised into frequency bands based upon the dominant brain function when these frequencies occur. Table 1.1 summarises the frequency range of each band along with the amplitude range. The waveforms shown in Figure 1.4 are examples of each category of EEG frequency and help to visualise the frequency and amplitude differences more readily.

Table 1.1 EEG brain waves along with their range of frequency bandings and amplitudes in the literature [20-26].

	Frequency band (Hz)	Amplitude (μV)	State of Mind
Delta	0.1 – 4	100 – 200	Deep sleep
Theta	4 – 7	5 – 100	Drowsy or meditative
Alpha	8 – 12	5 – 100	Relaxed
Beta	12 – 30	2 – 20	Alert or working
Gamma	30 – 100	0.5 – 2	Active thought

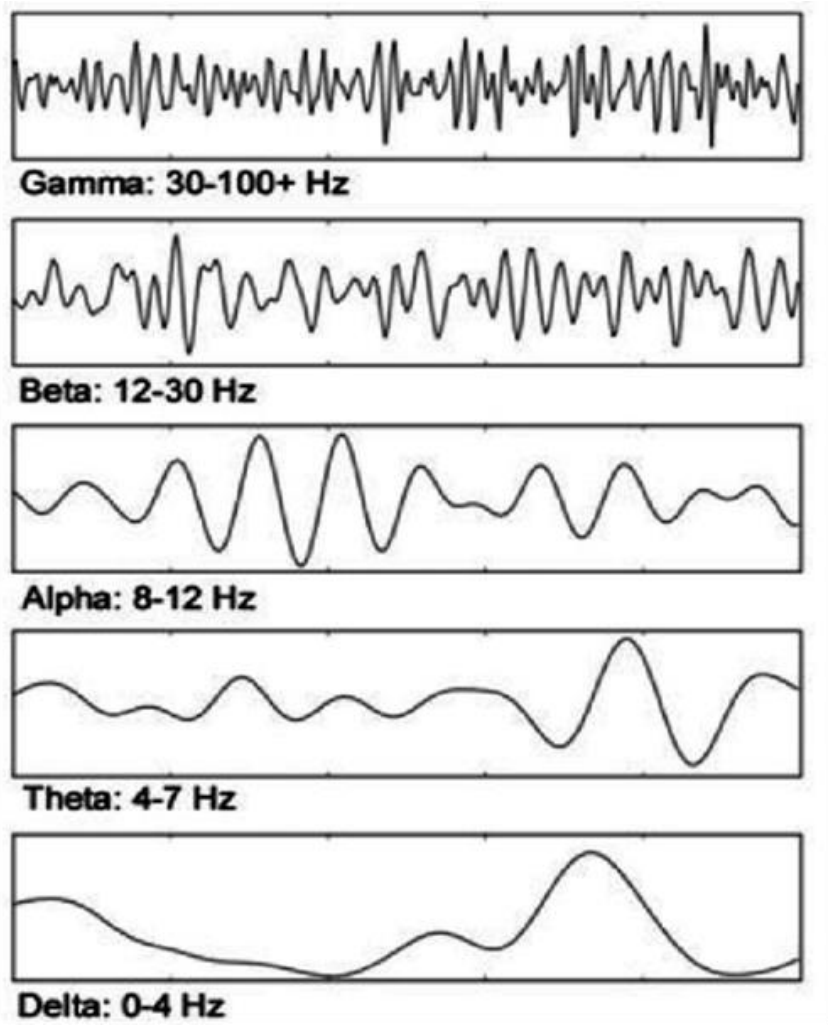

Figure 1.4 Comparison of EEG bands showing frequency range of each band. Modified from Nunez *et al*. [26].

1.1.3 Electrodes and placement

Correct EEG electrode placement is important not only to ensure proper location of electrodes in relation to cortical areas but also so that they can be reliably and precisely maintained from individual to individual.

1.1.3.1 International 10/20 system of electrode placement

The international 10/20 system is the standard naming and positioning scheme for EEG applications [27]. It divides the scalp up by taking a line from the nasion to the inion and between pre-auricular points. This provides the Cz electrode position at the centre of the scalp, and allows all other positions to be calculated relative to this. Figure 1.5 shows the subdivision of the scalp based upon the craniometric reference points (Figure 1.5a and b), and how high density EEG is also achieved by further subdivision (Figure 1.5c). The 10/20 system is comprised of 19 electrodes sites as can be seen in Figure 1.5b.

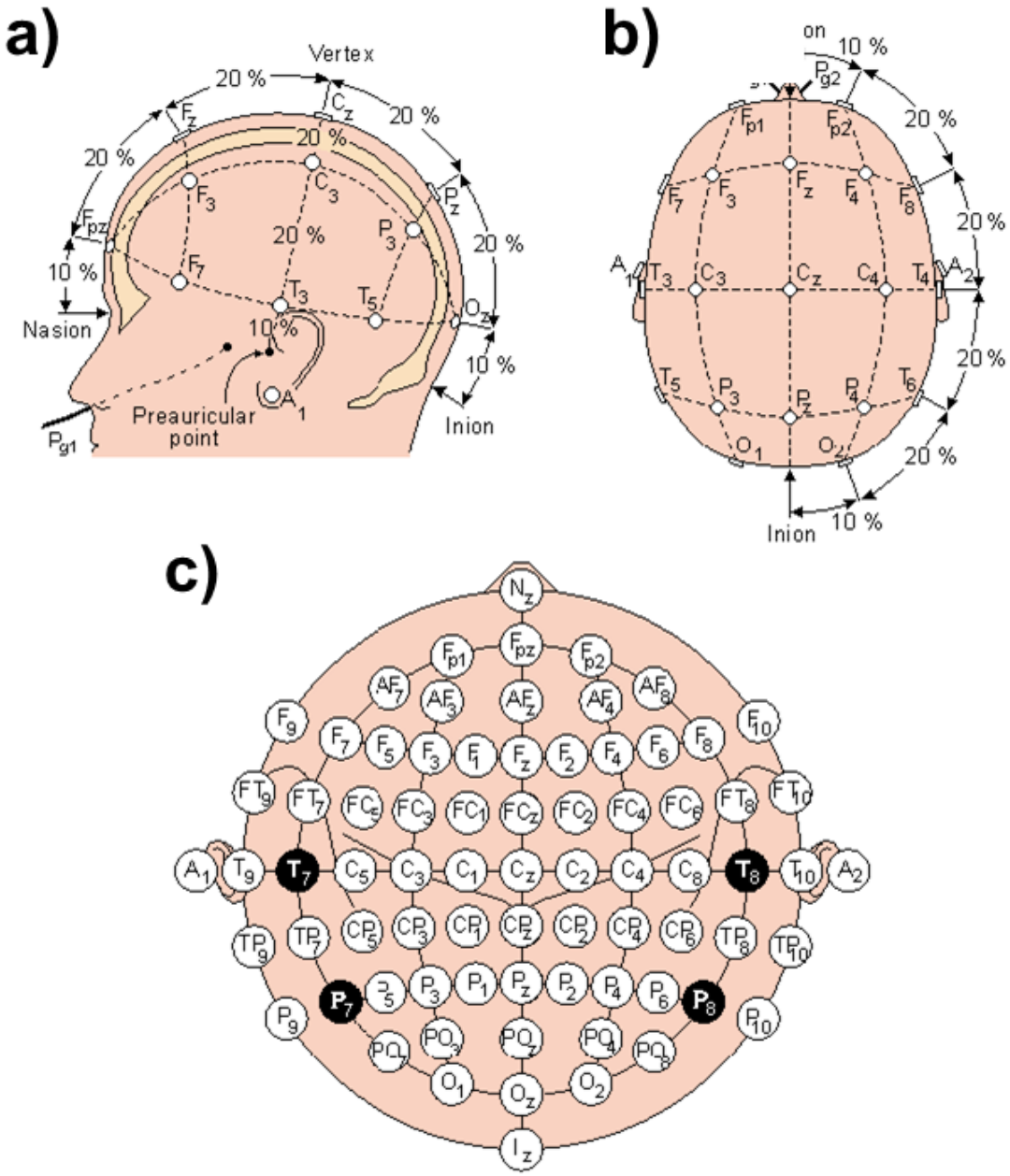

Figure 1.5 a) and b) 10/20 International System of electrode placement. **c)** 10/10 International System showing extra electrode positions for higher density EEG. Modified from bci2000.org website [28].

1.1.4 Artifacts

Although EEG is designed predominantly to record brain activity, it also records electrical potentials arising from sources other than the brain. Any recorded activity that is not of brain origin is referred to as an artifact. The causes of artifacts are numerous, but the key causes are discussed in the following section.

1.1.4.1 Eye movement artifacts

The eye blink artifact is very common in EEG data [29]. The potential difference between the cornea and retina is larger than that of cortical potentials [30], in the range of 0.4 – 1.0 mV. When the eye blinks the action causes the eye to move and it is this movement that causes the change in potential and the resultant artifact. The high comparative amplitude of an eye blink can corrupt data on EEG electrodes. Eye artifacts are often measured more directly in the electro-oculogram (EOG), using pairs of electrodes placed above and around the eyes. Eye blink artifacts, owing to their dominant nature, are suitable for use as data markers; participants could be asked to blink a set number of times at known points in a protocol. See Figure 1.6 b) and c) as an examples of eye blinks and eye movement, respectively.

1.1.4.2 Muscle artifacts

Electromyographic (EMG) artifacts can exhibit an amplitude of around 100 to 1000 µV, considerably greater than that of EEG (approximately 10 to 100 µV)[31]. Consequently, muscular activity can obscure neural potentials altogether. Muscle activity-related artifacts can be caused by activity in different muscle groups including neck and facial muscles. These signals have a wide frequency range 0 to 200 Hz and can be distributed across different sets of electrodes on the scalp depending on the location of the source muscles. This also overlaps the EEG data frequency band of 0 to 30 Hz [32]. See Figure 1.6e as an example of muscle activity and its effect on an EEG recording.

1.1.4.3 Cardiac artifacts

The pulse, or heartbeat, artifact can occur when an electrode is placed on or near a blood vessel. The expansion and contraction of the vessel introduce voltage changes into the recordings by displacing the electrode momentarily. The artifact signal has a frequency near 1.2 Hz, but can vary with the state of the patient [33]. See Figure 1.6f as an example of pulse artifact. Electrocardiographic (ECG) artifacts can also contaminate EEG signals due to the electrical activity of the heart conducting to the scalp.

1.1.4.4 Skin artifacts

Sodium chloride and lactic acid from sweat glands in the scalp can react with the metal of the electrode to alter impedance and thus signal amplitude [34]. If this occurs differentially across active and reference electrodes an impedance mismatch naturally results which can result in large baseline sways [35].

1.1.4.5 Electrode movement artifacts

Any movement which disturbs the contact of the electrode with the scalp can result in a sudden increase in electrode impedance leading to a resulting change in the EEG signal. While electrode movement is easily detected on the EEG signal, contaminated EEG from frequent movement can produce a great deal of data loss, and has been identified as one of the biggest challenges in mobile EEG [34] . Care must be taken to ensure a consistent low impedance contact with the skin as electrode displacement, or electrode impedance increases will produce artifacts that cannot be removed algorithmically [36].

1.1.4.6 Electrical interference

Owing to the large comparative amplitude of alternating current power supplies, EEG data are vulnerable to electromagnetic interference as it is transferred from the scalp electrodes to the recording device [37]. This artifact is often partially removed by notch filters, but for lower frequency line noise and harmonics this is often undesirable. If the line noise or harmonics occur in frequency bands of interest they interfere with EEG that occurs in the same band. Notch filtering at these frequencies can remove useful information. Line noise can corrupt the data from some or all of the electrodes depending on the source of the problem. See Figure 1.6d as an example of 50 Hz electrical interference.

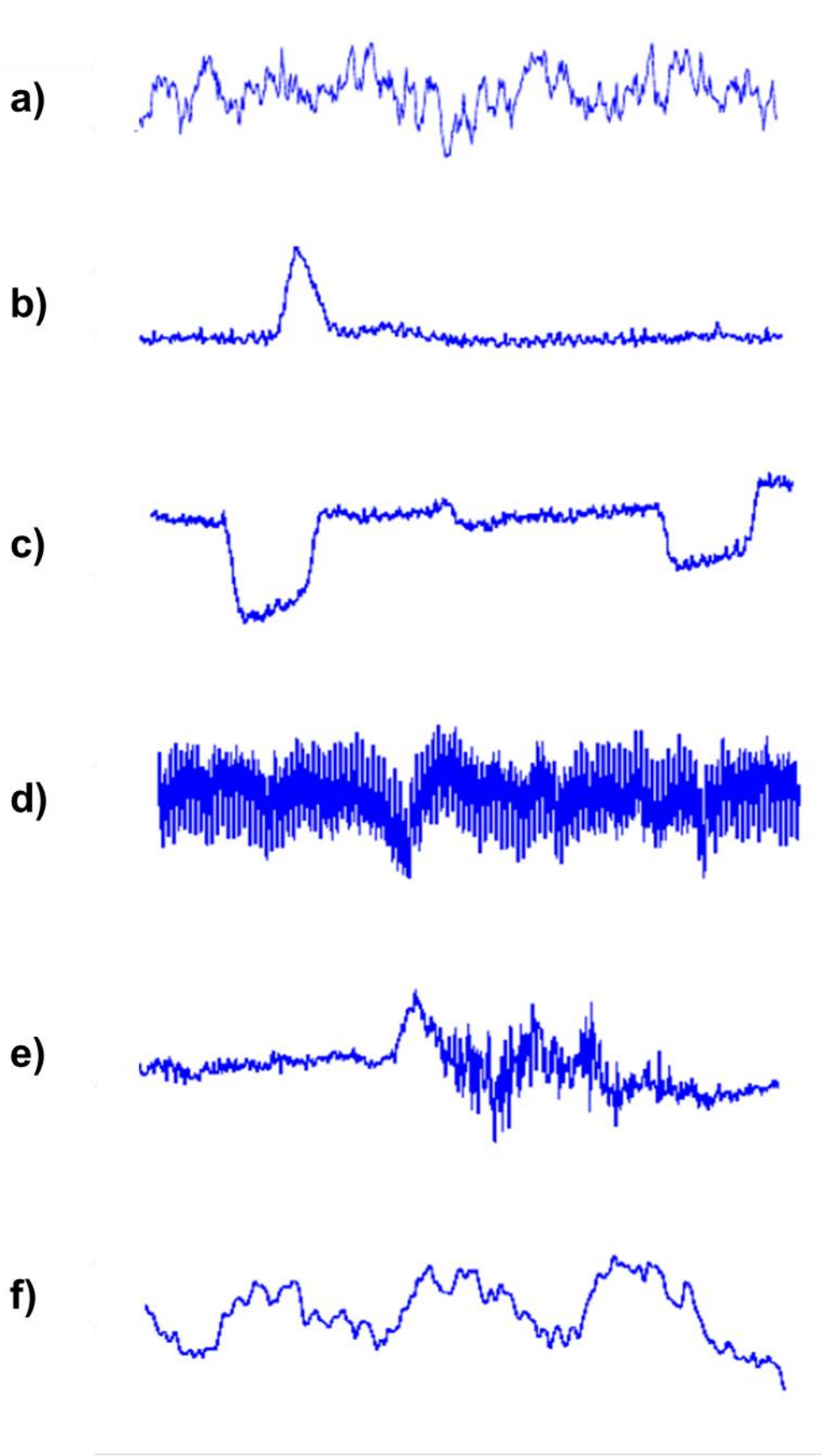

Figure 1.6a) Artifact free EEG, **b)** eye blink, **c)** eye movement, **d)** 50 Hz interference, **e)** muscle activity and **f)** pulse artifact. Modified from Fouad *et al*. [38].

1.2 Mobile EEG

Although EEG as a technique has been around for many years there are still advances to be made in its development when considering recordings made during participant movement. Mobile EEG is still in its infancy and significant advances in technology need to be applied to this area to enable greater utility in research investigations. A better understanding of the brain's activity while navigating and moving are important to investigate, and this is where little is currently known.

1.2.1 Why is mobile EEG important?

Mobile EEG seeks to obtain recordings while movement is taking place. Such recordings potentially provide more information about how the human brain works in real world scenarios (not artificial laboratory environments). For example, imagine navigating through a busy bookshop whilst trying to find specific books of interest. What cognitive processes are taking place at any one time during this activity in order for it to be successfully achieved? Using static EEG it is not possible to know. Mobile EEG, although more suitable for such applications, still has limitations relating to system specification, and the equipment mounting position. Commercial EEG systems suitable for mobile EEG applications, tend to have lower system specifications than their static EEG counterparts.

Researchers use the term 'mobile EEG' in a wide range of contexts. In the next chapter a review of literature will be conducted to address the ambiguity of the term and provide detailed information on mobile EEG systems along with how they have been used in published research studies.

Chapter 2: Development and application of the categorisation of mobile EEG (CoME): a researcher's perspective

2.1 Introduction

Mobile or ambulatory EEG is an increasingly active area of research utilised in a variety of applications and scenarios such as outdoor urban environments [39,40], sports activities [41], and brain-computer interfacing [42-44]. Typically, participant movement during EEG recordings is discouraged in order to reduce data artifacts. Mobile EEG seeks to obtain recordings while movement is taking place, but its success has been impeded by low system specification, and the mounting position of the EEG equipment. EEG systems are now becoming available that lend themselves to mobile applications, although in general they have lower system specifications when compared to static EEG systems.

Mobile EEG approaches include walking on a treadmill while tethered to immobile EEG equipment [10,45], walking outdoors with a wireless mobile EEG headset combined with a rucksack mounted PC [36], and being moved on a trolley while wearing a virtual reality headset to provide the sensation of movement [46]. These diverse approaches cause ambiguity because they are all termed 'mobile EEG' by researchers and yet exhibit wide variation in EEG device mobility, participant mobility, and system specification.

One technique that has been used to address the problem of misleading terminology in biomedical research, and the differing interpretation of some terms across practitioners, is categorisation based upon scales for parameters of interest [47,48]. An advantage of using a categorisation scheme is that it standardises scores so they can be exchanged between practitioners with greater clarity. Since the term 'mobile EEG' lacks this form of standardisation, a categorisation scheme that encompasses the range of mobility of EEG equipment, mobility of the participant and the main features of EEG system technical specification would provide researchers with a standardised way of quantifying 'mobile EEG' as used in studies.

A categorisation scheme for mobile EEG with sufficient measure and usability would allow researchers to determine the potential of specific EEG systems (and related equipment), and to guide development of new and more mobile experimental protocols. By extension, it would also allow EEG system developers to 'design in' attributes that are of importance to the research community as technology advances become possible. The literature contains a number of EEG system comparison studies where usability [49,50], signal quality [51], performance [52], and electrode types [53] were compared. However, no categorisation schemes are currently available for 'mobile EEG'.

In this chapter, thirty published research investigations were reviewed. They were selected because they either had 'mobile EEG' (or 'ambulatory EEG') in the paper title and/or involved some form of participant mobility whilst EEG recordings were being acquired. Key features related to equipment used, equipment mounting position, participant activity, and EEG system specification were extracted. Next, a novel categorisation scheme for 'mobile EEG' was developed based upon scoring the following key parameters: device mobility, participant mobility, and system specification. The specific parameter score descriptors for device mobility and participant mobility were derived from descriptions given in the twenty-nine 'mobile EEG' published research investigations and one static EEG study. The categorisation scheme was then applied retrospectively to the thirty published studies, and a subset of these was taken to illustrate the range of unique categorisation scores in the parameters covered by the developed scoring scheme.

2.2 Development of the categorisation of mobile EEG (CoME) scheme

To develop descriptors for device mobility, participant mobility, and system specification, a review of thirty published research studies was undertaken. More specifically, studies were selected that either had 'mobile EEG' (or ambulatory EEG) in the title and/or involved some form of participant mobility whilst EEG recordings were being taken. This enabled a range of each parameter to be derived from these studies, along with informative descriptors for each score. One investigation was selected which used EEG in a static setting [54], to provide contrast for the 'mobile EEG' studies and allow benchmarking appropriate scales from a 0 =static perspective. This study was particularly suitable as an example of static EEG since participant movement was actively discouraged via training provided to participants prior to recording.

The studies included are shown in Table 2.1, and detail the study, year published, equipment mounting positions, EEG system used, and participant activity during EEG recordings. This information was used to derive both the device mobility parameter scores and those of the participant mobility scores. Where information was either missing from the publication or ambiguously described this has been recorded in this table.

Table 2.1 Mobile EEG studies.

Study	Year	EEG System	Equipment Mounting Position	Participant Activity
Askamp[55]	2013	Mobita	Waist-mounted	Epileptic out-patients, stair climbing
Aspinall [39]	2015	EPOC	Head-mounted, wireless link to back-mounted laptop	Outside walking
Bulea [56]	2014	actiCHamp	Back-mounted (according to figure in paper)	Treadmill walking
Castermans [42]	2011	ANT	Presumed off-body but not stated	Treadmill walking
Davies & Gavin [54]	2007	ActiveTwo	Off-body	Seated watching & listening
Debener [36]	2012	Oldenburg Hybrid	Head-mounted, wireless link to back-mounted laptop	Indoor and outdoor walking
Debener [57]	2015	SMARTING	Head-mounted, wireless link to smart device	Seated indoors
De Vos [51]	2014	Oldenburg Hybrid	Head-mounted, wireless link to PC	Seated screen speller task
Doppelmayr [58]	2012	Varioport	Waist-mounted	Slow walking
Duvinage [52]	2013	EPOC & ANT	Presumed off-body but not stated	Treadmill walking
Ehinger[46]	2014	Asalab	Off-body	Constrained walking with trolley
Fitzgerald [59]	2013	ProFusion	Waist-mounted	Epileptic out-patients sleep monitoring
Gargiulo [60]	2008	Penso	Presumed waist-mounted but not stated	Seated, eyes open & closed, button pressing
Gramann [10]	2010	ActiveTwo	Off-body	Treadmill walking
Gwin [14]	2010	ActiveTwo	Off-body	Running on treadmill
Jungnickel [61]	2016	BrainAmp	Rucksack-mounted, wireless link to PC	Standing and pointing
Klonovs [62]	2013	EPOC	Head-mounted, wireless link to PC	Not made clear. Presume seated driving
Li [63]	2014	Not specified	Off-body	Human centrifuge
Lin [64]	2014	Cognionics	Head-mounted, wireless link to PC	SSVEP whilst treadmill walking
Liu [65]	2013	Mindwave	Head-mounted, wireless link to PC	Seated driving
Lotte [43]	2009	Polymate AP216	Back-mounted EEG device and laptop	Corridor walking
Maidhof [66]	2014	ActiveTwo	Off-body	Keyboard playing
Robertson [67]	2015	B-Alert	Head-mounted, wireless link to PC	Exercise cycling
Stopczynski [68]	2014	EPOC	Head-mounted, wireless link to smart device	Seated imagined finger tapping
Wagner [69]	2012	BrainAmp	Off-body	Robotic-assisted treadmill walking
Wang [70]	2014	NuAmp	Head-mounted, wireless link to PC	VR Simulated driving whilst seated

Table 2.1 continued…

Study	Year	EEG System	Equipment Mounting Position	Participant Activity
Wascher [40]	2014	BrainAmp	Back-mounted	Indoor physical box sorting task
Wong [71]	2014	Mindwave	Head-mounted, wireless link to PC	Screen based shape tracing while seated
Zander [72]	2017	V-Amp	Off-body	Seated driving
Zink [73]	2016	SMARTING	Head-mounted, wireless link to back-mounted laptop	Cycling

2.2.1 Device mobility

The device mobility score reflects the mounting position (off-body, waist-mounted, or head-mounted), along with the level of physical restriction placed upon the participant by the EEG acquisition system. Figure 2.1 shows examples of the various mounting positions of the device and associated equipment on the participant. Table 2.2 provides the device mobility scores and descriptors. The mounting modalities taken from the published studies (see Table 2.1) fit to the descriptors for scores 0 to 4. The descriptor for score 5 is aspirational and taking a logical projection of what could be developed from the descriptor for score 4.

When all of the equipment is off-body mounted and the participant is tethered to the equipment via cabling it is clear that the equipment is static and therefore is scored as 0. When the EEG amplifier is mounted on the waist (or the back) of a participant movement related artifacts are likely because of electrode displacement [36,74]. Leads cannot be fastened to the participant sufficiently well to completely remove electrode wire movement as this will then cause restricted head movement. When coupled with the length of electrode wires this can result in increased electromagnetic interference [75].This provides scores 1 and 2, where the difference between these is the restriction placed upon the participant. If additional equipment is placed in a rucksack on the participant this scores 1 as the participant is encumbered with this additional load and in turn increase the weight to be carried along with susceptibility to system movement artifacts [76]. When no additional equipment is used a higher of score of 2 is used to reflect that the participant is not encumbered with an additional load.

With EEG amplifiers that are completely head-mounted, movement related artifacts are reduced and head movements are not restricted [36]. However, in general the headset needs to wirelessly link to another piece of equipment such as a PC (see Table 2.1). This applies restrictions on the participant that take the form of either equipment placed in a

rucksack and therefore encumbering with an additional load, or the additional equipment is stored off-body and the participant is constrained by the wireless connection range. Both of these modalities score 3 as in both conditions participants are constrained in some way. When the equipment is replaced with a smartphone, which is inherently mobile, the participant is clearly far less constrained [57,68] and this condition scores 4. The next logical step is a modality where not even a smartphone is required and this scores 5. Although no example of such a system has been found it has been included as future EEG system developments could well achieve this level.

Table 2.2 Device mobility scores.

Device Mobility Score (D)	Descriptor
0	All equipment off-body mounted and participant tethered via cabling to EEG acquisition equipment.
1	Waist-mounted (or back-mounted) with additional equipment located in a rucksack.
2	All equipment is waist-mounted.
3	Head-mounted EEG system, with additional equipment located in a rucksack or off-body.
4	Head-mounted and requires smartphone/tablet.
5	Head-mounted and does not require any additional equipment.

Note that the level of participant mobility is not taken into account when considering device mobility. For example, if a study used a head-mounted system that did not require a PC or smartphone, and the participant was instructed by the researcher to remain as still as possible, the device would be scored as 5D.

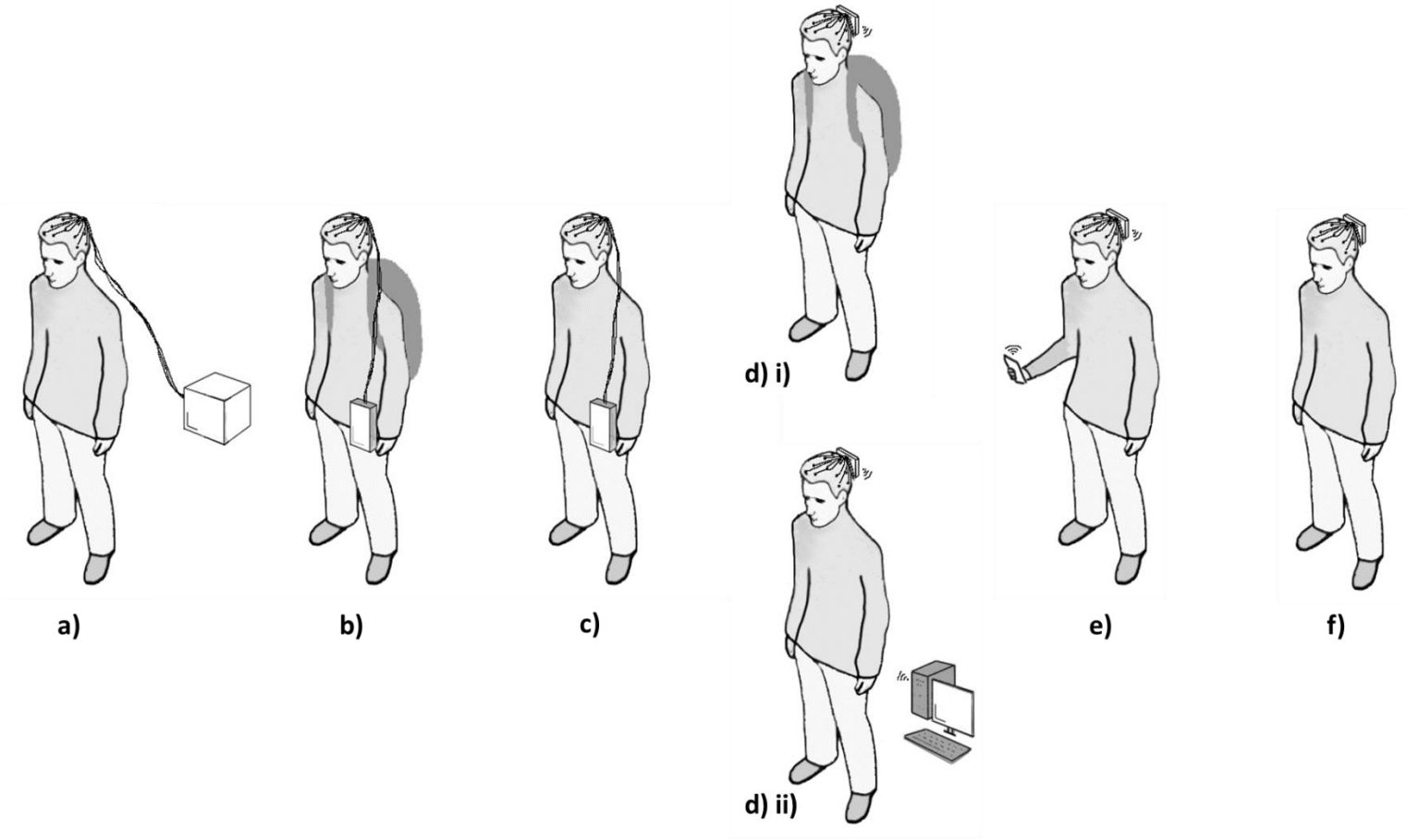

Figure 2.1 Various mounting positions of the EEG device and associated equipment on the participant. **a)** All equipment off-body mounted and participant tethered via cabling to EEG acquisition equipment. **b)** Waist-mounted (or back-mounted) with additional equipment located in a rucksack. **c)** All equipment is waist-mounted. **d)** Head-mounted EEG system, with additional equipment located **i)** in a rucksack or **ii)** off-body tethering participant via limited range wireless link. **e)** Head-mounted and requires smartphone/tablet. **f)** Head-mounted; acquisition, storage and analysis equipment is integrated within the headset.

2.2.2 Participant mobility

The scaling descriptors for participant mobility were based upon the activities described in the published EEG studies (see Table 2.1). Table 2.3 gives the score associated with each descriptor. This score reflects the level of participant mobility in the context of instructions given by the researcher to participants during a study. It is not unusual for participants to perform more than one type of activity, and in such cases, the activity involving the highest participant mobility was scored. From the list of studies, activities ranged from static to treadmill running. The scores captured this range from 0 to 4 with a score of 5 allowing for future work where participants run unconstrained or are playing sport.

Table 2.3 Participant mobility scores.

Participant Mobility Score (P)	Descriptor
0	Lying, sitting or standing still.
1	Lying, sitting or standing with localised movement, for example finger tapping or button pressing.
2	Constrained walking/cycling.
3	Unconstrained walking/cycling.
4	Walking and carrying, climbing stairs, constrained running.
5	Unconstrained running, vigorous physical exercise or sport.

When movement is discouraged by researchers it is generally done so in order to decrease the likelihood of movement related artifacts [14]. In protocols where participants were lying, sitting or standing still a score of 0 was applied as the participants are static and not mobile. In protocols where participants were lying, sitting or standing with localised movement (for example finger tapping or button pressing), a score of 1 was

given to recognise the introduction of movement, albeit localised. These localised movements are defined as occurring without actual displacement of the whole body.

Treadmill walking, although constraining the participant in terms of direction and pace of movement, is a further increase upon localised movement and this type of activity scores 2. Indoor or outdoor unconstrained walking scores 3 as the participant is not constrained in terms of direction and pace as is the case with a treadmill. The aspect of environment such as, indoor/outdoor or urban/rural whilst having a sensory impact on the participant [36,39] does not have a quantifiable impact on their mobility and are therefore not considered in the scoring or descriptors.

With treadmill running being the greatest level of mobility found in any of the studies in Table 2.1, a score of 4 was given to this level of activity. The same score was also given for a study where the participants had to carry packages of different sizes and weights (0.5 to 15Kg) whilst walking [40] and a study of epileptic outpatient data where stair climbing as assumed to be the most mobile activity [55]. The justification for scoring the two disparate activities the same is they both include activities that are more than just walking. This allows a score of 5 to be applied to unconstrained running or sport. No study was found to include such a level of mobility but this score allows for this to be captured in the future.

2.2.3 System specification

EEG system specification is an important consideration in mobile EEG research studies. A system that is considered to be highly mobile may only have a low system specification that adversely affects signal quality. Conversely, a system that is considered to be static (off-body mounted) typically has a higher system specification. Therefore, a system specification score was developed, in addition to the device and participant mobility

scores. Table 2.4 lists the EEG systems used in previously published studies (see Table 2.1) along with the sampling rate, bit resolution, number of channels, battery life and electrode type. These values were used to formulate scores to differentiate between differing system specifications.

The system specification score consists of four attributes added together, with each attribute ranging from 1 to 5. It was decided not to start the system specification scale for each parameter from 0 as the interpretation of this would be unclear, and even the most basic device would have some utility. It is also important to note that the impact of a device encumbering the participant has been incorporated into the device mobility score rather than the system specification score since it is a factor that affects participant mobility.

Since the emphasis is on mobility the electrode type has been captured as this impacts the likelihood and severity of motion artifacts. A specific example is that of dry electrodes that are much more difficult to secure to the participant and movement in relation to the participants body occurs more readily [77]. Gel-based electrodes provide improved signal quality in comparison to saline [36]. The EEG systems used in Table 2.4 can be broken down into either dry, saline or gel based electrodes that are either passive or active and unshielded or shielded. The scoring for this was 1 to 3 for the dry, wet and gel (or cream) respectively, with the addition of 1 score each if the electrodes are active and shielded, as given in Table 2.5. This provides a score range of 1 to 5; dry, passive and unshielded gives a score of 1, and gel, active and shielded a score of 5.

Table 2.4 Specifications of EEG systems as used in published research studies.

EEG System	Sampling rate (Hz)	Bit res. (bits)	No. of channels	Battery Life (Hours)	Electrode type		
					dry/saline/gel	passive/active	unshielded/shielded
ActiveTwo [10,14,54,66]	512, 1024, 8192	24	32, 248	10	gel	active	shielded
Asalab [46]	1024	24	128	10	gel	active	shielded
B-Alert [67]	256	16	20	8	conductive cream	passive	shielded
EPOC [39,52,62,68]	128	14	14	6	saline	passive	not stated
Mindwave [65,71]	500	16	1	10	dry	passive	shielded
Mobita [55]	2000	24	32	19	gel	passive	shielded
Oldenburg Hybrid [36,78]	128	14	14	6	gel	passive	shielded
Penso [60]	256	16	8	not stated	dry	passive	shielded
ProFusion [59]	512	16	32	15	gel	passive	not stated
SMARTING [57,73]	500	24	16, 24	5	gel	passive	not stated
Varioport [58]	2000	16	10	4 days	not stated	passive	not stated
ANT [42]	512, 2048	24	32,128	5	gel	passive	shielded
Polymate AP216 [79]	1000	16	3	18	gel	active	shielded
V-Amp [72]	2000	24	16	N/A USB	dry	active	shielded
BrainAmp [40,61,69]	500, 1000, 2500	16	28, 120, 156	30	gel	active	shielded
NuAmp [70]	500	22	32	N/A USB	gel	passive	unshielded
actiCHamp [56]	500	24	64	24	gel	active	shielded
Cognionics [64]	250	24	10 out of 32	8	dry	active	shielded

Table 2.5 Electrode type scoring

Electrode Type		
Passive (0)		Active (1)
Unshielded (0)		Shielded (1)
Dry (1)	Wet (2)	Gel (3)

Since the bit resolution impacts upon the accuracy of the data recorded and the sampling rate of the system governs the temporal resolution, both these parameters were included in the system specification scoring. These are also attributes that are usually reported by researchers. It should be noted that the sampling rates recorded from the EEG systems used in the thirty selected studies (see Table 2.1) fall into sequences of either 125, 250, 500,… or 128, 256, 512,... because of the underlying technology used. It was therefore decided that 125/128, 250/256, 500/512,… would score the same as their temporal resolutions are very similar.

The reporting of the system's specification in published studies does not always include the attributes required to be captured by the proposed scoring system. In these cases, system manufacturer specification details were sought to supplement the missing information. Where systems have been developed in-house, and therefore manufacturer specification details do not exist, a range of possible scores is reported to encompass the potential variation in specification score.

Battery life is an important consideration of mobile EEG. For an EEG system to be fully mobile it has to be battery powered and the charge life of the battery directly governs the period of active monitoring that can take place [80]. A battery life attribute was included in the system specification score so duration of use could be captured, and where equipment was not battery powered this was also reported.

A rating scale of 1 to 5 for each system specification attribute was used. The range for each attribute is from the lowest used in commercially available systems, up to the highest and beyond to cover future expected technological developments. The score assigned for each attribute of the system specification is dictated by the actual bit resolution, sampling rate, battery life and electrode type used in the research investigation. Table 2.6 shows the system attributes and scoring of the system specification.

Table 2.6 System specification scores

System Attribute[1]	**Scores**				
	1	**2**	**3**	**4**	**5**
Bit resolution (bits)	14	16	22	24	>24
Sampling rate (Hz)	125 or 128	250 or 256	500 or 512	1000 or 1024	>1000
Battery Life (Hrs)	Mains, USB or equivalent	1 to 8	9 to 16	17 to 24	>24

[1]A score of 1-5 is given separately for each system attribute, and summed, along with the score for electrode type from Table 2.5, to give a single total score (minimum score=4, maximum score=20).

Scores for bit resolution, sampling rate, battery life and electrode type were added together to form a single combined total score for system specification (S) out of a maximum possible score of 20. For example, a bit resolution of 14, sampling rate of 512 Hz, a battery life of 8 hours and active shielded gel electrodes would give a total system specification score of 1 + 3 + 2 + 5 = 11S.

2.2.4 Number of channels

To develop a scoring scale for the number of channels used in an EEG study, many factors would have to be considered that relate to the specific type of investigation being undertaken. The type of analysis to be performed quite often necessitates a certain number of channels for validity, such as distributed source reconstruction [81], and spatial filtering methods [82]. Although, in general, the range of possible analysis approaches systematically increases with spatial densities, and therefore a scale could be created on such a basis, the positioning of the electrodes presents another aspect of the problem. A steady-state visual evoked potentials experiment using electrodes only located at the posterior of the head is different from an imagined motor activity experiment that uses electrodes localised more to anterior of the head. Therefore, in the categorisation scheme it was decided to report the number of channels (C) separately, for example, 32C.

2.3 Application of the categorisation of mobile EEG (CoME) scheme

The developed CoME scheme was applied to all thirty published research studies listed in Table 2.1. The specification score (S) for each EEG system (bit resolution, sampling rate, battery life, and electrode type) is presented in Table 2.7. The scores for device mobility (D), participant mobility (P), total score for system specification (S), and number of channels (C) are presented in Table 2.8. Figure 2.2 presents in a 3D plot the D, P and S scores for a selected subset of the thirty studies (comprising of sixteen studies), which illustrate the range of specific scores obtained using the CoME scheme. For each of the selected studies, the resultant D, P and S scores, number of channels used, and the final categorisation score have been summarized below the EEG equipment and participant activity:

ActiveTwo -1 (Biosemi, Netherlands)

Davies & Gavin [54] used an off-body mounted system in which participants were seated, and therefore static. Consequently, device mobility (D) and participant mobility (P) were ranked at the lowest point of each scale (0D and 0P). This study used a BioSemi ActiveTwo EEG system with recordings made using 24 bit sampling resolution (score=4), at a sampling rate of 1024 Hz (score=4), battery life of 10 hours (score=3) and electrodes were active shielded and gel-based (score=5), yielding a system score of 16S. Since 32 channels were used the total score for the BioSemi ActiveTwo system as used in this study was (0D,0P,16S,32C).

ActiveTwo -3 (Biosemi, Netherlands)

The study by Gwin *et al.,* [14] also used a BioSemi ActiveTwo system, but involved participants walking and running on a treadmill with the EEG acquisition equipment mounted off-body on a rack above the treadmill. This configuration yields a device mobility score of 0D. The treadmill running of the participant scored 4P. The system score

is 15S, which is different from Davies & Gavin [54], because of the lower sampling rate of 512 Hz (score=3). However, the number of channels used was greater at 248 channels. The overall score is (0D,4P,15S,248C).

ActiveTwo -4 (Biosemi, Netherlands)

Motion capture was used in conjunction with EEG while participants played a digital piano in a study by Maidhof *et al*., [66]. A BioSemi ActiveTwo system was used but this time with a sampling rate of 8192 Hz (score=5), which combines with the bit resolution, battery life and electrode type to form a score of 17S. The device was mounted off-body and scores 0D. The participants were seated and performing localised movement which scores as 1P. The number of channels used was 32 making the overall score (0D,1P,17S,32C).

actiCHamp (BrainVision, USA)

User-driven treadmill walking was an investigation undertaken by Bulea *et al*., [56]. A figure in this paper shows participants wearing an EEG cap that is then wired to one of several back mounted pieces of equipment. This arrangement has been scored as 1D, and because the study used treadmill walking the score for participant mobility was 2P. The EEG system consisted of 24 bit sampling (score=4), 500 Hz sampling frequency (score=3), battery life of 24 hours (score=4) summed to form a score of 16S. 64 channels of EEG were used for this study providing a combined score of (1D,2P,16S,64C).

Asalab (ANT Neuro, Netherlands)

Ehinger *et al*.,[46] used the term 'mobile EEG study' to describe participants moving with a trolley. The trolley was used to mount all of the equipment in a static EEG system format. Since the device was mounted off-body (on the trolley) it was given a score of 0D for device mobility. As part of the study participants moved by pushing the trolley within guide rails, and a score of 2P for participant mobility was given. The EEG equipment

system specification was 24 bit resolution (score=4), with a 1024 Hz sampling rate (score=4), battery life of 10 hours (score=3), and active shielded gel electrodes were used (score=5) combining to give 16S. Since 128 EEG channels were used the overall score was (0D,2P,16S,128C).

B-Alert (Advanced Brain Monitoring, U.S.A.)

Monitoring responses in the prefrontal cortex (PFC) and motor cortex (MC) during cycling-based exercise was the purpose of the investigation by Robertson *et al.,*[67]. They used a B-Alert mobile EEG system to capture the data; since this is a head-mounted system that connects to a PC via a wireless connection it was given a score of 3D. The participants were seated on fixed exercise cycles during the study which scored 2P. The B-Alert system specification as used, consisted of a 16 bit sampling resolution (score=2), 256 Hz sampling rate (score=2), battery life of 8 hours (score=2), and passive shielded conductive cream-based electrodes were used (score=4) combining to give 10S. Overall scores including the 20 channels score was (3D,2P,10S,20C).

BrainAmp-1 (Brain Products, Germany)

Participants stood in front of a projection screen and had to point, in a study by Jungnickel *et al*., [61]. The EEG system is placed in a backpack and consequently scores 1D. The participants in this study were standing still and pointing which is a localised movement and scores 1P. The BrainAmp system specification as used, consisted of a 16 bit sampling resolution (score=2), 500 Hz sampling rate (score=3), battery life of 30 hours (score=5), and active shielded gel-based electrodes were used (score=5) combining to give 15S. The overall score including the 156 channels score was (3D,2P,15S,156C).

BrainAmp-3 (Brain Products, Germany)

Wascher *et al*., [40] also used a BrainAmp EEG system in a study that recorded EEG while participants carried packages of various weights (0.5 to 15Kg) while walking. The EEG equipment was mounted on the participants in a belt bag located at their lower back and scored 1D. A score of 4P was attributed to the activity carried out by participants since it went beyond unconstrained walking with the inclusion of package carrying. The system score is 16S, which is different from Jungnickel *et al*., [61], because of the higher sampling rate of 1000 Hz (score=4). The combination of scores provides an overall score of (1D,4P,16S,28C).

Mindwave (NeuroSky, U.S.A)

Participants were seated during a driving simulation study undertaken by Liu *et al*.[65] They used a head-mounted Mindwave system that requires a wirelessly linked PC to process and store the EEG data. The device mobility was scored as 3D as the laptop/PC restricts the range of the participants. Since the participants were undertaking a seated driving simulation task in which small amounts of localised physical movement were involved it was scored as 1P. The Mindwave system has a sampling resolution of 16 bit (score=2), a 500 Hz sampling rate (score=3), battery life of 10 hours (score=3) and with a dry passive shielded electrode (score=2), to give a combined score of 6S. The overall score for this study with a single channel used was (3D,1P,6S,1C).

Mobita (TMSi, Netherlands)

The Mobita EEG system was evaluated in a study by Askamp *et al*., [55]. The device was waist-mounted and did not require any additional equipment and thus scored 2D. Since participants in the study were out-patients it was assumed that everyday home activities would be the type of activities undertaken. Stair climbing was therefore considered the most mobile of activities within a home environment and so scored 4P. The EEG system provided a sampling resolution of 24 bit (score=4), a 500 Hz sampling rate (score=3),

battery life of 19 hours (score=4) and with a gel-based passive shielded electrodes (score=4), to give a combined score of 17S. The overall score for this study with 32 EEG channels used was (2D,4P,17S,32C).

Oldenburg Hybrid-1 (modified Emotiv, U.S.A.)

Debener *et al*.,[36] undertook a study in which participants walked outside unconstrained. This investigation used what is referred to as the Oldenburg system, comprised of the data acquisition electronics from an EPOC system fitted to an electrode cap (Easycap, Germany). This modified system was developed in an attempt to increase data quality by improving electrode connection to the participant's scalp. However, the resulting data recordings are still limited by the comparatively low system specification of the acquisition electronics. The device mobility was scored as 3D since the EEG acquisition equipment was in a rucksack mounted on the participant. This study scored relatively high for participant mobility (3P) as participants were walking outside (constrained only by the weight of the rucksack-housed laptop). Since the acquisition electronics are from an EPOC EEG system with a bit resolution of 14 (score=1), sampling rate of 128 Hz (score=1), battery life of 6 hours (score=2) and the upgrade of electrodes to gel-based passive shielded (score=4), gives the score of 8S. The system was still limited to 14 channels and the categorisation gave an overall score of (3D,3P,8S,14C).

Oldenburg Hybrid-2(modified Emotiv, U.S.A.)

De Vos *et al.,* [51] compared the performance of the Oldenburg Hybrid to that of a traditional amplifier in a seated brain-computer interface (BCI) speller task. Although the participants were not required to carry additional equipment in a rucksack, they were still limited by the range of the wireless link to a corresponding PC and therefore scored 3D. With the participants being seated whilst performing a visual event related potentials (ERP) speller task they were seated without moving and gain a score of 0P. The acquisition electronics and electrode types remain the same as with Debener *et al*.,[36] and

therefore score 8S.The system again has 14 channels with the categorisation score becoming (3D,0P,8S,14C).

Penso (non-commercial)

Gargiulo et al., [60] studied seated participants performing imagined motor activity. They built their own EEG system which was waist-mounted and scored 2D. Since the participants were seated and physical movement was limited to eyes opening and closing and button pressing a score of 1P was assigned. Their EEG system provided them with 16 bit sampling resolution (score=2), a 256 Hz sampling rate (score=2). The battery life was not mentioned in the publication and since it is not a commercial product, documentation could not be used. A score range of 1 to 5 was given to capture the range of possible scores, and along with electrodes that were dry passive and shielded (score=2), this gave a score for the system specification of 7-11S, and with 8 EEG channels an overall score of (2D,1P,7-11S,8C).

Polymate AP216 (TEAC Corp., Japan)

Lotte *et al.,* [43] studied EEG recordings from participants performing corridor walking. The EEG system and a laptop were stored in a backpack which the participants wore and scored 1D. Since the participants were walking in an unconstrained manner it scored 3P. The Polymate EEG system provided them with 16 bit sampling resolution (score=2), a 1000 Hz sampling rate (score=4), battery life of 18 hours (score=4)and active shielded gel-based electrodes (score=5) summed to give 15S. Three channels were used during this study, and contributes to the overall score of (1D,3P,15S,3C).

SMARTING-1 (mBrainTrain, Belgrade, Serbia)

Debener *et al.,*[57] used a mobile EEG system with participants seated indoors. The emphasis was on the unobtrusive flexible printed electrodes they had used that were located around the ears. EEG recordings were made using SMARTING, which is a head-

mounted system that transmits data wirelessly to a smartphone or PC. Since a smartphone was used in their study the device mobility scored 4D. The participant movement were essentially static whilst seated indoors when recordings took place and scored 0P. The SMARTING EEG system provided the researchers with samples at 24 bit sampling resolution (score=4), a sampling rate of 500 Hz (score=3), battery life of 5 hours (score=2), electrodes are gel-based passive and unshielded (score=3), totalling 12S. The overall score with 16 EEG channels used was (4D,0P,12S,16C).

Varioport (Becker Meditec, Germany)

Doppelmayr *et al.,*[58] performed static EEG recordings during rest periods in ultra-long running events. They also performed EEG recordings with participants walking slowly with eyes closed (hand-led by a member of support crew), and it is this part of the study which was scored since it contained the most physical movement. EEG recordings were made using a light weight, waist-mounted system called Varioport which scored 2D. The participant movement involved periods of slow walking, and scored 3P. The Varioport EEG system provided the researchers with samples at 16 bit sampling resolution (score=2), a sampling rate of 2000 Hz (score=5), battery life of 96 hours (score=5). No information regarding the type of electrodes used in the study are supplied in the publication, and attempts made to find this missing information via manufacturer documentation has also failed to help. A score was applied by taking the only information available (passive) and applying the lowest scores for the unknown parameters (score=3). A total score of 10S is given but this could be higher with a score range of 10-15S. With the Varioport being used to provide 10 channels the overall score was (2D,3P,10-15S,10C).

Table 2.7 Scoring of EEG system specification (S).

EEG System (Published Study)	Bit resolution (score)	Sampling rate Hz (score)	Battery Life (score)	Electrode Type[1] (score)	Total system specification score (S)
ActiveTwo-1 (Davies & Gavin [54])	24 (4)	1024 (4)	10 (3)	gel, active, shielded (5)	16
ActiveTwo-2 (Gramann *et al.*[10])	24 (4)	512 (3)	10 (3)	gel, active, shielded (5)	15
ActiveTwo-3 (Gwin [14])	24 (4)	512 (3)	10 (3)	gel, active, shielded (5)	15
ActiveTwo-4 (Maidhof [66])	24 (4)	8192 (5)	10 (3)	gel, active, shielded (5)	17
actiCHamp (Bulea [56])	24 (4)	500 (3)	24 (4)	gel, active, shielded (5)	16
ANT-1 Castermans [42]	24 (4)	512 (3)	5 (2)	gel, passive, shielded (4)	13
ANT-2 Duvinage [52]	24 (4)	2048 (5)	5 (2)	gel, passive, shielded (4)	15
Asalab (Ehinger *et al.*[46])	24 (4)	1024 (4)	10 (3)	gel, active, shielded (5)	16
B-Alert (Robertson *et al.*[67])	16 (2)	256 (2)	8 (2)	cream, passive, shielded (4)	10
BrainAmp-1 (Jungnickel [61])	16 (2)	500 (3)	30 (5)	gel, active, shielded (5)	15
BrainAmp-2 (Wagner [69])	16 (2)	2500 (5)	30 (5)	gel, active, shielded (5)	17
BrainAmp-3 (Wascher [40])	16 (2)	1000 (4)	30 (5)	gel, active, shielded (5)	16
Cognionics (Lin [64])	24 (4)	250 (2)	8 (2)	dry, active, shielded (3)	11
EPOC-1 (Aspinall [39])	14 (1)	128 (1)	6 (2)	saline, passive, not stated (2)	6
EPOC-2 (Klonovs [62])	14 (1)	128 (1)	6 (2)	saline, passive, not stated (2)	6
EPOC-3 (Stopczynski *et al*. [68,83])	14 (1)	128 (1)	6 (2)	saline, passive, not stated (2)	6
Mindwave-1 (Liu *et al.*[65])	16 (2)	500 (2)	10 (3)	dry, passive, shielded (2)	9
Mindwave-2 (Wong [71])	16 (2)	500 (2)	10 (3)	dry, passive, shielded (2)	9
Mobita (Askamp [55])	24 (4)	2000 (5)	19 (4)	gel, passive, shielded (4)	17
NuAmp (Wang [70])	22 (3)	500 (2)	N/A (1)	gel, passive, unshielded (3)	9
Oldenburg Hybrid-1 (Debener *et al.*[36])	14 (1)	128 (1)	6 (2)	gel, passive, shielded (4)	8

Table 2.7 continued…

EEG System (Published Study)	Bit resolution (score)	Sampling rate Hz (score)	Battery Life (score)	Electrode Type[1] (score)	Total system specification score (S)
Oldenburg Hybrid-2 (De Vos [51])	14 (1)	128 (1)	6 (2)	gel, passive, shielded (4)	8
Penso (Gargiulo *et al.*[60])	16 (2)	256 (2)	N/A (1)	dry, passive, shielded (2)	7
Polymate AP216 (Lotte [43])	16 (2)	1000 (4)	18 (4)	gel, active, shielded (5)	15
Profusion (Fitzgerald *et al.*[59])	16 (2)	512 (3)	15 (3)	gel, passive, unshielded (3)	11
SMARTING-1 (Debener *et al.*[57])	24 (4)	500 (3)	5 (2)	gel, passive, not stated (3)	12
SMARTING-2 (Zink *et al.*[73])	24 (4)	500 (3)	5 (2)	gel, passive, not stated (3)	12
Varioport (Doppelmayr *et al.*[58])	16 (3)	2000 (4)	96 (5)	not stated, passive, not stated (1)	13
V-Amp (Zander [72])	24 (4)	2000 (4)	N/A (1)	dry, active, shielded (3)	12

[1] Selected from dry/saline/gel (or cream), passive/active, unshielded/shielded. N/A, not applicable.

Table 2.8 Overall scores for device mobility (D), participant mobility (P), system specification (S), number of channels (C), and total categorisation scores.

EEG System (Published Study)	Device Mobility Score (D)	Participant Mobility Score (P)	System Specification Score (S)	Number of Channels (C)	Total Categorisation Score (D,P,S,C)
ActiveTwo-1 (Davies & Gavin[54])	0	0	16	32	**(0D,0P,16S,32C)**
ActiveTwo-2 (Gramann *et al.*[10])	0	2	15	248	**(0D,2P,15S,248C)**
ActiveTwo-3 (Gwin [14])	0	4	15	248	**(0D,4P,15S,248C)**
ActiveTwo-4 (Maidhof [66])	0	1	17	32	**(0D,1P,17S,32C)**
actiCHamp (Bulea [56])	1	2	16	64	**(1D,2P,16S,64C)**
ANT-1 (Castermans [42])	0	2	13	32	**(0D,2P,13S,32C)**
ANT-2 (Duvinage [52])	0	2	15	128	**(0D,2P,15S,128C)**
Asalab (Ehinger *et al.*[46])	0	2	16	128	**(0D,2P,16S,128C)**
B-Alert (Robertson *et al.*[67])	3	2	10	20	**(3D,2P,10S,20C)**
BrainAmp-1 (Jungnickel [61])	1	1	15	156	**(1D,1P,15S,156C)**
BrainAmp-2 (Wagner [69])	0	2	17	120	**(0D,2P,17S,120C)**
BrainAmp-3 (Wascher [40])	1	4	16	28	**(1D,4P,16S,28C)**
Cognionics (Lin [64])	3	2	11	10	**(3D,2P,11S,10C)**
EPOC-1 (Aspinall [39])	3	3	6	14	**(3D,3P,6S,14C)**
EPOC-2 (Klonovs [62])	3	1	6	14	**(3D,1P,6S,14C)**
EPOC-3 (Stopczynski *et al*. [68,83])	4	0	6	14	**(4D,0P,6S,14C)**
Mindwave-1 (Liu *et al.*[65])	3	1	9	1	**(3D,1P,9S,1C)**
Mindwave-2 (Wong [71])	3	1	9	1	**(3D,1P,9S,1C)**
Mobita (Askamp[55])	2	4	17	32	**(2D,4P,17S,32C)**
NuAmp (Wang [70])	3	1	9	32	**(3D,1P,9S,32C)**
Oldenburg Hybrid-1 (Debener *et al.*[36])	3	3	8	14	**(3D,3P,8S,14C)**
Oldenburg Hybrid-2 (De Vos [51])	3	0	8	14	**(3D,0P,8S,14C)**
Penso (Gargiulo *et al.*[60])	2	1	7	8	**(2D,1P,7S,8C)**
Polymate AP216 (Lotte [43])	1	3	15	3	**(1D,3P,15S,3C)**
Profusion (Fitzgerald *et al.*[59])	2	1	11	32	**(2D,1P,11S,32C)**
SMARTING-1 (Debener *et al.*[57])	4	0	12	16	**(4D,0P,12S,16C)**

Table 2.8 continued…

EEG System (Published Study)	Device Mobility Score (D)	Participant Mobility Score (P)	System Specification Score (S)	Number of Channels (C)	Total Categorisation Score (D,P,S,C)
SMARTING-2 (Zink *et al.*[73])	3	3	12	24	**(3D,3P,12S,24C)**
Varioport (Doppelmayr *et al.*[58])	2	3	13	10	**(2D,3P,13S,10C)**
V-Amp (Zander [72])	0	1	12	16	**(0D,1P,12S,16C)**

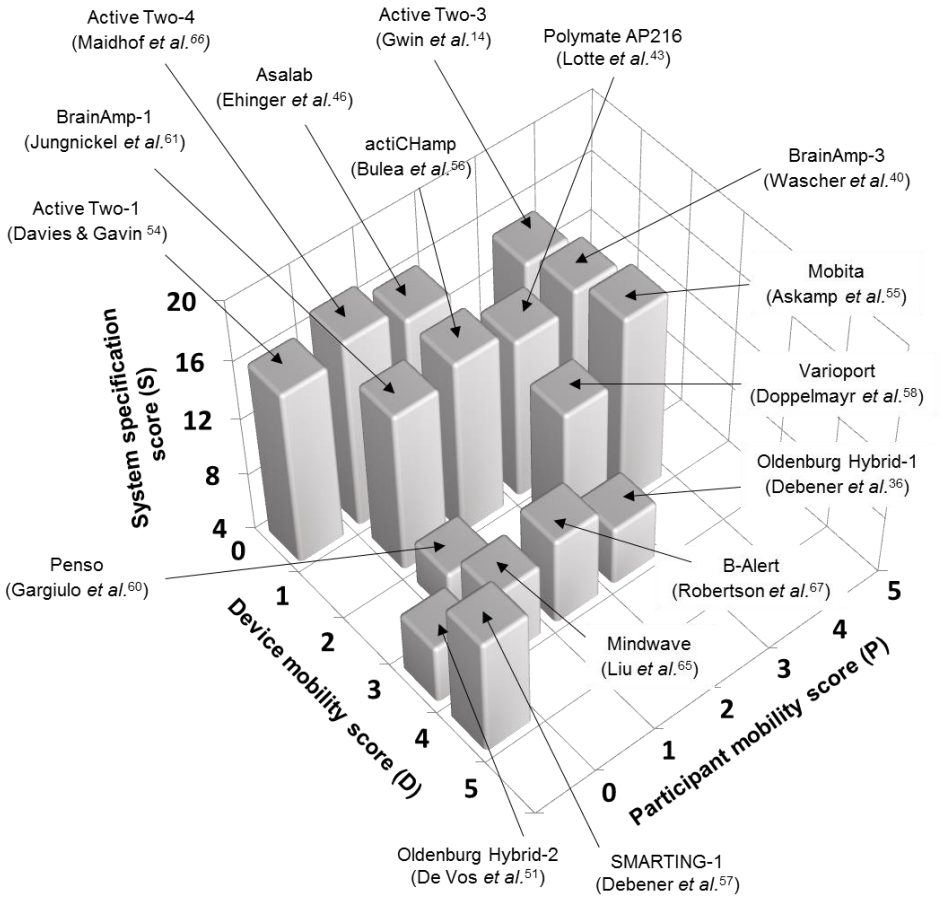

Figure 2.2 3D plot showing the device and participant mobility scores and the system specification scores for each selected research investigation and associated EEG systems. Refer to Table 2.8 for the number of channels used in each selected study.

2.4 Discussion

In the current investigation, thirty published research investigations have been reviewed and used to develop a novel categorisation scheme for 'mobile EEG' based upon scores of the following parameters: device mobility, participant mobility, and system specification whilst also reporting the number of channels used. The parameter score descriptors were derived following review of thirty published research investigations. The categorisation scheme was then applied retrospectively to all thirty published studies and a subset of these (sixteen studies) was taken to illustrate the range of specific categorisation scores in the parameters covered by the developed scoring system.

The results show a broad range in the scores for device mobility, participant mobility and system specification. The results highlight the need for such a categorisation scheme to be adopted and utilised by researchers, as it provides a quantitative and more accurate description than the vague term 'mobile EEG'. In addition, the categorisation has been designed to provide the scores in a convenient format. This allows researchers to readily capture and compare the actual meaning of the term 'mobile EEG' in the context of a specific researcher's study. Researchers are encouraged to apply the categorisation scheme to their own mobile EEG systems and research contexts when using the ambiguous term, 'mobile EEG' in their publications and reports. It should be noted that users of the categorisation scheme should not equate lower or higher scores with subjective judgements. The intention is only to quantify the level of device mobility, participant mobility, system specification and number of channels used in a comparable way across studies.

Based upon the categorisation scores of the thirty published studies, there may be an indication that EEG systems with higher system specification scores are associated with lower scores for device mobility. For example, the studies by Maidhof *et al.,*[66] and Ehinger *et al.,*[46] have higher device specification scores of 17S and 16S respectively,

but lower scores for device mobility of 0D. In contrast, EEG systems with lower scores for system specification scored higher for device mobility. For example, the studies by Debener *et al.,*[36] and Stopczynski *et al*.,[68,83] scored 8S and 6S respectively for system specification, but scored 3D and 4D, respectively for device mobility. The developed CoME scheme could enable researchers, in future investigations using a larger number of included studies, to determine whether there are any relationships between device mobility, participant mobility and system specification.

The categorisation scoring scheme will aid in the development of new mobile EEG systems, by both research and commercial communities, by making it possible to clearly identify quantifiable improvements and to clarify reporting of 'mobile EEG' in publications. Fully head-mounted EEG systems are especially appropriate for recordings to be acquired in mobile settings. Combining such a head-mounted system with a smartphone would give a high score for device and participant mobility.

The categorisation scheme is capable of informing investigators of the potential for increasing device and participant mobility, and thereby highlighting future research possibilities. For example, in the study by Gargiulo *et al.,*[60] the imagined motor activity could be undertaken while participants walk, as the device mobility score of 2D, in principle, allows a higher level of mobility to be introduced. In the studies by Stopczynski *et al.,*[68,83] using the EPOC system, device mobility scores were 4D, but since the investigation involved participants sitting still, the participant mobility scores were limited to 0P. This indicates that there is the potential for additional investigations to be designed in which participant mobility could be introduced or increased. A further example is in the studies by Zink *et al.,*[73] and Debener *et al.,*[57] who both used the SMARTING system. If Zink *et al.,*[73] were to use a smartphone instead of a PC, as in the study by Debener *et al.,*[57] to record the transmitted data then the study score for device mobility would increase from 3D to 4D to enable novel protocols.

Another usage of the categorisation scheme by researchers could be in determining the degree of device mobility, participant mobility, system specification, and number of channels used within and between research investigations. To better facilitate this process, a CoME scheme form has been included in Appendix 1. It is hoped by including this easy to use resource, researchers will be encouraged to quantify their research in terms of the categories covered. From the perspective of the categorisation scheme, an ideal 'mobile EEG' system would score a maximum of (5D,5P,20S), and represents a fully head-mounted system that does not require additional equipment for data recording. The participant would be able to undertake extreme activities such as unconstrained running, and the system specification would be greater than 24 bit resolution, sampling at greater than 1000 Hz with a battery life of more than 24 hours. No study-EEG system combination with this level of device and participant mobility coupled with this level of system specification could be found. The expectation is that given the pace of current developments, the higher scores for system and device/participant mobility descriptors are likely to be achievable in the foreseeable future.

There are two ways in which the CoME scheme can be applied: 1) retrospectively and 2) prospectively. In the current study it was applied retrospectively to thirty published studies and scored according to what the research reported. There is usually a reason why researchers have not maximised the settings. This could also relate to the equipment used as some systems are modular and in order to use the equipment in a certain way compromises may have been made. If the scheme is used to plan a study and therefore the scheme is to be applied prospectively, a system's maximum settings would be scored.

2.4.1 Limitations of the CoME scheme

In the CoME scheme, the total system specification is a combined score reflecting the electrode type, bit resolution, sampling rate and battery life. The recommendation is that researchers consider both the total system specification score as well as the individual scores for these parameters. It is possible that the CoME system specification score is not fully reflective of a researchers expected change in EEG signal quality within a certain research context. For instance, an improvement in systems specification when using active electrodes instead of passive may be considered by a researcher to represent an increase in signal quality, but using the CoME scheme there would only be a score change from 0 to 1. However, when gel-based electrodes with wires of minimal length and associated electronics are in close proximity (head-mounted configuration), using active electrodes may not produce an increase in signal quality and a CoME score allocation of one may be considered as high.

There are potentially a wide range of system specification parameters which could have been included such as impedance, and wireless connection range but only bit resolution, sampling rate, battery life and electrode type were included in the categorisation scheme. These four attributes were included as they are usually reported in published EEG research studies or can be found with relative ease from manufacturer's documentation. Some publications do not report details of the EEG system used and corresponding settings. A recommendation resulting from this finding is that research investigators, as part of good publication practise, report at least the following parameters: EEG system name, EEG system manufacturer (where appropriate), bit resolution, sampling rate, battery life, electrode type and number of channels used.

For electrode impedance, published research studies typically only provide a general statement such as '*impedance was kept below 5kΩ'* rather than giving a precise value for each channel and for each participant. In addition, impedance is a dynamic variable

that changes throughout the course of a study and it is assumed that researchers will deal with this as a matter of course when obtaining research data fit for publication. Another reason for selecting the parameters chosen is that a scoring scale can be generated with increasing gradations, for example, increasing sampling rate gives a higher score. Such an increasing gradation scale is not possible to generate for different electrode metal types (tin versus silver versus gold), where the application rather than the level of mobility of participants is the main factor of consideration.

Although the categorisation scheme has been developed from the perspective of the researcher and has descriptors which cover EEG equipment mobility, participant mobility and system specification, it does not consider the perspective of the participant. It is possible that the participant may have experienced, for example, some discomfort relating to the EEG equipment that the researchers had been unaware of, or that items of equipment were encumbering during the investigation. Participants could be asked to provide scores for comfort, weight, aesthetic form and these could be added to the categorisation scheme. For example, the study by Hairston *et al.,*[49], which utilised participant reported comfort ratings for EEG systems (1=very comfortable, 7= very uncomfortable), could potentially be incorporated into the categorisation scheme. The subjectivity of comfort assessments would be a problem when developing a participant-focused scoring system using descriptors, particularly as participant assessments may change over time. The addition of several participant-focused parameters to the categorisation scheme would make the format less concise and make comparisons more difficult. Perhaps a separate participant categorisation scheme could be developed to address these issues, but it would have to accurately capture and quantify participant perspectives, which are rarely sought.

In the next chapter, the CoME scheme is utilised in the design process to aid in the development of a system specification for a smartphone-based waist-mounted mobile EEG system.

2.5 Conclusions

In this chapter a review was undertaken of thirty published research studies that use the term ‘mobile EEG’ or contain participant mobility whilst EEG is being acquired. From this review a categorisation scheme for ‘mobile EEG’ studies based upon scoring for device mobility, participant mobility, system specification, and number of channels used was developed in order to remove the inherent ambiguity in the way this term is used by researchers. The results of applying the categorisation retrospectively to a range of published research shows that it captures the degree to which the EEG equipment is mobile, the degree of participant movement in the study, the main attributes of the system specification that are readily available along with the number of channels used. The format of the resultant scores is concise and enables convenient comparison across different research studies. The CoME scheme form is intended to be a useful aid for researchers to conveniently categorise their mobile EEG studies as well as in the design and development of mobile EEG equipment (see Appendix 1).

2.6 Aims of the thesis

Having reviewed the mobile EEG literature and developed the CoME scheme, the remainder of the research presented in the thesis aims to develop a smartphone-based mobile EEG system that has sufficient capability to produce research quality recordings. The CoME scheme will be used to help define the system specification.

The aims of this thesis are to:

1. design and build a prototype smartphone-based mobile EEG system that can be utilised for research and is adaptable and upgradable (Chapter 3).

2. validate the developed smartphone-based waist-mounted EEG system against a commercial grade mobile EEG system in study participants in various postures (lying, sitting, standing, and standing with arms raised) and walking (Chapter 4).

3. develop an ERP capability of the smartphone-based waist-mounted EEG system (Chapter 5).

4. upgrade the smartphone-based waist-mounted EEG system to a head-mounted configuration and undertake an ERP study (Chapter 6).

Chapter 3: Design and development of a smartphone-based waist-mounted mobile EEG system

3.1 Introduction

In this chapter, a research quality smartphone-based waist-mounted mobile EEG system is proposed, with its specification defined with the aid of the CoME scheme. Constraining factors such as how the resultant system will be validated and what electrodes to use will be considered within the process of defining the system's specification. Once the system specification has been produced, the system will be scored to show how it compares to the scores of published mobile EEG studies (see Chapter 2).

Traditional static EEG recordings are made while constraining the participant movement to such a degree that movement-related artifacts are minimised. Participant movement during EEG experiments adversely affects signal quality through mechanisms such as variation of the electrode-skin interface and signals generated by muscles. Strategies to deal with the problem of these artifacts are largely confined to removal of the sections of adversely affected data, or the aforementioned constraining of participant movement. Neither of these strategies results in usable continuous brain activity data being recorded during participant movement. The lack of continuous data limits advances in the understanding of human brain activity in real world scenarios. There is a growing interest in studies that employ mobile EEG in settings outside of a traditional laboratory setting [12,36,39,78,84]. Hardware and experimental protocols are required to obtain continuous brain activity data while a participant is moving and undertaking a range of tasks in a variety of environments. The purpose of mobile EEG is to obtain recordings of electrical activity of the brain at the scalp surface outside of a static EEG laboratory setting and during various participant movements. However, currently available commercial mobile EEG systems have limited success in achieving this [36,52].

A mobile EEG system's specification (including sampling rate, bit resolution, battery life, electrode type and number of channels) affects data quality. Its weight, size and

mounting-position impact upon participant mobility. Consequently, the EEG system used can impose constraints upon a research study when, for example, a large, heavy, high specification system is used it cannot be carried by a participant. Conversely, a small, light, low specification system may be carried but only provides lower quality data recordings. Researchers have adopted a wide variety of approaches to mobile EEG when working within the constraints of device mobility and system specification. Such approaches have included walking on a treadmill while tethered to immobile EEG equipment [10,45], walking outdoors with a wireless mobile EEG headset combined with a rucksack-mounted PC [36], and being moved on a trolley while wearing a virtual reality headset to provide the sensation of movement [46]. Where heavy and bulky EEG systems have been used to record human brain signals during participant movement, the equipment has been located off-body, thereby tethering the participant to the equipment and restricting overall mobility [10,45,46]. When researchers have used small, lightweight and head-mounted EEG systems, the equipment has been located on the participant's body [36,39]. Such systems, in general, have a lower system specification in comparison to static systems as a means to meet the constraints of size and weight. Lower specification systems typically measure fewer channels, have a slower sampling rate and/or lower bit resolution. These EEG systems usually 'partner' with equipment that receives, processes, and records the EEG data, and in ERP experiments, provide stimuli and the associated data marker. This 'partner' equipment typically takes the form of a PC or laptop, and in cases where walking is required, this has to be carried in a rucksack by the participant [39].

Although EEG is considered a relatively low-cost technique [85], the cost of research quality EEG equipment can still be prohibitive and this, along with size, weight and specification issues has encouraged researchers to build their own EEG systems [60,86]. One approach taken by researchers has been to modify low-cost, low-specification EEG equipment to improve data quality attained from such systems. Debener *et al.* [36] chose to modify a commercial 14-channel wireless EEG system by taking the acquisition electronics and attaching them to an EEG cap with sintered Ag/AgCl electrodes and 10/20 system of electrode placement [87]. The benefits of this approach include improved EEG signal quality due to the low-impedance gel electrode connection in

comparison to the dry electrodes and standardisation of electrode positioning without the need to design and build an entire EEG system.

When considering the differences between dry and gel electrodes there is sufficient evidence to show that although dry electrodes are an improving technology, gel electrodes provide higher signal quality and produce less movement-related artifacts [88]. An international standard for electrode placement exists and is known as the international 10/20 system, which is comprised of 19 channels distributed across the scalp [89]. Gel-based EEG caps that make use of this placement system provide an advantage over individual cup electrodes since the participant setup time is reduced. Developing a mobile EEG system that utilises a gel-based EEG cap would enable comparisons with commercial EEG systems using the same cap. The ways in which improvements in the size and weight of equipment carried by participants could then be investigated. Further improvements to this approach would be realised if the researcher designed and built the entire system as this would enable improvements and modifications to be made as aspects of the technology used improved over time. Smartphones are an example of such a technology.

Several research groups have developed mobile EEG systems that link to smartphones [68,86,90]. This approach to EEG system development has the benefit of reducing the size and weight of participant carried equipment since a smartphone (used to record data or deliver stimuli) is smaller and lighter than a laptop PC. The reduction in size and weight comes at a cost since smartphones are generally inferior to laptop PCs in terms of processing power. However, since smartphone technology is improving at a rapid rate [91], and advances in low-power, high-performance microcontroller technology are at the centre of such improvements, it is unlikely to be a long term problem. By incorporating a smartphone into the design of a mobile EEG system, immediate benefits from equipment size and weight reductions are realised and longer-term smartphone developments will only improve such a system's performance and capability. Furthermore, current smartphone devices typically have 64-bit chipsets with octa-core processors, secure digital (SD) card storage, along with Wi-Fi

connectivity and therefore have potential to process and store large amounts of wirelessly transmitted data.

To utilise a smartphone for recording EEG data, an application (app) is required to take the received data and store it in a file. Developing a smartphone app can be undertaken using a variety of different approaches such as Google's Android Studio and Apples Xcode. However, such development tools are designed for a limited number of platforms and therefore restrict the range of platforms on which the app can be used. These restrictions can be removed by using a game engine that has support for a wide range of platforms, including mobile devices. Game engines such as Unity [92] and Unreal [93] provide support for a range of platforms that include (but are not limited to) smartphones.

The aim of this chapter is to design and develop a 24 channel, 24 bit mobile EEG system with a 250 Hz sampling frequency. The mobile EEG system is intended to partner with a smartphone via a Wi-Fi link with an app developed using a gaming engine and running on a smartphone facilitating recording and plotting of live data. Electrode coverage will provide a sufficient number of channels to be compatible with the international 10/20 system, and also five additional channels available for ECG, EOG or EMG recordings. The CoME scheme developed in the previous chapter will be utilised to help define the mobile EEG systems design specification. The prototype system presents many potential advantages over buying a commercially available system. Since the design and production process is known and documented, improvements and adaptations to the system and smartphone app are possible. This will allow bespoke solutions to be produced and enable specific research problems relating to EEG system limitations to be directly addressed. Additionally, as technology continues to advance, the components (e.g. Wi-Fi module, microcontroller, battery etc.) of the EEG system can be readily upgraded.

3.2 Developing the io:bio mobile EEG system design methodology and specification

The intended system was named as the io:bio mobile EEG system. Before the designing and fabrication of a prototype smartphone-based mobile EEG system could be started a design specification was required. Various requirements had to be factored into the design specification. For example once fabricated, the io:bio system needed to be capable of providing EEG recordings during participant movement. Another being that the data quality (sampling rate, bit resolution and number of channels) of the recordings made needed to be comparable to other mobile EEG systems used in published mobile EEG studies. Since these requirements are represented in the CoME scheme scores and the comparison was best achieved by utilising the CoME scheme (see Chapter 2). This enabled scores of mobile EEG systems and how they were utilised in published studies generated in the previous chapter to serve as a comparison for the proposed io:bio system design specification. Furthermore, this information was already available in graphical form (see Figure 2.2). A design specification was generated by selecting desired score ranges, and then further refined by considering what was achievable with available technology.

To complete the specification, the details of what capabilities were required for the system to be regarded as 'research quality' were needed first. These requirements then had to be satisfied within the constraint of the system requiring to be used in a mobile context. Device mobility comes with small and lightweight systems and therefore size and weight are attributes that need to be considered as a part of the specification. The physical footprint of electronic components were considered as they are factors that impacted upon the overall size of the electronics which in turn impacted upon the size of the enclosing case and ultimately the weight of the overall system. Before the specification was developed, design constraining factors were first considered in the context of the proposed mobile EEG system specification and how they impact upon it.

3.2.1 Design constraints

A number of factors needed to be considered when forming the specification for the io:bio mobile EEG system if the resultant system was to be comparable to other mobile EEG systems in the context to which they have been used in published research studies. Firstly, the io:bio mobile EEG system was required to be mobile and therefore body-mounted in some way. Secondly, it required validation once a working prototype had been constructed. The validation process along with the gold standard device to be used for comparison needed to be identified, and this had implications upon the selected participant protocol and participant setup procedure. Thirdly, the EEG electrodes used with the gold standard system were also used for the io:bio EEG system as this maintained the standard of this aspect of the overall system quality. Finally, where the system recorded data to (memory card, PC or smartphone) was important and has implications on participant mobility (see Chapter 2, Section2.2.2). Once the constraining factors had been explored in more depth, the next stage was to define design specifics such as the minimum rates of bit resolution, sampling, battery life, electrode type and number of channels.

3.2.1.1 Gold standard mobile EEG system for comparison

A commercially available waist-mounted EEG system known as Morpheus was selected as the gold standard for comparison (Micromed, Italy), as it is mobile and a clinically Food and Drug Administration (FDA) approved device. This waist-mounted EEG enabled participant mobility to be undertaken because of its relatively small and lightweight design. The io:bio mobile EEG system was constrained to a waist-mounted configuration to provide an optimal comparison with this selected gold standard system.

3.2.1.2 Gel-based 19 electrode EEG cap

The Micromed mobile EEG system connects to a 19 channel electrode cap that utilises the international 10/20 system of electrode positioning [94]. The connection to the cap was made via a 25-way D-type connector, and provided a mechanism of easy connection and disconnection with the EEG device. By using the same electrode cap (and therefore the same 25 way connector) in the design of the io:bio system it was possible to exchange the gold standard and the io:bio EEG systems without having to disturb the electrode connections at the participant's scalp surface. This facilitated an easy system exchange within the same participant during the validation process and therefore was incorporated into the io:bio EEG system design.

3.2.1.3 Partnering a smartphone with io:bio

Whilst defining the descriptors for device mobility that form part of the CoME scheme (see Chapter 2, Section 2.2.1) it was noted that some researchers had used EEG systems that partner with a smartphone. By adopting this approach with the io:bio mobile EEG system design, a number of advantages were made available. The inherent mobile nature of a smartphone, coupled with its high processing power made it a viable option to replace a PC or laptop in a research study scenario. Smartphones also have the potential ability to present participants with stimuli (auditory and visual), a feature that could be utilised in mobile EEG research settings. A smartphone was thus integrated with the io:bio EEG system (Asus Zenfone 2).

3.2.2 Application of CoME scheme to the design specification of io:bio

With the known constraints identified, the next stage was to ensure that the design of the io:bio mobile EEG system was of research quality rather than consumer grade. The CoME scheme was used in a prospective manner for this. Figure 2.2 of Chapter 2 shows a range of systems used in research studies in terms of their scores for participant mobility, device mobility and system specification. This was used to perform a comparison with the systems used in these studies to the io:bio system's design specification. This approach enabled comparisons to be made between the io:bio system and mobile EEG systems used in research studies.

3.2.2.1 Device mobility

From the device mobility descriptors (Chapter 2, Table 2.2), a fully head-mounted system would provide scores in the range 3-5D for device mobility. However, once the mobile EEG system had been designed and built, it required validating against a gold standard system to ensure that the system performed the process of EEG data recording to a similar quality. This is a design constraint in the current context as the gold standard system to be used for the validation process was a waist-mounted Micromed EEG system. By constraining the design specification of the EEG system to a waist-mounted modality the two systems could be readily compared. By designing the io:bio system to partner with a smartphone, the score for device mobility was 2D.

3.2.2.2 Participant mobility

Since the io:bio mobile EEG system was constrained to a waist-mounted modality (see Chapter 2, Section 2.2.1) this has implications for participant mobility. Participant running could be unsafe with a waist-mounted system that connects via long cables to an electrode cap. It is also likely that movement-related artifacts will occur using this mounting position. Thus, unconstrained walking was a reasonable level to aim for as a means to validate the mobile EEG system. This was scored as 3P using the CoME scheme.

3.2.2.3 System specification

While it would have been desirable to maximise all of the system specification attributes and achieve a score of 20S, this was not achievable. The constraints of the system having to be waist-mounted in the context of size and weight were considered and the EEG signal acquisition electronics designed and selected accordingly.

The bit resolution of the majority of the EEG systems used to derive the CoME scheme scales and descriptors was 16 bit or higher. Only the EPOC system (and Oldenburgh [36] which uses the acquisition electronics from the EPOC system) had bit resolutions lower than 16 bit (14 bit). For the prototype io:bio EEG system to be comparable to the majority of the EEG systems used to derive the CoME scheme scales, the analogue to digital converters used in its design would have had to be 16 bits or higher. An analogue to digital convertor specifically designed for EEG applications is available from Texas Instruments (Texas, USA); the ADS1299 [95] has a bit resolution of 24, and provides 8 differential channels. By using this integrated circuit (IC) to sample the EEG data, a suitably high bit resolution was designed in. All other facets of the system requirements were made only within the context ADS1299 IC as no other comparable convertor was identified with greater specification.

The EEG systems used within the studies reviewed for the CoME scheme (Chapter 2, Table 2.1) had sampling rates of 128 Hz or higher. When considering the frequency content of EEG signals and Nyquist sampling theory, a sampling rate of 128 Hz would enable frequencies up to 64 Hz to be recorded without aliasing occurring. Furthermore, the standards published by the International Federation of Clinical Neurophysiology (IFCN) [96] state that sampling rates should be multiples of 50 or 64 at a minimum rate of 200 Hz. The ADS1299 has a programmable sampling rate that ranges from 250 to 16000 Hz. This enabled a starting sampling rate of 250 Hz to be selected which meets the requirements of the IFCN, and provides the possibility of increasing the sampling rate in future developments. The io:bio system scored 2 for a sampling rate of 250 Hz using the CoME scheme.

A battery life of approximately 8 hours was aimed for as many research studies are much shorter in duration than this. Since battery life is largely affected by the power consumption of the system, power consumption is another constraint on the design process, and where applicable was factored in when making design choices. This approach helped to reduce the factors affecting battery life down to a choice of how large (and heavy) could the battery be, since larger batteries (of the same voltage and technology) relate to longer battery life. The io:bio system scored as 2 for a battery life of 8 hours.

The choice of electrode type to be used with io:bio was constrained by the electrode cap selected (Softcap, SPES Medica). Since it was a gel-based (score = 3), passive electrode (score = 0), unshielded electrode cap (score = 0), for the waist-mounted version of io:bio the total electrode score was 3. This results in an initial system specification score of 11S (24 bit = 4, 250 Hz = 2, 1 to 8 hours = 2 and gel passive unshielded = 3) for the io:bio system in a waist-mounted modality.

3.2.2.4 Number of channels

A minimum of 19 channels were required if a full comparison with the gold standard Micromed EEG system was to be made. The ADS1299 provided 8 channels, and by combining three of these ICs, 24 channels were achievable. The additional 5 channels were dedicated as differential channels for recording of ECG, EOG and EMG. These differential channels are potentially useful for artifact rejection purposes such as those created by eye blinks [40,97].

3.2.3 Scoring the prototype using the CoME scheme

In summary, the system specification for developing the io:bio mobile EEG was for a 24 bit, 24 channel, and 250 Hz sampling system. This was then designed to fit within an enclosure that was small and light enough to be waist-mounted, and able to connect a to 19 channel EEG cap via a standard 25 way D type connector. EEG data was designed to be received and recorded by a smartphone via Wi-Fi. The combined scores for device mobility, participant mobility, system specification and number of channels result in an overall CoME scheme score of (2D, 3P, 11S, 24C) for the first prototype version of io:bio system.

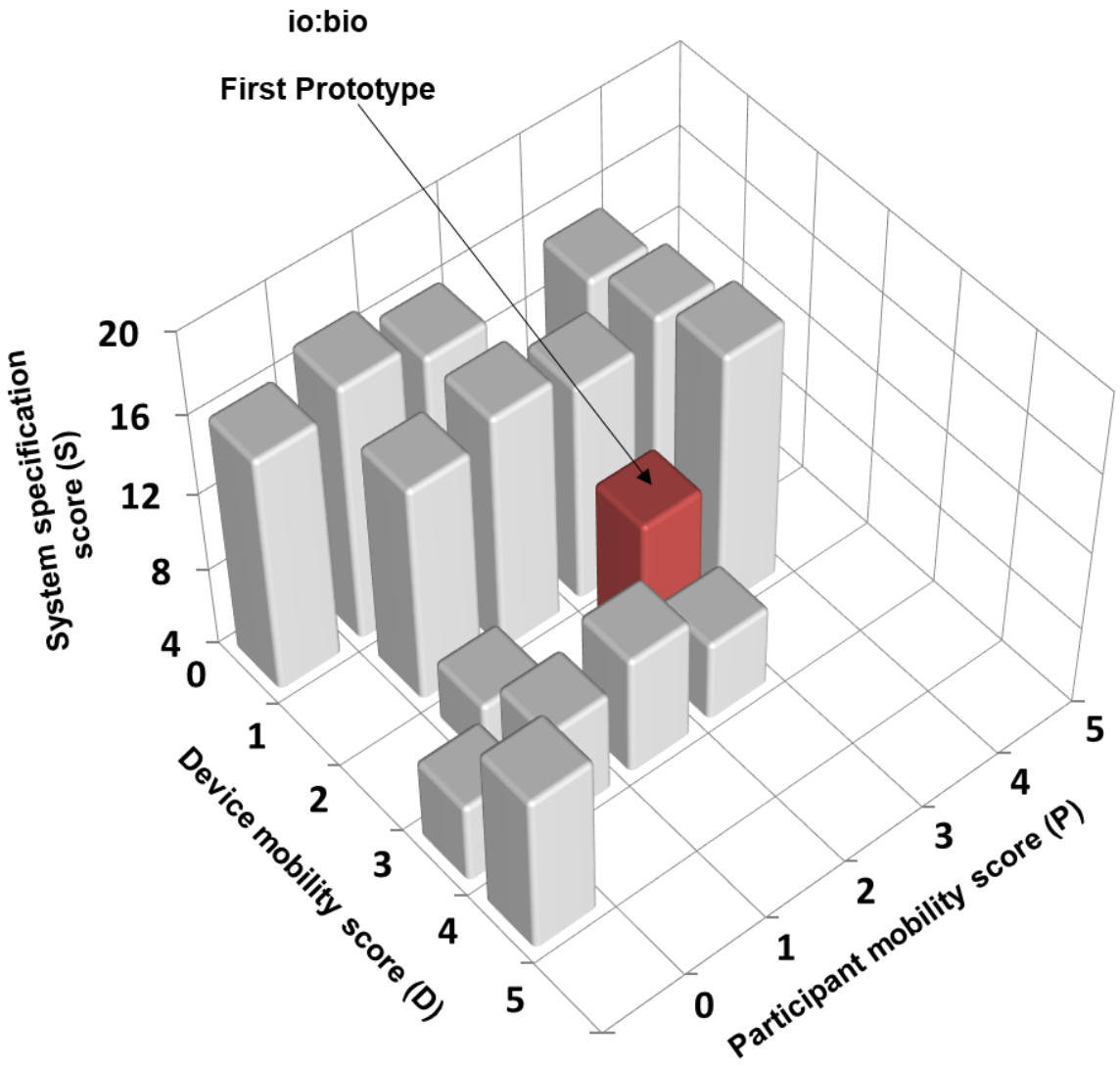

Figure 3.1 3D plot showing the device and participant mobility scores, and the system specification scores for each selected research investigation and associated EEG systems covered in the CoME study (for details see Chapter 2, Figure 2.2), along with the score for the io:bio EEG system.

3.3 Smartphone-based EEG system development

The design and development of the complete io:bio mobile EEG system covers the electronic hardware, embedded software, and smartphone application software. A combination of software and hardware development methodologies were utilised during the prototype mobile EEG system development. The methodologies were selected for their applicability to a specific sub-system of the overall design, thus facilitating a sub-division of the project as follows:

- **Top-down:** a development and testing methodology that lends itself to software development, especially where User Interfaces (UIs) are required. Software is written largely with the UI in mind and the underlying functions that drive the hardware are included as function stubs (empty software function) that are completed later. This was the smartphone app section of the project and was required to send commands to, and receive data from, the waist-mounted electronics sub-system.

- **Bottom-up:** a development and testing methodology that lends itself to hardware development. Individual sub-components of a hardware system are developed and tested individually and then combined to provide a staged development process. Some software is written at this stage, for example device drivers, so that each module can be tested before and after integration with other modules. This was the waist-mounted electronic sub-system that responded to commands to perform tasks such as sample EEG data and send it via Wi-Fi to the smartphone.

- **Sandwich testing:** Bringing top-down and bottom-up methodologies together by using a methodology known as sandwich testing facilitates the cross linking of the software and the hardware development. At this stage the function stubs are replaced with hardware device drivers as appropriate. This brings together the top-down approach and the bottom-up approach to provide a

middle layer. This middle layer links the waist-mounted electronic section of the system with the smartphone app via the commands sent and responses received.

The hardware, embedded software (software running on the io:bio mobile EEG prototype) and smartphone app software are next presented in detail.

3.3.1 Electronic hardware development

Acquiring EEG data from the scalp surface involves a number of signal processing stages. The ADS1299 makes use of high levels of integration of the signal processing stages to enable the creation of scalable medical instrumentation systems at lower power, smaller size and lower cost [95]. The use of three ADS1299 ICs formed the centre of a design capable of providing 24 channels at 24 bit resolution at 250 samples per second. Each ADS1299 device provides 8 differential channels and therefore a combination of 3 of these ICs provided the required 24 channels. The linking of these devices is not a trivial stage of the development, and the manufacturer's datasheet details two distinct methods of connecting the devices together (Figure 3.2):

1) **Daisy Chain Mode:** The DOUT pin of one device is connected to the DAISY_IN pin of the next device in the link, thereby creating a chain. Only one chip select pin is used for all of the devices.

2) **Standard Mode:** Each device has its own chip select connection and allows independent access to the IC and its registers.

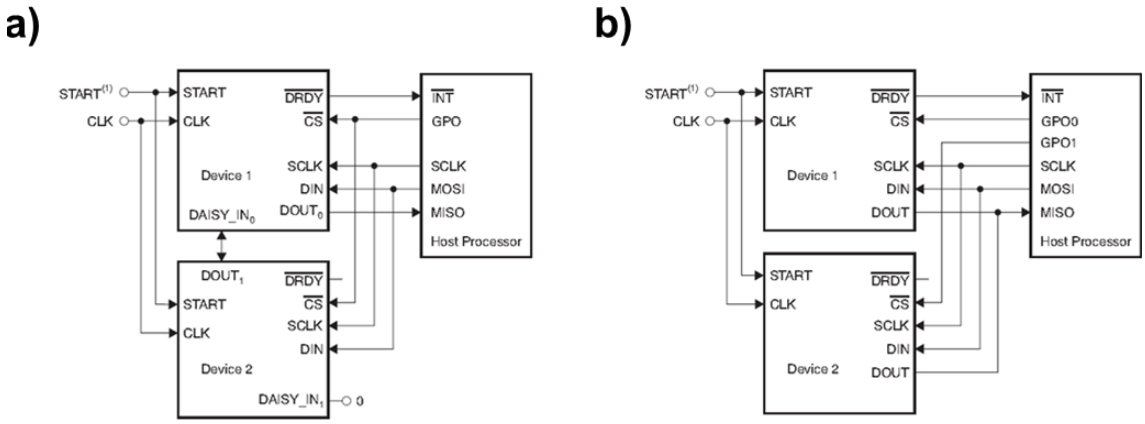

Figure 3.2 Multiple device configuration options: **a)** Daisy chain configuration and **b)** Standard mode configuration. Taken from Texas Instrument ADS1299 datasheet [95].

Both modes of connecting multiple devices together to provide more channels were constructed and tested. The daisy chain mode of connection was found to be inappropriate as it did not provide access to the register settings of each individual device (only the first device in the chain). Access to the register settings was required in order to be able to configure individual channel settings and gains. With a plan to include 19 EEG channels, and 5 differential channels to be used for ECG, EMG and/or EOG, having the same gain and channel settings would not have been viable since the amplitudes of the EEG signals are much lower than those of ECG, EOG and EMG. When using the daisy chain mode the sampled data forms a collective chain that comprises all of the channels data. However, one bit of data (always set to zero) is inserted in-between the data from each device. The resultant formatting of the data did not match up with the expected 8 bit packets of data normally used and thereby made data capture problematic. The standard mode of multiple device connection was thereby selected and the daisy chain mode was rejected.

In the standard mode of connection adopted, the three devices shared the same serial peripheral interface (SPI) bus connected to the microcontroller, but each device also had individual chip select pin connection. Connecting the three devices to a microcontroller in this manner facilitated individual reading and writing of register values, which in turn facilitated individual channel configuration. The three devices were synchronised by utilising an external clock signal to maintain synchronous sampling across the three devices.

The approach taken to selecting a suitable microcontroller was to consider the size, weight and power consumption aspects taken from the specifications of currently available microcontroller devices whilst ensuring the device was also capable of transferring the sampled data via a wireless local area network (LAN) module to a smartphone. An LPC1769 ARM processor [98] was selected as the microcontroller for the design as it provided low power consumption, a small physical footprint and has high processing performance relative to its size and power consumption. A RN131 wireless LAN module [99] was connected to the microcontroller via a serial connection (using the

RS232 standard) to provide a means of wirelessly connecting to a smartphone via a Wi-Fi link. The Wi-Fi link was further enhanced by using an omni-directional external antenna (Molex, USA) with a gain of 3.5 decibels (dB). The power supply and power management of the design were accomplished by using a MCP73871 power management IC [100] that allows battery powering of the system via a lithium-ion battery as well as charging of the battery through a universal serial bus (USB), when connected to a power source. The USB connection was also wired to allow firmware updating of the microcontroller to take place via In-Circuit Programming (ICP). The complete functional block diagram of the io:bio system is shown in Figure 3.3.

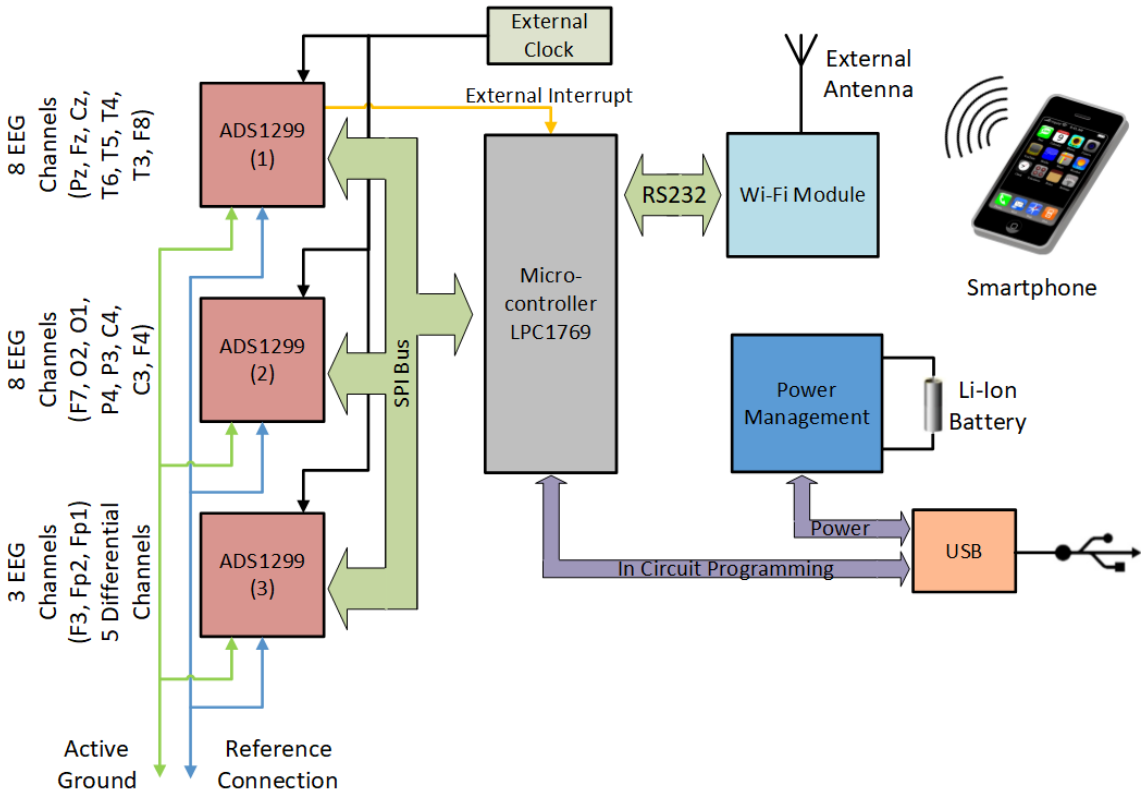

Figure 3.3 io:bio system functional block diagram showing the key sub-systems and their interconnections. The EEG channels, active ground and reference connections are labelled.

The printed circuit board design was produced using Xpedition printed circuit board (PCB) computer aided design (CAD) software (Mentor Graphics, Netherlands). The resultant PCB was populated with electronic components, and then housed in a commercially available aluminium case (Hammond Manufacturing, Canada). The case measured 43mm high, 78mm wide and 120mm deep, which is a reasonable size for a waisted-mounted mobile EEG system and comparable with the Micromed system that measures 44mm high, 83mm wide and 120mm deep at its extremes. The total weight of the io:bio mobile EEG system (including electronics and battery) was 338 g and the Micromed system weighed 250g. The case provided a robust housing for the io:bio mobile EEG system.

3.3.2 Embedded software development

The embedded software was written in the programming language C [101]. The manufacturer of the LPC1769 microcontroller (NXP, Netherlands) provided a software development environment called LPCXpresso [102], which utilised the C programming language, and was used for the embedded software development. In addition, an operating system was used to provide the software framework and hardware support needed for the EEG system. FreeRTOS is the market leading Real Time Operating System (RTOS), and a free-to-use de-facto standard solution for microcontrollers written in the C programming language [103]. It provided support for the chosen microcontroller (LPC1769) along with accompanying software libraries and example code. A command line interface (CLI) was available as a part of FreeRTOS, and Figure 3.4 shows the various layers and their associated communication paths.

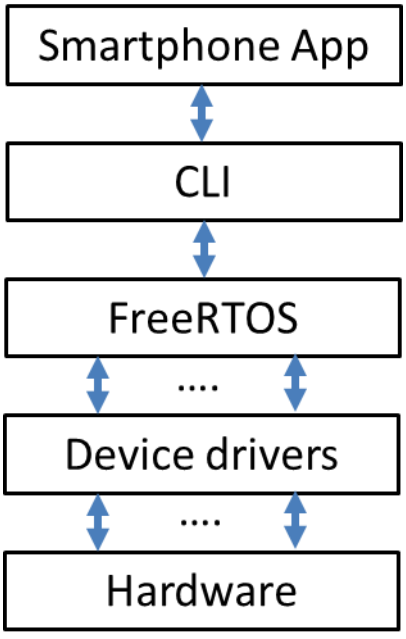

Figure 3.4 io:bio mobile EEG system layer diagram showing the various system layers and associated communication paths.

FreeRTOS was used to provide the system with the ability to perform certain tasks under instruction. The tasks included starting and stopping data acquisition, performing impedance checks and plotting live data. Tasks could be conveyed to the EEG system from any script language and therefore provided flexibility in ways in which the system could be controlled via a smartphone app or other methods.

Since the smartphone app was to be written at a later stage, alternative methods of testing the CLI were important to ensure correct performance. The CLI and the associated lower level functionality of the io:bio mobile EEG system was tested on a PC by connecting to it via a USB to serial lead, and running a terminal program [104]. This enabled the functionality testing of the embedded electronics and software to take place prior to developing the smartphone app and the associated UI. Each command used in the CLI had to be defined in software, and although many commands were written for testing purposes, only a small subset of these commands were actually used in the final version of the smartphone app software (Table 3.1). The testing was repeated with the wired link between the io:bio mobile EEG system and the PC being replaced by a Wi-Fi link.

Table 3.1 A list of the main CLI commands, their associated parameters and descriptions.

Command	Parameters	Description
`start`	Destination Encoding	Puts all ADS1299 ICs into constant conversion mode and sends the resultant data packets to the selected destination (1=internal SD card, 2=Wi-Fi link). The data will be uuencoded if the encoding parameter is set to 1 e.g. `start 2 1` sends uuencoded sampled data via Wi-Fi.
`stop`	Destination	Takes all ADS1299 ICs out of constant conversion mode and stops sending data packets to the selected destination (1=internal SD card, 2=Wi-Fi link) e.g. stop 2 stops sending sampled data via Wi-Fi.
`rreg`	ADS Register	Returns the value of the selected register from the selected ADS IC e.g. `rreg 2 1` returns the contents of register 1 from ADS 2.
`wreg`	ADS Register Value	Sets the value of the selected register in the selected ADS IC e.g. `wreg 2 1 1` writes the value 1 into register 1 of ADS 2.
`adcinit`	Mode	Configures all ADS1299 ICs according to mode (1=normal, 2= impedance check and 3=off) e.g. `adcinit 1` sets up all ADS1299 ICs in normal mode.
`cpureset`	None	Performs a software reset of the LPC1769 microcontroller.

3.3.3 Transmitted data packet structure

When data is read from the ADS1299 it is formatted as 24 status bits + 24 bits x 8 channels, giving a total of 216 bits (27 bytes). The format of the status bits is '1100' + LOFF_STATP + LOFF_STATN + bits 4 to 7 of the GPIO register (LOFF_STATP and LOFF_STATN are the lead off detection registers and not used). By limiting the status bits to one byte (the bits relating to LOFF_STATN and the GPIO register), a saving in data of 2 bytes per sample per ADS1299 device is achieved. Therefore, a packet structure was formed as follows:

(((8 status bits + (24 bits × 8 channels)) = 200 bits) × 3 ADS1299) × 6 samples = 450 bytes

The number of samples sent in a single packet of data was 6.

Since the data was being processed by the FreeRTOS CLI, steps had to be taken to ensure that the data was constrained to the 7 bit ASCII [105] character range in order to constrain the range to printable characters and avoid ASCII control codes. This was achieved by performing a form of binary to text encoding known as uuencoding (Unix to Unix encoding) on the data before transmission and then decoding it after reception. This approach increased the size of the data packet from 450 bytes to 600 bytes, and placed a data processing overhead at each end of the transmission.

The GPIO register bits that have been retained from the status bits indicate the logic level of the four GPIO pins of each ADS1299. The GPIO pins of each of the three ADS1299 ICs were wired to IO pins of the microcontroller, thus enabling the marking of data at a per sample resolution to take place. The first GPIO pin for the first ADS1299 was wired externally to a participant push button switch to allow event marking by participants.

3.3.3.1 File header structure

At the start of a data capture process, a header is transmitted from io:bio mobile EEG system to the smartphone; the same header is also logged at the start of the saved data file. This header contains information relating to the data file including the date and time it was created, sampling rate and number of channels. The complete header structure along with the size taken up in bytes of each data item can be found in Table 3.2. The information stored in the header is also used to reconstruct the sampled data into microvolt amplitudes from the output codes of the ADS1299's.

Table 3.2 Header data structure showing information stored along with size in bytes.

Data	Description	Size
EEG1.0	version number	6 bytes
Date and time	Year, month, day, hour, minute, second.	6 bytes
Samples per second	6=250 Hz, 5=500 Hz, 4=1 kHz, 3=2 kHz, 2=4 kHz, 1=8 kHz and 0=16 kHz	1 byte
No of channels	1 to 24	1 byte
Bytes per channel	set to 3	1 byte
Channels gains	3 bits per channel	3 bytes
Reserved for future development	set as '*' to indicate not being used.	9 bytes

3.3.3.2 Converting file structure to EDF+ structure

The European Data Format (EDF) is a standard file format designed for the exchange and storage of medical time series data [106]. An extension of the EDF file format (EDF+) was created in 2002 and as well as containing signal samples also can contain annotations, stimuli and events [107]. A signal in an EDF+ data record is composed of a series of 2-byte samples (16 bit), the subsequent samples representing subsequent integer values of that signal, sampled with equal time intervals. This data format was selected because the gold standard for comparison, the Micromed system, exports data in this format.

A Matlab script was coded to read in the data file and write out an EDF+ equivalent file. Relationship between input signal amplitude and output code are presented in Table 3.3. Since the Vref is 4.5V in this case, and the weight of the least significant bit (LSB) is equal to (2*Vref/Gain/2^24), the data output from the ADS1299's is converted to voltage using the following formula:

$$sample * (\frac{4.5}{gain})/2^{23}\ Volts$$

Table 3.3 Relationship between input signal amplitude and output code (hexadecimal). V_{REF} = 4.5 Volts. Modified from Texas Instrument ADS1299 datasheet [95].

Input Signal, V_{IN} (AINP –AINN)	**Ideal Output Code**
≥ V_{REF}	7FFFFFh
+V_{REF}/(2^{23}-1)	000001h
0	000000h
-V_{REF}/(2^{23}-1)	FFFFFFh
≤-V_{REF}/(2^{23}/2^{23}-1)	800000h

3.3.4 Smartphone app development

The smartphone app was developed using the Unity game engine [92]. The scripts for Unity were developed in a script language called C# [108]. The main thread utilising a state machine methodology to provide a structured approach towards the development and enable additional states to be added in the future should additional functionality be required (Figure 3.5). The states for 'updating hardware settings' and 'read ADS Statuses' have been included to facilitate future development. The ADS1299 has a set of registers that dictate its sampling rate and individual channel gain as well as other potentially useful settings. The capability to read and write these settings from within the app can be added at a later stage.

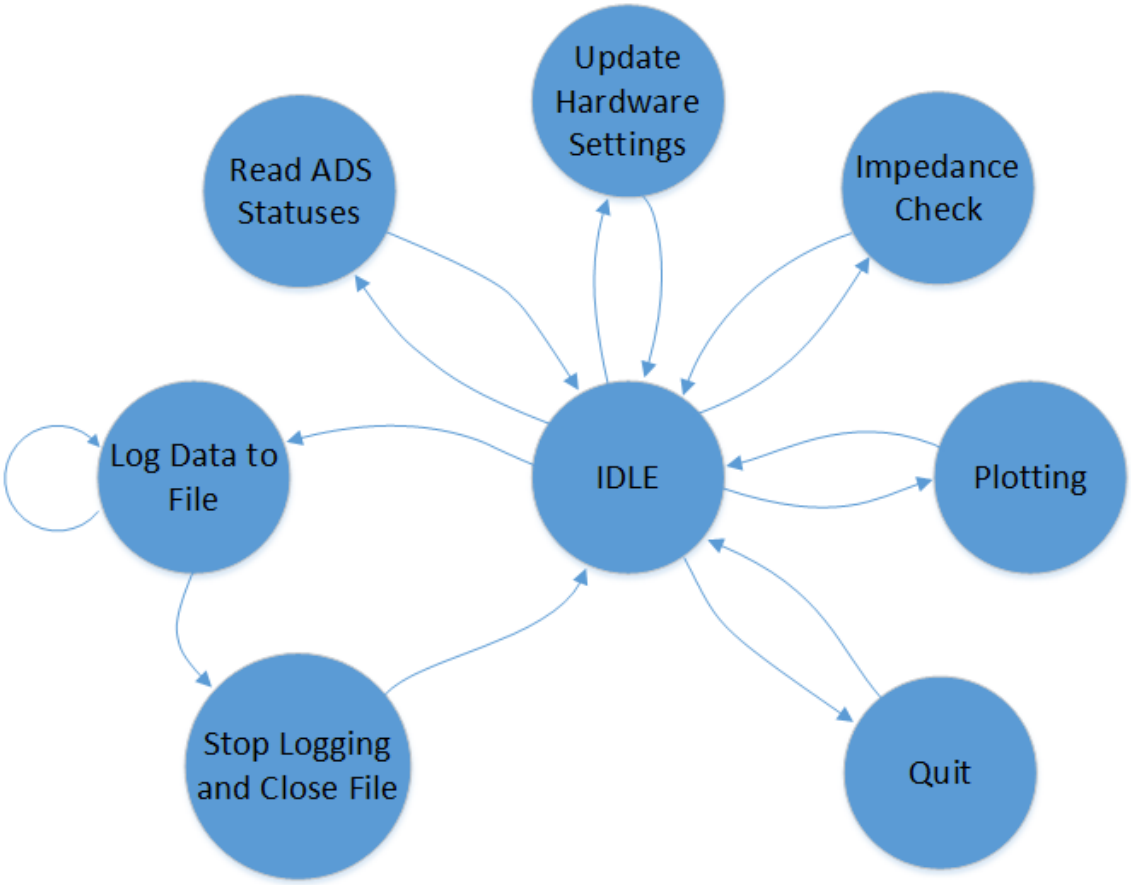

Figure 3.5 State diagram for the state machine used in the smartphone application development.

3.4 Testing the prototype

The testing of the io:bio mobile EEG system was divided into two stages. The first stage was performed using internally generated test signals only. The second stage was performed with a healthy human participant.

3.4.1 Internal test signals

EEGLAB is an open source interactive Matlab toolbox for plotting and processing EEG data that is commonly used in EEG research. Once accurate recordings of the test signal were plotted in EEGLAB, this first phase of testing was deemed successful. The test signals were generated in the ADS1299 ICs via a built-in channel input option. The datasheet of the ADS1299 [95] shows the register settings required to enable the test signal on each of the eight channels. The test signal takes the form of a square wave and as such has both a frequency and an amplitude. The datasheet provides details of register settings to set the frequency and amplitude based upon two options, these can be seen in the datasheet extract in Figure 3.6.

The datasheet states the signal amplitude, for the highlighted option, as:

$$\text{test signal amplitude (mV)} = 1*(\text{VREFP-VREFN})/2.4$$

Since the VREF is 4.5V the equation shows the amplitude to be as follows:

$$\text{test signal amplitude (mV)} = \frac{4.5 - (-4.5)}{2.4} = 3.75 \text{ mV}$$

The frequency of the square wave test signal was configured to be:

$$\text{test signal pulse frequency} = F_{CLK}/2^{21}$$

With F_{CLK} = 2.048 MHz the resultant test signal frequency should be:

$$\text{test signal pulse frequency} = 2.048\text{x}10^{6}/2^{21} = 0.977 \text{ Hz}$$

CONFIG2: Configuration Register 2

Address = 02h

BIT 7	BIT 6	BIT 5	BIT 4	BIT 3	BIT 2	BIT 1	BIT 0
1	1	0	INT_CAL	0	CAL_AMP0	CAL_FREQ1	CAL_FREQ0

This register configures the test signal generation. See the *Input Multiplexer* section for more details.

Bits[7:5] **Must always be set to '110'**

Bit 4 **INT_CAL: TEST source**

This bit determines the source for the Test signal.
0 = Test signals are driven externally (default)
1 = Test signals are generated internally

Bit 3 **Must always be set to '0'**

Bit 2 **CAL_AMP0: Test signal amplitude**

This bit determines the calibration signal amplitude.
0 = 1 × (VREFP – VREFN) / 2.4 mV (default)
1 = 2 × (VREFP – VREFN) / 2.4 mV

Bits[1:0] **CAL_FREQ[1:0]: Test signal frequency**

These bits determine the calibration signal frequency.
00 = Pulsed at f_{CLK} / 2^{21} (default)
01 = Pulsed at f_{CLK} / 2^{20}
10 = Not used
11 = At dc

Figure 3.6 An extract from the manufacturer's ADS1299 datasheet showing the configuration register that controls test signal settings and parameters (CONFIG2). Highlighted text shows selected parameters (yellow colour). Taken from Texas Instrument ADS1299 datasheet [95].

3.4.2 Participants

The participant completed a health questionnaire and consent form prior to participation, and was healthy with no history of neurological disorders. Hull York Medical School's Ethics Committee provided ethical scrutiny and approval for the research. Recordings of 10 minutes were taken while the participant was seated to provide optimal conditions for artifact-free EEG recordings, therefore if any problems were encountered they would be most likely attributable to design or construction errors. All 19 EEG channels of the Softcap (SPES Medica, Italy) were used in the test recording and the resultant data file converted to EDF+ format. The conductive electrode gel used was Neurgel (SPES Medica, Italy). The ground electrode was located at AFz and the reference electrode was located at the right ear.

3.5 Results

The results for this chapter include the completed state of the prototype smartphone-based io:bio mobile EEG system and are presented as follows: Firstly, the enclosure of the prototype along with its various connections and components; secondly, the CLI and its command set functionality upon which the app development makes use, and finally, the smartphone app and functionality. The results also include the internally generated test signal, and EEG signals from a single participant.

3.5.1 First prototype of the smartphone-based mobile EEG system

The finished version of the first prototype of the io:bio smartphone-based mobile EEG system is seen in Figure 3.7. Connection to a standard 10/20 electrode cap is provided by a 25way D-type connector and its wiring is detailed in Figure 3.8 and Table 3.4. Each electrode is connected to one input of a differential amplifier (one amplifier per pair of electrodes); a common system reference electrode is connected to the other input of each differential amplifier internally.

Figure 3.7a shows the connection for the electrode cap via the 25 way D-type connector, as well as the touch-proof connectors (as used in the Micromed system) for the differential channels, reference electrode and active ground connections (see Table). Figure 3.7b shows a connector for an external participant push button which provides participant induced data markers. Figure 3.7c shows the location of the external Wi-Fi antenna, positioned beneath a layer of sticky-backed foam rubber used to protect the antenna.

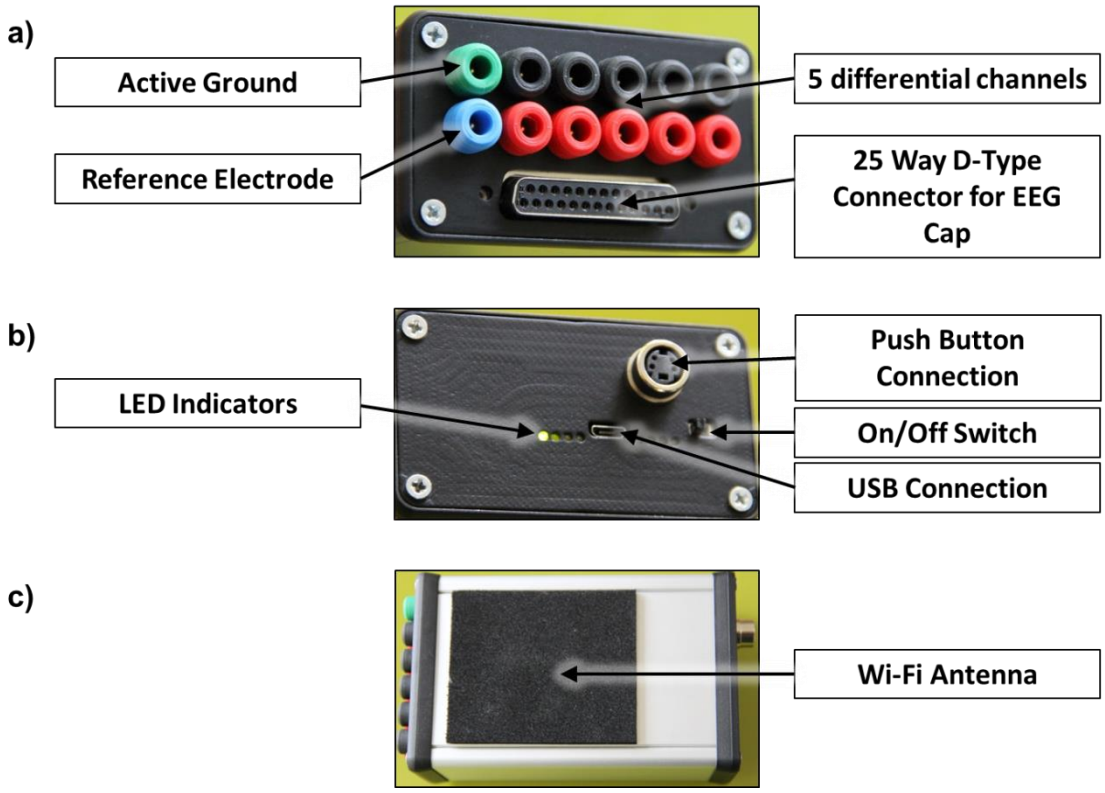

Figure 3.7 Photographs of the io:bio system detailing **a)** top panel connections (active ground, reference electrode, differential channels and EEG cap), **b)** bottom panel connections (USB, and event marker push button), LED indicators (from left to right are power, charging, connection status and data activity) and On/Off switch, and **c)** Wi-Fi antenna (located under the rubber foam pad).

Table 3.4 Pin out of the electrode cap connector.

Pin	Electrode	Pin	Electrode	Pin	Electrode
1	FP1 – Brown	11	N.C.	21	T6 – Grey
2	F3 – Red	12	N.C.	22	CZ – White
3	C3 – Orange	13	N.C.	23	PZ - Black
4	P3 – Yellow	14	FP2 - Brown	24	N.C.
5	O1 – Green	15	F4 – Red	25	N.C.
6	F7 – Blue	16	C4 – Orange		
7	T3 – Pink	17	P4 – Yellow		
8	T5 – Grey	18	O2 – Green		
9	GND – White	19	F8 – Blue		
10	FZ - Black	20	T4 – Pink		

N.C. = not connected.

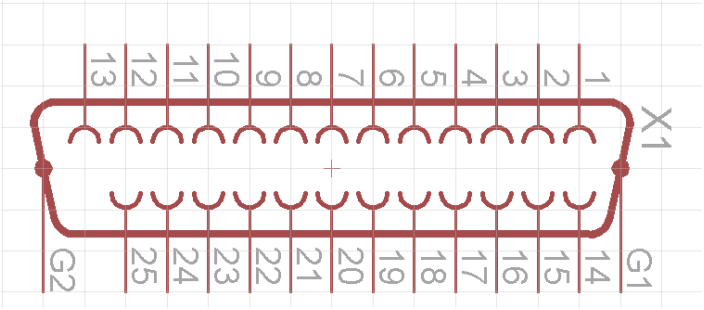

Figure 3.8 Pin labelling of the 25 way D type connector used for EEG electrode cap connection.

3.5.2 Command line interface testing

The development of the CLI was an important intermediate step used to check functionality of the EEG system, including commands, and data acquisition, prior to the development of the smartphone app. The methodology for the development of the smartphone app was to provide the commands (or sequence of commands) via a graphical user interface. Recording data issues a 'START 2 1' command in order to put all ADS1299 ICs into constant conversion mode and initiate the sending of the resultant data packets to the selected destination (2=Wi-Fi link). An example screenshot of the CLI in operation can be seen in Figure 3.9.

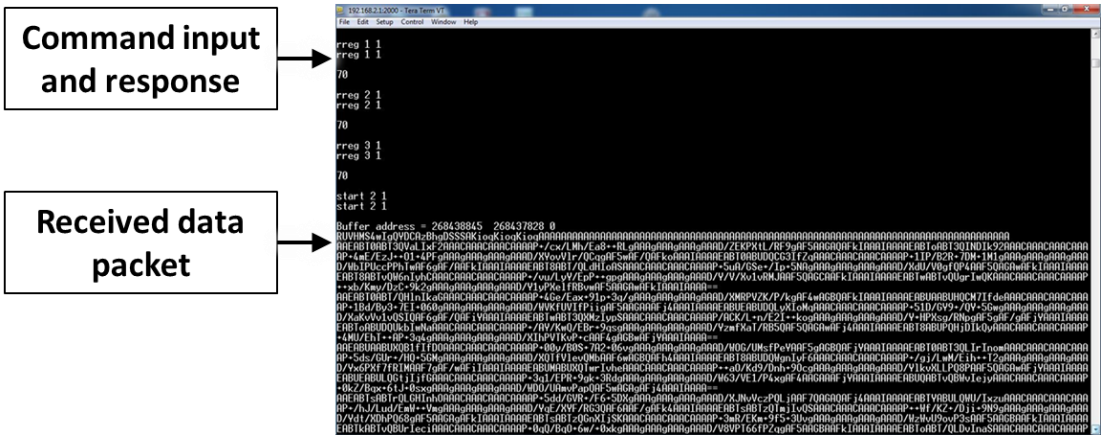

Figure 3.9 io:bio EEG system testing by means of its CLI through a terminal program running on a PC linked via Wi-Fi.

3.5.3 Test signal reconstruction

To test the io:bio prototype using the ADS1299s internally generated test signals, a recording was made on the smartphone, the resultant file converted to EDF+ format and then plotted in EEGLAB. A basic version of the smartphone app was used for this testing stage, and consisted of only starting and stopping a recording.

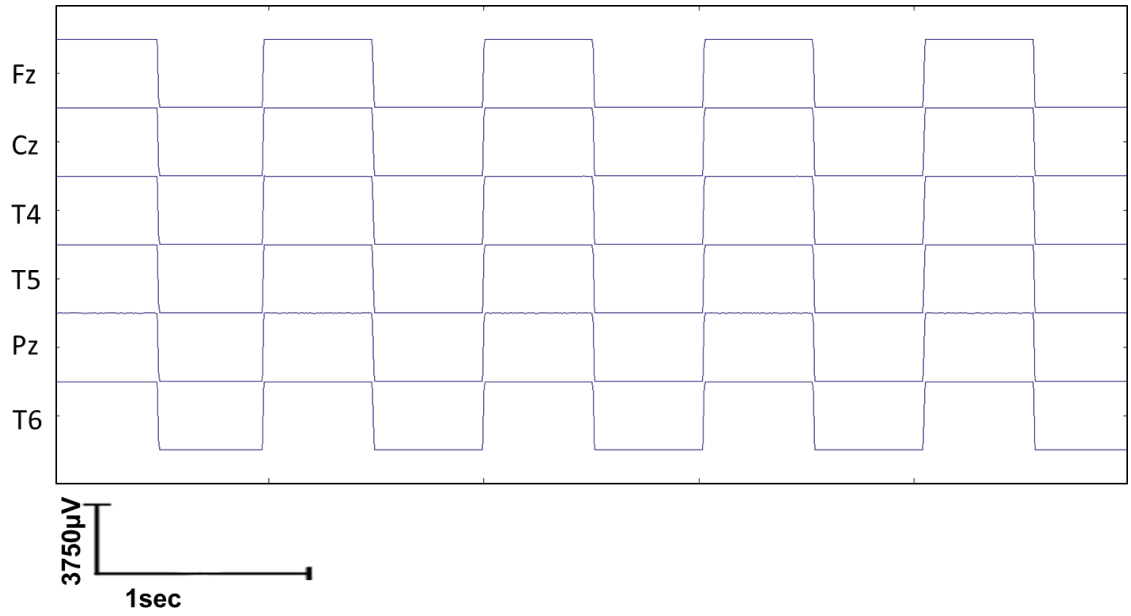

Figure 3.10 Test signals generated internally at 3.75mV. Fz gain = 1, Cz gain = 2, T4 gain = 4, T5 gain = 6, Pz gain =8 and T6 gain = 12.

Amplitudes of 3.75mV were recorded for all 6 channels and correspond with the expected amplitude (see Figure 3.10). The frequency is less than 1 Hz and matches with the expected frequency of 0.977 Hz. The test shows the gain calculation is working correctly and that the data path from the ADS1299 ICs through to the Matlab script to convert the recorded data into EDF+ format works correctly. Different gains were used for each channel to shows that gain is correctly used in the calculations relating to signal amplitude.

3.5.4 Smartphone app

The app was coded to provide impedance check, live data plotting and data recording features as a minimum set of options a researcher is likely to require. The impedance check is important during the electrode cap gelling stage of the participant setup, and provides a visual indication of the level of impedance for individual electrodes. The live data plotting is useful to check that the signals being captured are acceptable, and in the case of the differential channels of the correct polarity.

The impedance check feature provides an approximate indication of the impedance of all 19 EEG electrodes via a diagrammatic representation of the electrodes in a 10/20 standard EEG electrode configuration (Figure 3.11a). When the impedance of an electrodes connection exceeds 8kΩ the corresponding electrode on the diagram changes to red. However, when the impedance of an electrode connection to the scalp is less than 3kΩ, the corresponding electrode on the diagram is green. The intermediate range of 3kΩ to 8kΩ is indicated by the corresponding electrode on the diagram as amber.

The live data-plotting feature displays the channels in groups of eight that can be cycled through to provide a means of visually inspecting signal quality (Figure 3.11c). This feature was important to provide reassurance that EEG data quality was of an acceptable level prior to data recording. The data recording feature records the received EEG data to the smartphone. Every block of received data is indicated by an incremental count on the smartphone; time duration of the recording is also displayed (Figure 3.11b). This enables a loss of data to be detected by the researcher, as in such a case the time count would advance, but the received data count would not.

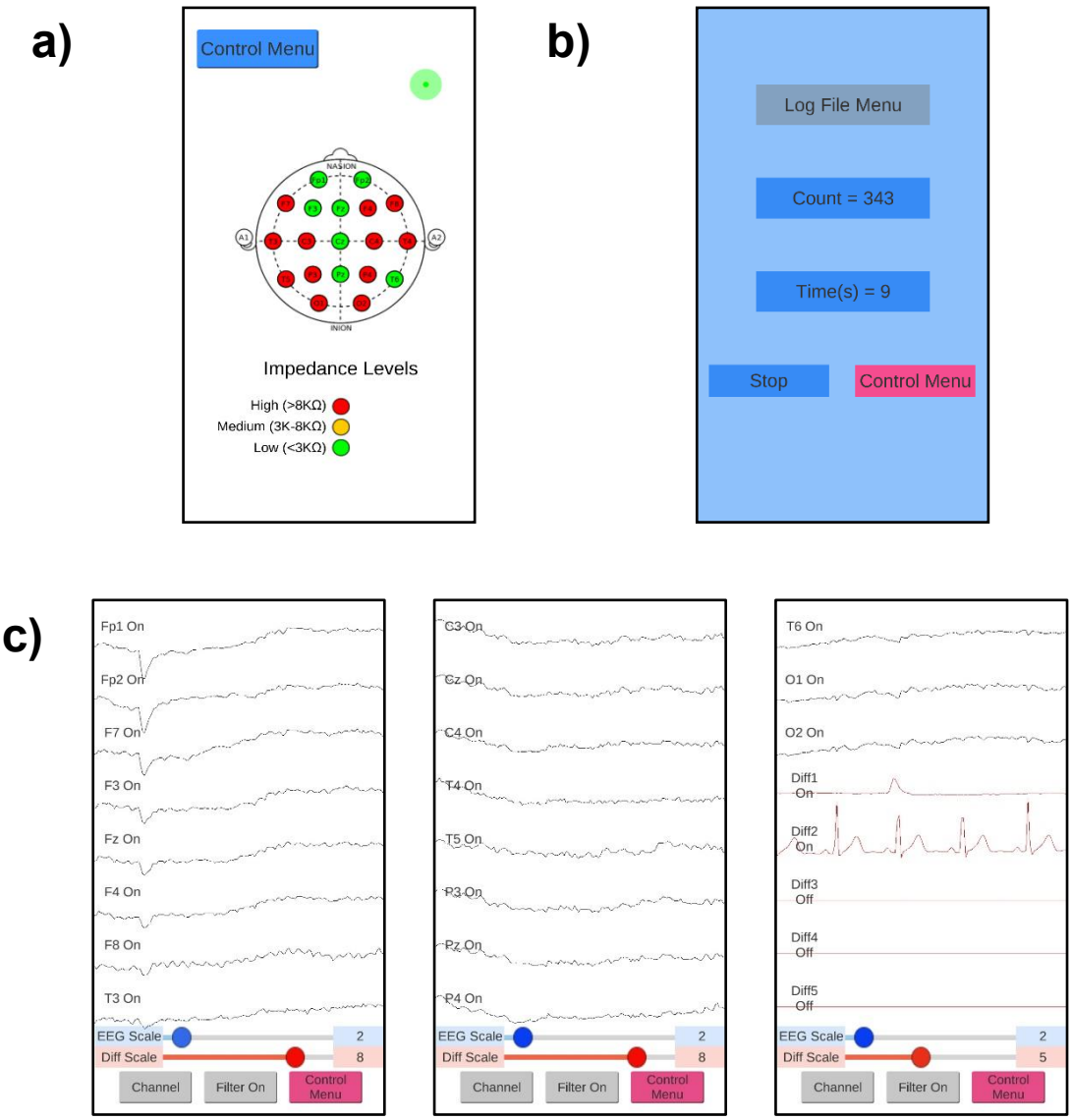

Figure 3.11 Smartphone app showing **a)** impedance checking, **b)** data recording and **c)** live data plotting (high pass filtering 0.1 Hz) of 19 EEG channels , an EOG channel (differential channel 1) and an ECG channel (differential channel 2). Note that a blink artifact is visible in the frontal EEG electrodes.

19 channels of EEG were successfully recorded from a seated participant. The data file was converted into an EDF+ file format and loaded into EEGLAB. Figure 3.12 shows a section of the successfully plotted EEG data.

3.5.5 Plotting participant data in EEGLAB

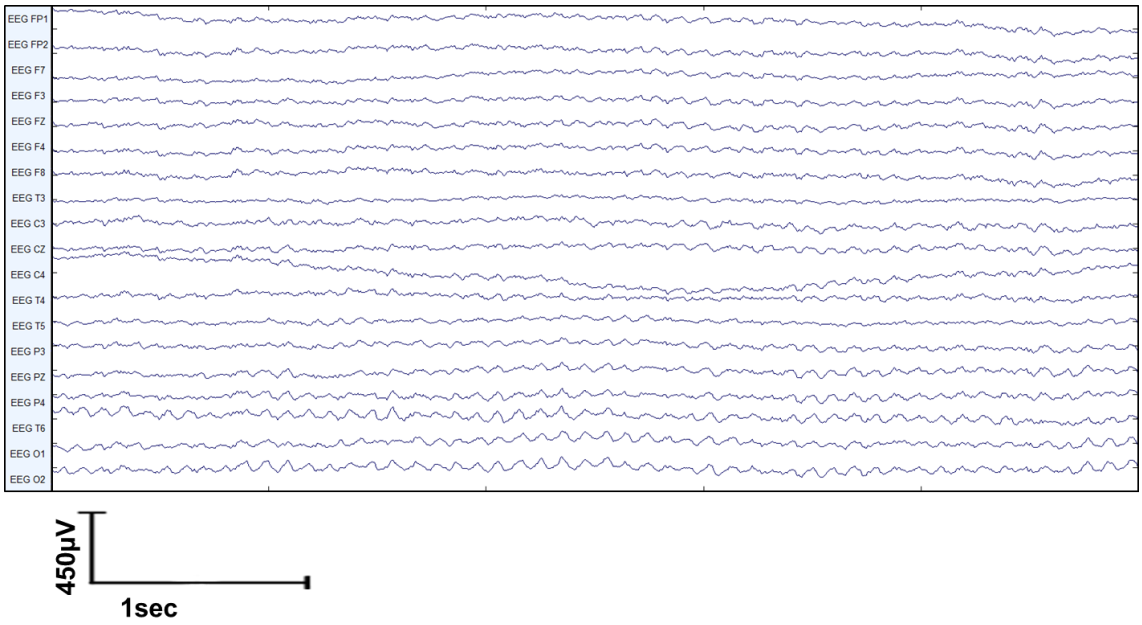

Figure 3.12 EEG data recorded using the io:bio prototype with a seated participant (eyes closed). Data converted to EDF+ file format and plotted in EEGLAB. Channels are displayed with FP1 at the top, down through to O2 at the bottom.

3.6 Discussion

This chapter has demonstrated the successful fabrication of a waist-mounted mobile EEG system (io:bio) with the specification to record 24 channels (19 EEG and 5 differential) at a resolution of 24 bit with a sampling frequency of 250 Hz onto a smartphones SD card via a Wi-Fi link. The smartphone app facilitates recording and plotting of live data, as well as impedance measurements of electrodes at the scalp surface. A Matlab script was produced to write the recorded EEG data to an EDF+ file format for subsequent loading into EEGLAB [109]. This enabled io:bio system data recordings to be readily analysed using an established research analysis platform and expedite the data capture and analysis process.

The CoME scheme shows where the io:bio smartphone-based mobile EEG system fits within the context of the current literature and this is visualised in Figure 3.1. This figure indicates, that the io:bio system has higher CoME scores (2D,3P,11S,24C) compared to most of the published mobile EEG studies for participant mobility and device mobility. An exception is the study by Askamp *et al.* [55] using the Mobita mobile EEG system which had a higher CoME score of (2D,4P,17S,32C).

Although the CoME scheme covers many design attributes of the io:bio system the type of wireless technology utilised is not one of them. The io:bio system utilises Wi-Fi technology for the wireless link between the acquisition electronics and the smartphone. Blum *et al.,* used a Smarting EEG system in combination with a smartphone to form a BCI system [110]. The wireless link between the smartphone and the acquisition electronics used Bluetooth technology. Other studies that have used a smartphone in conjunction with an EEG system have also used Bluetooth technology. Wi-Fi allows peer-to-peer connection (EEG to smartphone) without additional infrastructure. Wi-Fi can also be used to connect to network infrastructure in a hospital, home or research facility and thus enable cloud storage and processing. This is a clear advantage over Bluetooth technology in terms of future research possibilities

relating to clinical and home monitoring applications. Furthermore, Bluetooth has a restricted range which in the case of the SMARTING system is 10 metres. The data rate is generally much lower than Wi-Fi and is also less energy efficient [111].

It should be noted that the io:bio mobile EEG system (see Figure 3.1) has the potential for improvement in scores for device mobility. For example, there is the potential to improve device mobility scores from a waist-mounted (1-2D) configuration to a head-mounted (3-5D) one. In addition, there is the potential for the io:bio system to be utilised in participants where a greater degree of movement is required, for example during constrained (participant CoME score of 2P) or unconstrained (score of 3P) walking.

Another section of the io:bio system, the smartphone app was designed and coded so that it would partner with the EEG system hardware via a Wi-Fi link. The app functionality was purposely restricted to impedance checking, live plotting and data recording as these functions were regarded as the core functions required. Limiting the first version of the app to core functionality has facilitated ease of use of the system whilst also providing the opportunity for future expansion. Unity was used to develop the app and although it is a game engine, it is not restricted to producing games and allows projects to be deployed to a range of platforms which includes smartphones. The features in Unity include support for UI development which was required for the app design. By using Unity to develop the smartphone app, it allowed for the potential of deploying the app to other platforms such as virtual reality (VR) and augmented reality (AR) headsets, PCs, games consoles and smartTVs. Such an array of potential platforms could be used to form neurofeedback systems [74,83,112], gamification projects [113-115], and BCI testbeds [116,117].

The io:bio mobile EEG system next requires validation against a commercial grade mobile EEG system and this will be undertaken in the next chapter.

3.7 Conclusions

In this chapter, a waist-mounted smartphone-based mobile EEG system, known as io:bio, was designed, built and initially tested. The io:bio system and associated app is able to record 24 channels (19 EEG and 5 differential) at a resolution of 24 bit with a sampling frequency of 250 Hz onto a smartphones SD card via a Wi-Fi link. The design specification was defined with the aid of the CoME scheme and has the potential score for participant walking of (2D, 3P, 11S, 24C).

Chapter 4: Validation of a novel smartphone-based waist-mounted mobile EEG system

4.1 Introduction

All medical devices require validation to ensure that they measure correctly and accurately [118,119]. Many medical devices produce an absolute single measurement, for example blood pressure [120]. In such cases the validation process can be reduced to a comparison of values and a statistical method then applied to ascertain significance. However, in the case of EEG, measurements are a series of data taken over time and with many electrodes. The process of validating such recordings is less obvious as no single value is available for comparison. Since EEG data exhibits large variability between participants and occasions [121], validation would ideally be undertaken by connecting both EEG systems to the electrode cap simultaneously. However, this is not practical as electrode caps are designed to be connected to only one system at a time. There is also the concern that with two systems connected to a single electrode head cap at the same time via some form of signal splitter, interaction between them may occur.

Comparing two mobile EEG systems by taking recordings sequentially in time is an alternative to connecting the systems to a cap simultaneously. The drawback with recordings made sequentially is that brain activity changes over time and such changes are difficult to differentiate from systematic differences (bias toward one system resulting from predominantly higher, or lower, values obtained from that system). The degree to which the brain activity changes across sequential recordings could be mitigated if participants were engaged in a protocol which promoted a clear predictable signal in the EEG recordings. This would reduce the likelihood of changes in brain activity being a source of any difference found. This can be achieved by selecting a participant stimulus and task combination to provide such an EEG signal response. Gasser *et al*., stated that the alpha band has the best test-retest reliability compared with other EEG bands, and therefore can be considered as an intra-individual stable state [122]. By focusing upon the alpha band for EEG data analysis, intra-individual repeatability should be obtainable using mobile EEG systems. Application of power spectral density analysis in the frequency range of the alpha band (8 to 13 Hz) would

provide the peak amplitude, the frequency at which this peak occurs, and area under the curve. These quantitative measures derived from the EEG time series would enable statistical comparisons between recordings from both the Micromed and io:bio EEG systems to be undertaken. Bazanova *et al*., found that intra-individual correlation coefficient (ICC) was strongest in the posterior brain area with eyes closed and weakest in the anterior areas with eyes open [123]. Furthermore, Goljahani *et al*., reported that the alpha band peak amplitude, during eyes closed, dominates the EEG spectrum [124]. Periods of participants lying down with eyes closed provide an ideal protocol to capture a distinct peak within the alpha frequency range [125]. By including more than one period of participants lying down with eyes closed in a protocol, intra-system and inter-system variability can additionally be investigated. This would enable a measure of intra-system agreement (repeatability) in each mobile EEG system as well as inter-system agreement (validity).

A test of significance identifies when two methods (of recording EEG data) are related, but it does not quantify agreement between them. Furthermore, usually a paired t-test will have a null hypothesis that states there is no difference, and a hypothesis that a difference exists. In the current context, the opposite is the case with the null hypothesis being that a difference exists and the hypothesis that no difference exists between the two systems. This presents a potential problem when applied in the current context as the Bonferroni correction reduces the likelihood of a difference being found, and therefore an additional approach was sought to overcome this potential criticism. The agreement between metrics extracted from EEG data recorded from the same group of participants using two different systems can be quantified using differences between the observations. Bland and Altman proposed a graphical method to compare two measurement techniques [126], that incorporates the difference of individual measurements between the two systems by plotting these against the mean of each paired measurement. The inclusion of 95% limits of agreement (derived as mean difference ±1.96 standard deviations (SD) of the differences), provides limits in which 95% of the measurements should lie. When considering a Bland-Altman plot, it is important to be mindful that this method only defines the intervals of agreement between the two systems, it does not ascertain if those limits are acceptable within

the specific research context [127]. If the differences within the mean ± 1.96 SD are not contextually important, then the two systems can be used interchangeably.

The approach to statistically validating the io:bio mobile EEG system is not obvious since there are only a few published studies that have validated an EEG system against a gold standard [128-130]. In the three studies published, each involved some form of correlation analysis. However, correlation examines the relationship between one variable and another, not the differences between them, and it is not recommended as a method for assessing the comparability between measurement instruments [131]. An alternative approach to validating the io:bio mobile EEG system would be to perform a paired t-test (with Bonferroni correction for multiple comparisons due to 19 EEG channels) on values for alpha peak frequency, amplitude and area under the curve for the alpha band (8 to 13 Hz). However, when using a paired t-test information is lost regarding individual measurement differences, and although a test of significance identifies when two methods (of recording EEG data) are related, it does not quantify agreement between them [126]. Moreover, the application of a Bonferroni correction in the current context increases the likelihood of the null hypothesis (h_0 = that a significant difference between measures exists) being rejected. In addition to the paired t-tests an alternative statistical approach was sought to investigate individual differences in measures which are not assessed when performing a comparison of means. Interestingly, Kassab *et al*., [132] tested two EEG systems (Neuroscan SynAmps2 EEG/EP system versus a novel in-house system) using a Bland-Altman statistical analysis approach.

Bland and Altman proposed a graphical plot which displays the difference scores of two measurements against the mean for each subject and argued that if the new system agrees sufficiently well with the old system, it may be replaced with the new one[126]. This statistical method incorporates the difference of individual measurements between the two systems by plotting these against the mean of each paired measurement. The Bland-Altman plots have been used to compare two systems in clinical [133] and non-clinical contexts [132]. The Bland-Altman plot also evaluates bias

between the mean differences and thus indicates if a systematic bias toward one system is evident.

The aim of the present study is to validate a research quality, waist-mounted smartphone-based mobile EEG platform with healthy human participants against a clinically (FDA) approved commercial EEG system (Micromed) as the gold standard for comparison. Periods of participants lying down with eyes closed will be recorded with both mobile EEG systems. Alpha peak amplitude, frequency and area under the curve (AUC) are to be derived from power density analysis. Intra-system and inter-system comparisons of the alpha peak parameters will be determined to inform on each systems repeatability and the io:bio mobile EEG system's validity. Paired sample t-tests will be used to perform a test of significance. Bland Altman plots will be generated and utilised to make a statistical assessment of the io:bio system for intra-system and inter-system comparisons.

4.2 Methods

To validate the data recordings made by the developed io:bio system, a gold standard mobile EEG system was used for comparison. In addition, a convenient participant setup was essential, so that mobile EEG systems could be exchanged without disturbing electrodes and their connection to the scalp surface.

4.2.1 Gold standard mobile EEG system

A commercially available waist-mounted EEG system was selected as the gold standard for comparison (Micromed, Italy) that stores its data to a compact flash card that can then be loaded into a PC and is shown in Figure 4.1. It was connected to a 19 channel electrode cap that used the 10/20 system for electrode positioning, via a 25-way connector. The design of the prototype enabled it to be connected to the same electrode cap, thus enabling easy and convenient EEG system exchange during a validation study, without disturbance to the electrodes which could result in changes to the impedance of the connections to the scalp surface. An EEG cap with 20 tin electrodes was used with 19 electrodes conforming to the international 10/20 standard, and a ground electrode connection. Both systems were mounted on the participant via a waist-mounted harness and connected to the EEG cap as shown in Figure 4.2a (Micromed) and Figure 4.2b (io:bio).

Figure 4.1 Micromed mobile EEG system, defined as the gold standard system [134].

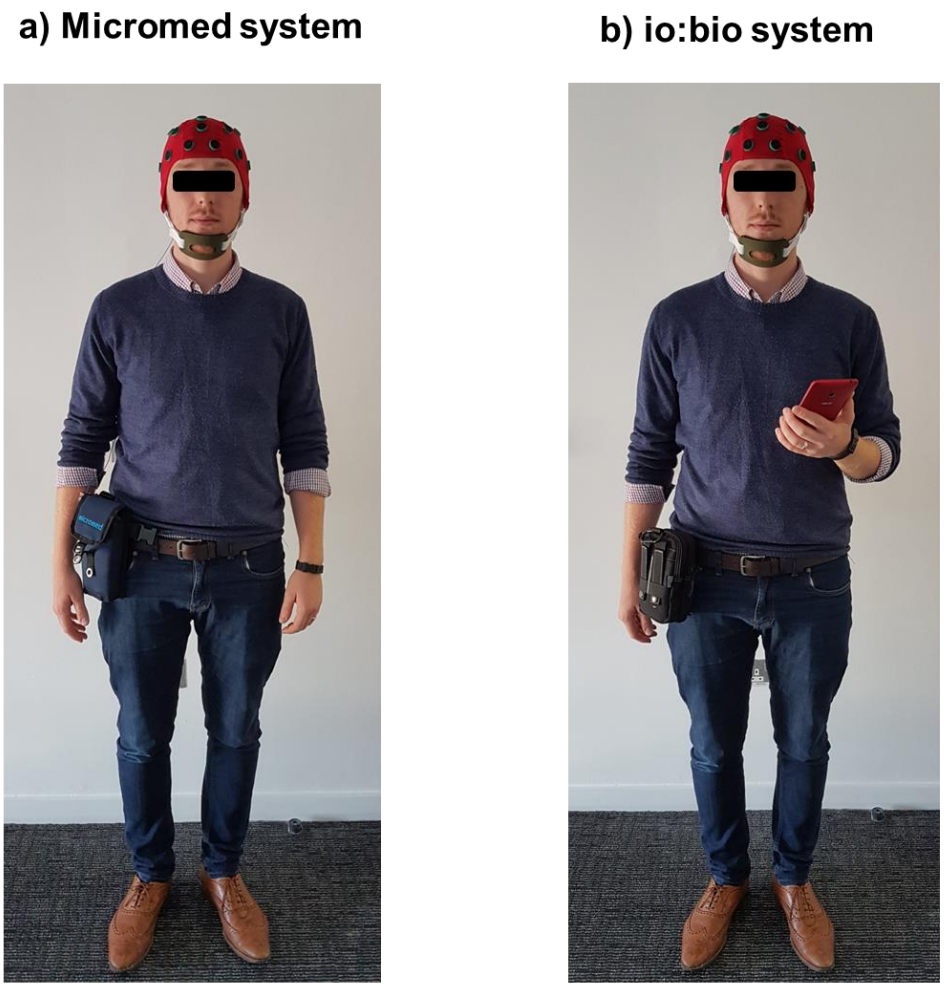

Figure 4.2 Participant wearing **a)** the Micromed system (left) and **b)** the io:bio system (right).

4.2.2 Participants

Twenty-one participants were recruited (range 18 to 55 years, mean ± standard error of the mean (SEM) age 35.4 ± 3.1, 5 males and 16 females), and all completed a health questionnaire and consent forms prior to participation. All participants were healthy with no history of neurological disorders. The Hull York Medical School Ethics Committee provided ethical scrutiny and approval for the study. The EEG cap used was a Softcap by SPES Medica with the ground located at AFz.

4.2.3 Experimental procedure

The experimental procedure consisted of two parts: firstly, the measurement of the electrical noise floor of each system, and secondly, the participant protocol for the validation process.

4.2.3.1 Measuring the electrical noise floor

Only signals that are greater in amplitude than the electrical noise floor of the EEG system used to record them can be measured with any degree of certainty. Hence, quantifying the electrical noise floor of an EEG system is important. A measure of the underlying noise level of each EEG system was obtained by recording a channel, with the inputs short-circuited to the active ground. The recordings were taken at the same time, with the two systems placed next to one another, so that they were exposed to the same potential sources of interference.

4.2.3.2 Participant protocol for validation of io:bio EEG system

The electrode wells of the EEG head cap were filled with conductive gel (Neurgel, SPES Medica, Italy) and the impedance was kept below 5kΩ to maintain signal quality. All scalp electrodes were referenced to the right ear. Data recordings were converted to EDF+ file format for both systems and imported into EEGLAB [109]. The sequence in which the mobile EEG systems were tested was pseudo-randomised for each participant so as to mitigate for potential ordering effects. The testing of the second system was performed within 30mins of the first system.

When the io:bio system was under test, the accompanying smartphone (Asus Zenfone 2) was placed on a bench in a central location in the laboratory rather than asking the participant to carry it, to maintain consistency with the Micromed system which does

not use a smartphone. The participants were guided through a protocol of activities via a PowerPoint presentation with accompanying audio instructions for each of the two systems under test. The protocol consisted of periods of ‘eyes open’ and ‘eyes closed’ in different postures as detailed in Table 4.1. This approach was used to maintain consistency of instructions across participants. Three consecutive intervals of lying down (participants were inclined to an angle of 45° whilst supine on a clinical examination couch) with eyes closed were recorded for each participant using each system. The first period served to acclimatise the participant. The remaining two periods are referred to as period 1 and period 2 respectively, and were used for the intra-system and inter-system comparison studies.

Incremental posture changes from lying down, to sitting, standing , standing with arms raised and walking were incorporated within the participant protocol, to compare how both systems coped with posture changes during EEG recordings. The walking section of the protocol was included to provide a challenging condition for EEG recording in terms of electrode displacement artifacts.

Table 4.1 Timeline of participant protocol detailing sequential participant postures with eyes open or closed, and the durations.

Participant Postures	Eyes	Duration (sec)
1. Lying Down		
Acclimatisation Period	Closed	20
	Open	20
Period 1	Closed	60
	Open	60
Period 2	Closed	20
	Open	20
2. Sitting		
	Open	20
	Closed	20
	Open	20
3. Standing		
	Open	20
	Closed	20
	Open	20
4. Standing Arms Raised		
	Open	15
	Closed	15
	Open	15
5. Slow Paced Walking		
	Open	60

4.2.4 EEG data analysis methodology

Analysis of the recorded data was achieved via Matlab scripts that made use of EEGLAB functions. The types of analysis consisted of power spectral density (PSD) and AUC techniques. Band pass filtering was performed on the recorded data (0.5 to 40 Hz) to remove unwanted high frequencies and baseline wander. The quantitative measures of alpha peak frequency, and amplitude and AUC for the alpha band were used for statistical comparison. The alpha band AUC in the current context was defined to be the alpha band power (area under PSD 8 to13 Hz) divided by the EEG power in the spectral range 2 to 30 Hz. These three data parameter values (for each individual, for periods 1 and 2), were used for evaluating the performance of the developed io:bio mobile EEG system compared to the gold standard Micromed system.

4.2.5 Statistical analysis

Often, metrics extracted from group EEG data, such as spectral peaks and area under the curve relating to specific frequency bands (theta, alpha, and beta), are used to perform a paired t-test [135-137]. It was therefore also applied in the current context, as an initial analysis step. Group mean alpha peak amplitude, frequency and AUC values were extracted from EEG recordings made using both the Micromed and io:bio systems, for periods 1 and 2 of participants lying down with eyes closed. A paired t-test was performed between the extracted metrics from periods 1 and 2 and for all 19 channels, providing intra-system comparisons for both systems. Paired t-tests were also performed between period 1's recorded on each system, and again for period 2's recorded on each system to provide inter-system comparisons. Since each individual paired t-test was repeated for all 19 channels, a Bonferroni correction was applied to correct for multiple comparisons i.e. p value = 0.05/19=0.002632.

Bland-Altman plots study the mean difference, and construct 95% limits of agreement. The limits of agreement defined in this way do not comment whether the limits are acceptable or not, so they must be defined *a priori*, based upon judgement of the context, such as clinical importance, and not statistical importance [126]. In the case of EEG, and more specifically the alpha peak (amplitude and frequency), it is relevant to know what factors can result in intra-individual variations that are biological in nature, and not generated by the EEG system, if acceptable limits of agreement are to be defined *a priori*. The prior decision on acceptable limits of agreement was made whilst considering a number of factors; firstly, Bazanova & Vernon [123] indicated that a plus or minus 2–2.5 Hz variation in association with intra-individual peak alpha frequency is to be expected. Secondly, intra-individual variability of the alpha peak amplitude can be affected by cognitive task involvement [138,139]. Thirdly, the alpha band increases in amplitude in relation to an increase in electrode-to-scalp impedance [140-142]. Finally, any developed mobile EEG system should have limits of agreement that are comparable to those of a gold standard mobile EEG system performing the same measurements and

under the same conditions. These points were then rationalised to generate the following *a priori* parameters:

1. The alpha peak frequency recorded from both systems, when comparing intra-system (i.e. period 1 of participant lying down with eyes closed against period 2 of the same participant lying down with eyes closed), should have limits of agreement that are within ± 2.5 Hz to demonstrate repeatability in each system while allowing for natural biological variations that are known to occur.

2. The alpha peak frequency recorded from both systems, when comparing inter-system (i.e. period 1 of participant lying down with eyes closed recorded using the Micromed system against period 1 of the same participant lying down with eyes closed recorded using the io:bio system, and again for period 2), has limits of agreement that are larger than the previously stated ± 2.5 Hz. The justification for increasing the limits of agreement are that the mean of each system is unlikely to be the same, and this will therefore add to the overall differences between the two system EEG recordings. Consequently, the limits were increased and set to ± 3 Hz.

3. The alpha peak amplitude recorded from both systems can vary according to impedance changes as well as unintended cognitive task involvement. Even though the same cap is used for both mobile EEG systems, the electrode impedance can still change as a result of participant movement. Neither cognitive task involvement nor electrode impedance variations can be controlled by the mobile EEG system and it is thus difficult to quantify acceptable limits of agreement when they are considered. As a result, it was decided that the io:bio system's intra-system comparison of amplitude limits of agreement should not be greater than those obtained for the gold standard system (Micromed). The inter-system comparison would be expected to have wider limits of agreement and therefore a limit of twice that of intra-system limits of agreement was selected.

4. The AUC of the alpha band recorded from both systems is largely affected by the same factors as the alpha peak amplitude, i.e. impedance changes as well as cognitive task involvement, and therefore the limits of agreement have been assessed in a similar manner.

5. The limits of agreement for intra-system comparisons for the io:bio system are to be less than or equal to those of the gold standard system (Micromed).

As well as for periods of participants lying down with eyes closed, Bland-Altman plots were also generated for sitting, standing, and standing with arms raised while participants had their eyes closed. Alpha peak frequency, amplitude and alpha band AUC were extracted from EEG recordings made with each system. The aim here was to identify differences in the Bland-Altman plots generated for comparison between the two systems for each of the participant postures.

It is appropriate to report 95% confidence intervals (CIs) for bias (mean difference), as well as upper and lower limits of agreement [143]. However, CIs are not added to the Bland-Altman plots, as this would detract from the visual simplicity that is a strength of this technique. Instead, CIs are reported in the text of the results section. The CIs have also been used to ascertain if a bias is significant or not based upon if the line of equality is inside or outside the CIs of the bias (mean difference). Bland-Altman plots were generated for channels O1 and O2 as these channels cover the occipital region of the brain where the alpha peak is prominent during periods of eyes closed [125].

4.2.6 Power spectrum analysis of participant walking data

As participant walking with eyes closed is both impractical and dangerous, analysis techniques other than those relating to alpha peak during eyes closed had to be considered. Walking with participant eyes open does not produce a clear alpha peak in the participant's EEG [144] and therefore it is not possible to use the statistical approaches taken previously for the analysis of peak frequency, amplitude and AUC of the alpha band during eyes closed. Instead, power spectral density plots were generated for the first 15 seconds of data capture during participant walking and compared to those for participants lying down. The resulting plots taken from eight example channels (Fp1, Fp2, Fz, Pz, T3, T4, O1 and O2) were plotted on the same axes as power spectral density plots for participants lying down, as a comparison. This comparison should identify the effects of walking upon the power spectrum caused by electromagnetic effects, impedance change and electrode displacement. Although electromagnetic interference exists during stationary EEG recordings, there is the potential for this type of interference to increase because of the movement of electrode wires even when these wires are securely taped to the participant.

4.3 Results

The results are presented starting with electrical noise floor comparisons of both systems. This is followed by a single participant example, where a comparison of time series EEG data recorded using both mobile EEG systems is made along with associated power spectrum plots are made. Alpha peak analysis of the participant group data for both systems is then detailed followed by Bland-Altman plots for intra-system and inter-system comparisons. Finally, PSD plots for both mobile EEG systems are presented from data recorded during participant walking.

4.3.1 Electrical noise floor

The peak-to-peak amplitude of the Micromed system electrical noise floor has an amplitude of approximately 4 μV (Figure 4.3a), compared to the io:bio system of approximately 1 μV (Figure 4.3b). The results of performing PSD analysis upon the noise floor recordings are presented in Figure 4.3c, and show that the power differences between the two system noise floors extend across the band of frequencies shown (0 to 60 Hz). A peak at 50 Hz is present in the PSD plot for the io:bio system. Although a peak at 50 Hz is not present in the PSD plot for the Micromed system, it should be noted that the amplitude at 50 Hz is above that of the corresponding amplitude in the io:bio system.

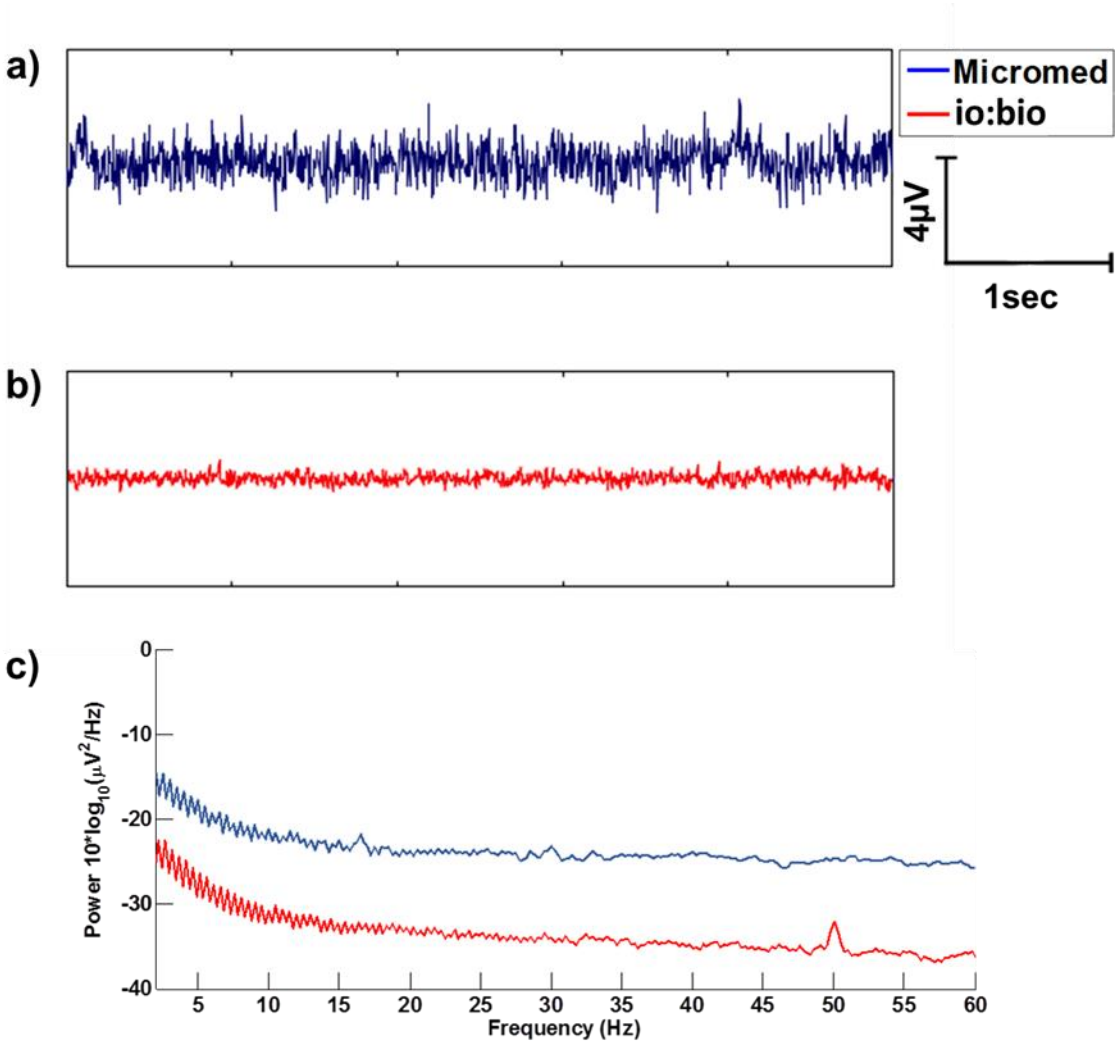

Figure 4.3 The electrical noise floor of each system with channel inputs shorted, **a)** Five seconds of time series data for Micromed system (blue), **b)** Five seconds of time series data for io:bio system (red), **c)** Associated PSD plots of the Micromed and io:bio systems.

4.3.2 Time series EEG data

Figure 4.4a,b shows a single participant example ten second period of time series data for each system, taken during period 1 of lying down with eyes closed. The time series plots are similar in amplitude and frequency content. The PSD plots display a comparison of the frequency band 0 to 30 Hz of the two systems EEG systems. Figure

4.4c shows the overlapping profiles of the individual PSD plots for channels O1 and O2 for both systems.

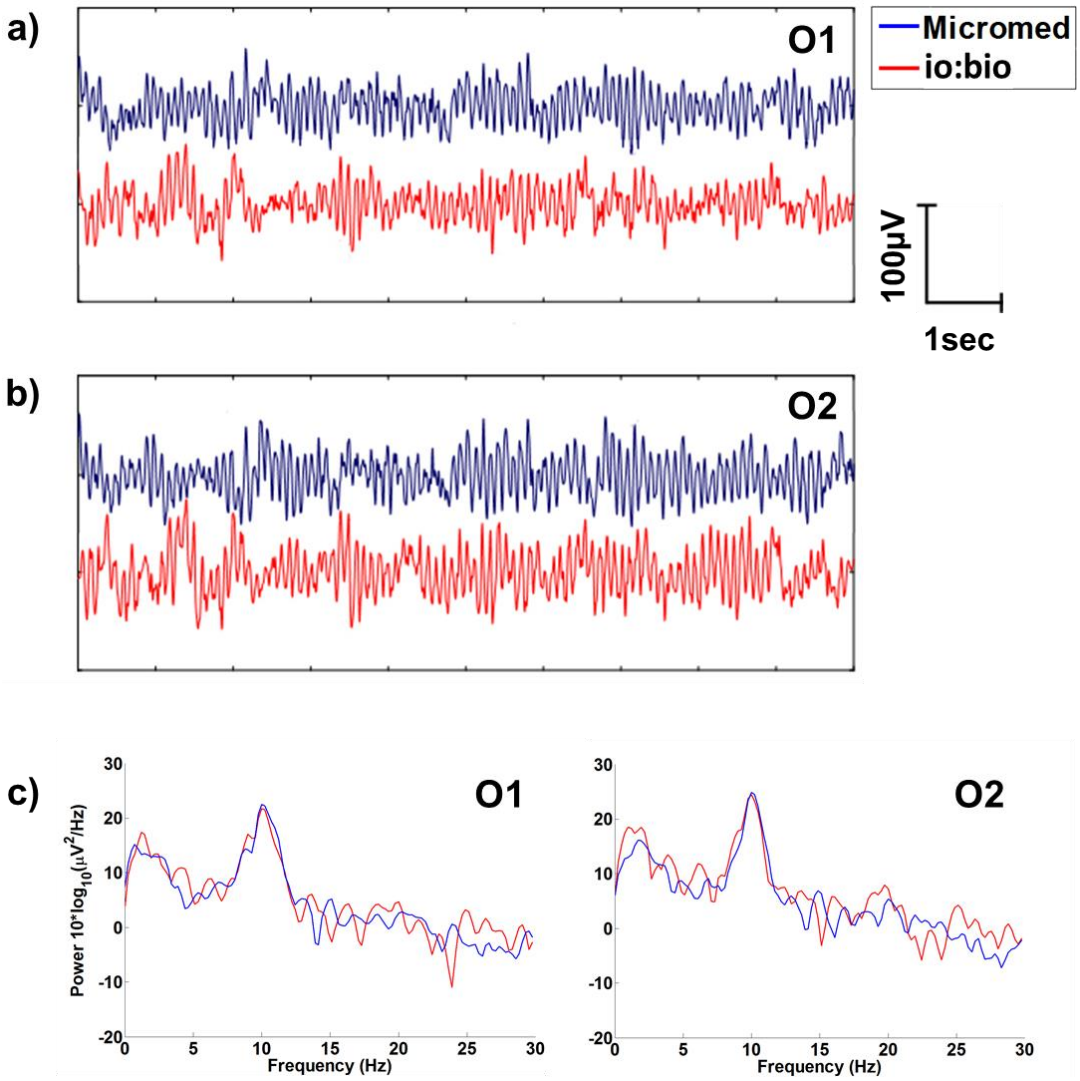

Figure 4.4 Example 10 s period of single participant time series EEG data for each system under test, taken sequentially during period 1 of lying down with eyes closed for a single participant (Micromed first followed by io:bio), at electrodes **a)** O1 and **b)** O2. The respective power spectrum plots for channels O1 and O2 are presented in **c)** and have been filtered (0.5 to 40 Hz).

4.3.3 Intra and inter-system alpha peak analysis

Values of alpha peak amplitude, frequency, and AUC of the alpha band were extracted from the recorded EEG data to provide quantitative parameters for statistical comparison between the two systems. Figure 4.5a shows the grand mean PSD plot for period 1 of lying down with eyes closed, recorded using both systems at electrodes O1 and O2. Figure 4.5b shows the grand mean PSD plot for period 2 of lying down with eyes closed, recorded using both systems at electrodes O1 and O2. The spectral activity recorded by the io:bio system is comparable to that recorded by the Micromed system, and follows a similar profile.

Grand mean bar charts of alpha peak amplitude, frequency, and AUC, for all channels, positioned on a head distribution that mimics the 10/20 electrode positions have been generated for intra-system and inter-system comparisons. Some channels were lost during the recordings (e.g. excessive impedance, contamination from artifacts) and where this occurred, channel data for both systems was removed for the participant in question to maintain valid pairs of data. This resulted in a range of 16 to 21 participant's data contributing to the grand means for each channel.

Figure 4.6 shows a comparison, for all channels, between period 1 and 2 of participants lying down with eyes closed recorded using the Micromed system. The distribution of power across the electrodes shows highest powers in occipital and parietal electrodes for both peak amplitude and AUC. No significant differences ($p>0.00263$) were found between the compared periods for alpha peak amplitude (Figure 4.6a), alpha peak frequency (Figure 4.6b) and area under the curve (Figure 4.6c).

The comparison for all channels, between period 1 and 2 of participants lying down with eyes closed recorded using the io:bio system is shown in Figure 4.7. The distribution of power across the electrodes mirrors that of the Micromed system with

highest powers in occipital and parietal electrodes for both peak amplitude and AUC. No significant differences (p>0.00263) were found between compared periods for alpha peak amplitude (Figure 4.7a), frequency (Figure 4.7b), and area under the curve (Figure 4.7c).

Figure 4.8 displays a comparison of Micromed (blue) and io:bio (red) systems during period 2 of eyes closed for alpha band peak power amplitude (Figure 4.8a), peak frequency (Figure 4.8b), and area under the curve (Figure 4.8c). No significance was found (p>0.00263).

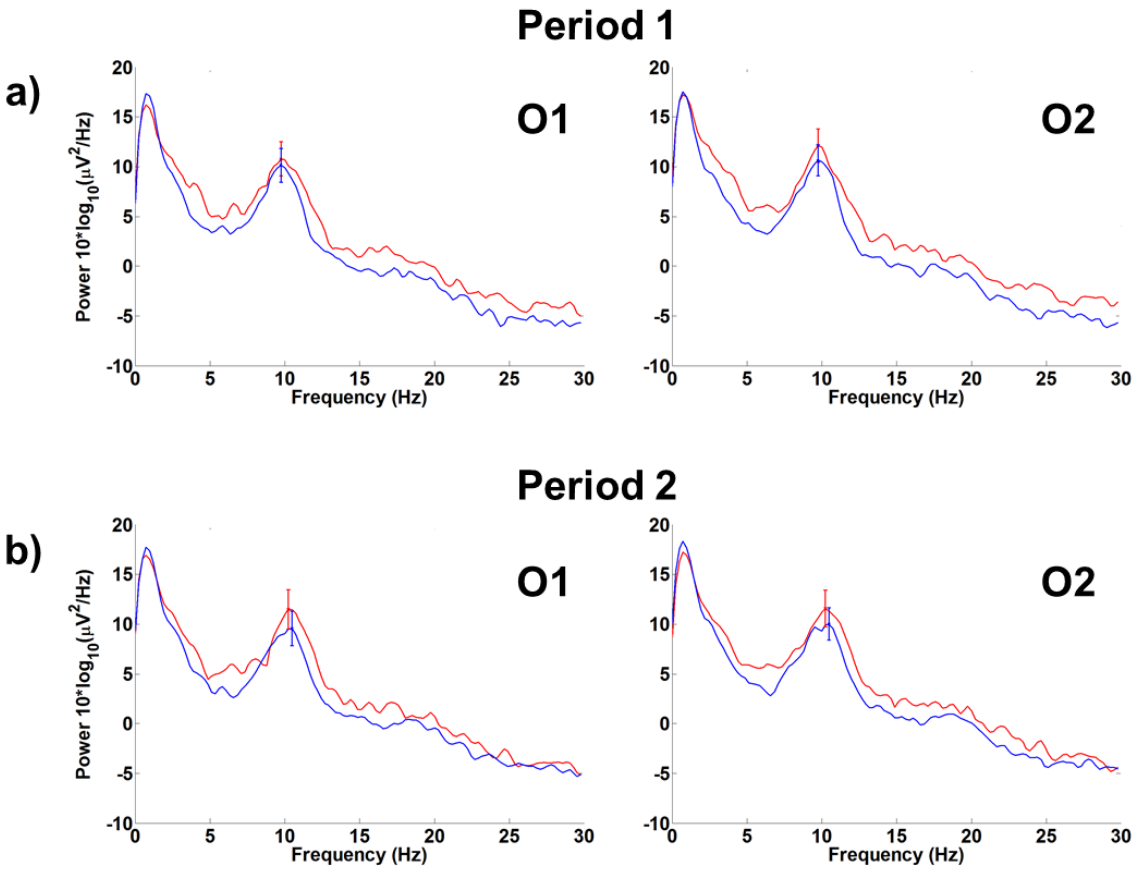

Figure 4.5 Grand mean power spectrum density plots for **a)** period 1, and **b)** period 2 of participants lying down with eyes closed using Micromed system (blue colour) and io:bio system (red). Data are presented as mean ± SEM for the alpha peak only, n=18.

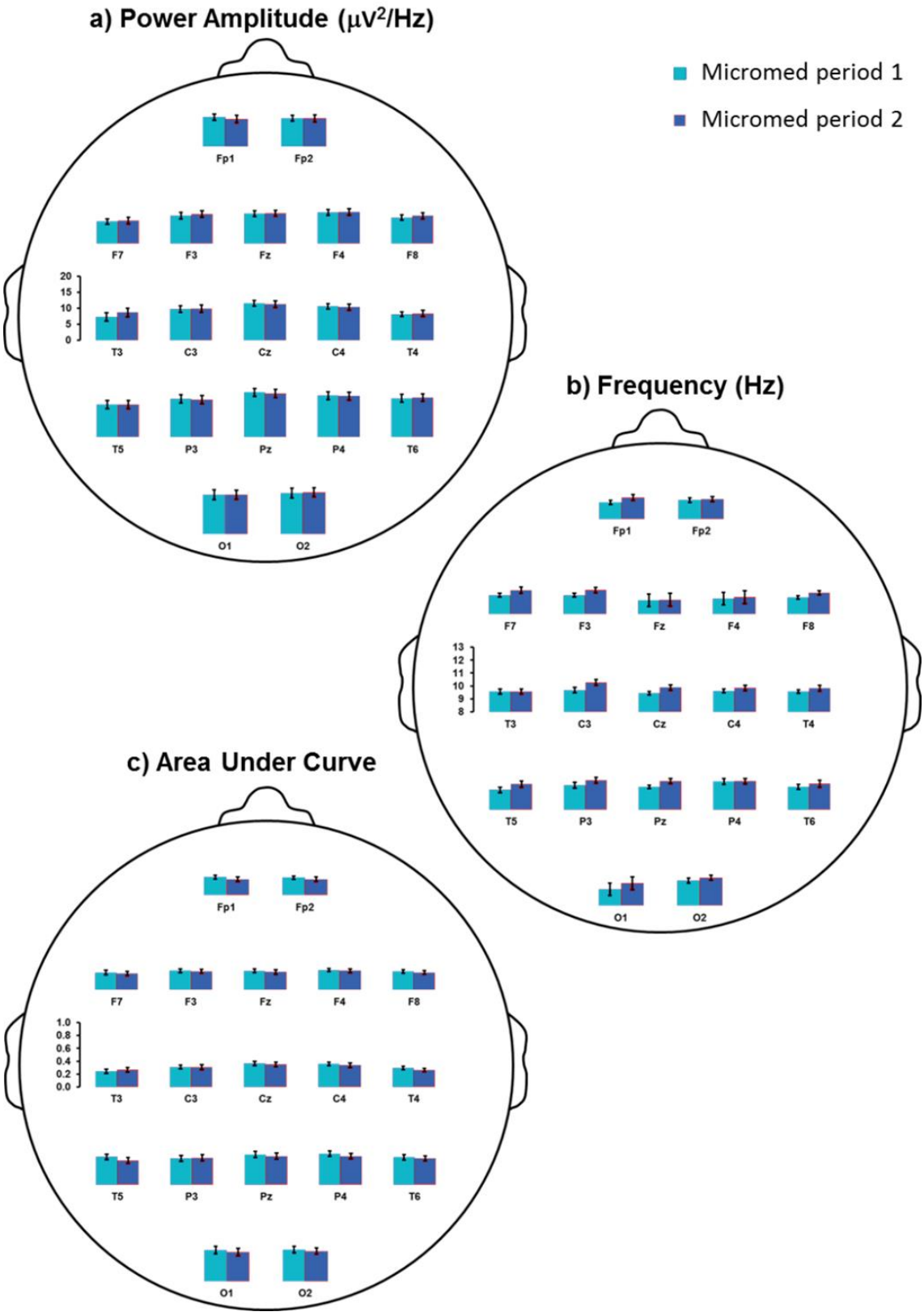

Figure 4.6 Grand mean bar charts for the Micromed system comparing periods 1 (cyan) and 2 (blue) for all EEG channels during eyes closed for alpha band **a)** peak power amplitude, **b)** peak frequency, and **c)** area under the curve (normalised). Data are presented as mean ± SEM, n=16-21. No significance was found (p>0.00263).

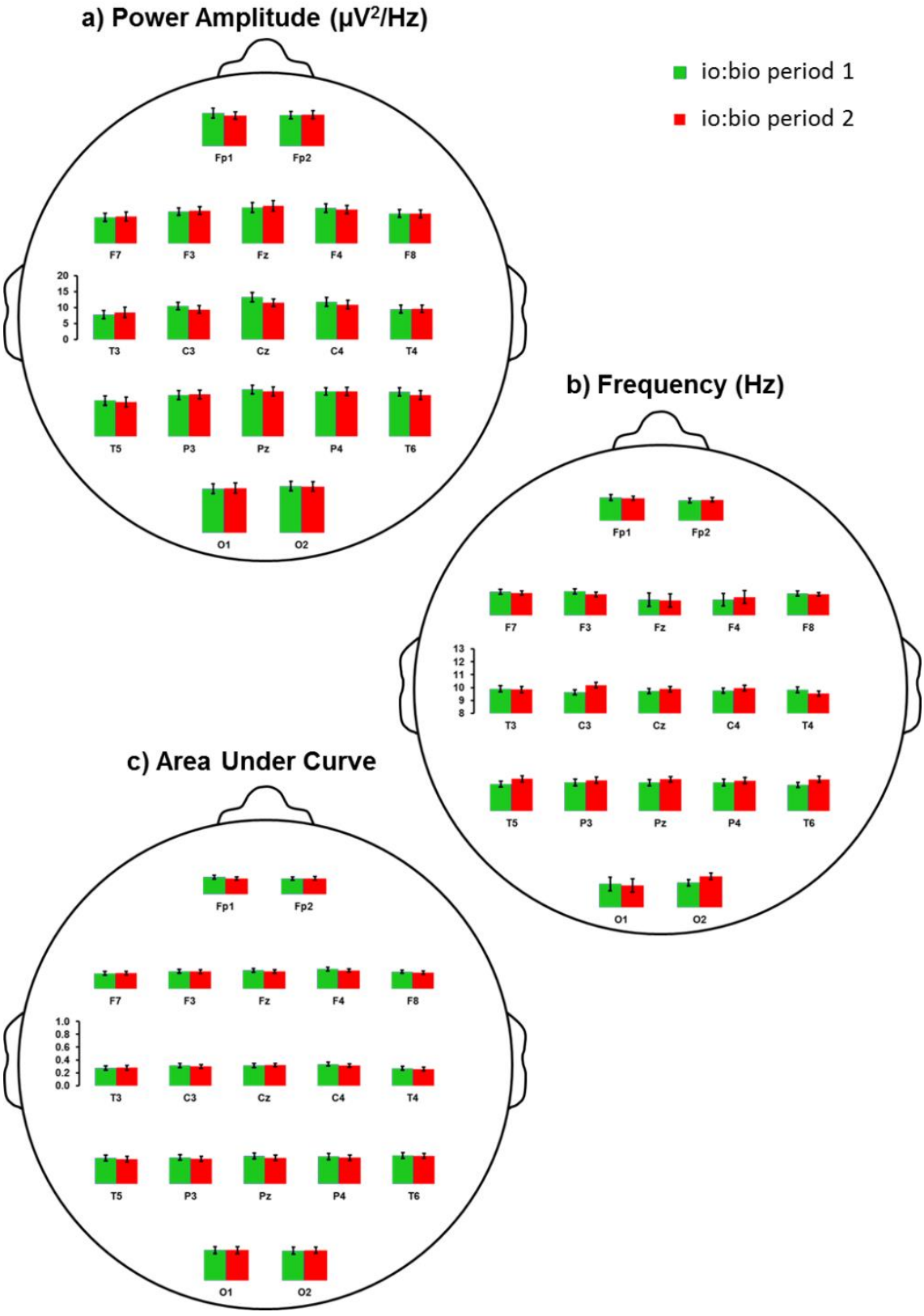

Figure 4.7 Grand mean bar charts for the io:bio system comparing periods 1 (green) and 2 (red) for all EEG channels during eyes closed for alpha band **a)** peak power amplitude, **b)** peak frequency, and **c)** area under the curve (normalised). Data are presented as mean ± SEM, n=16-21. No significance was found (p>0.00263).

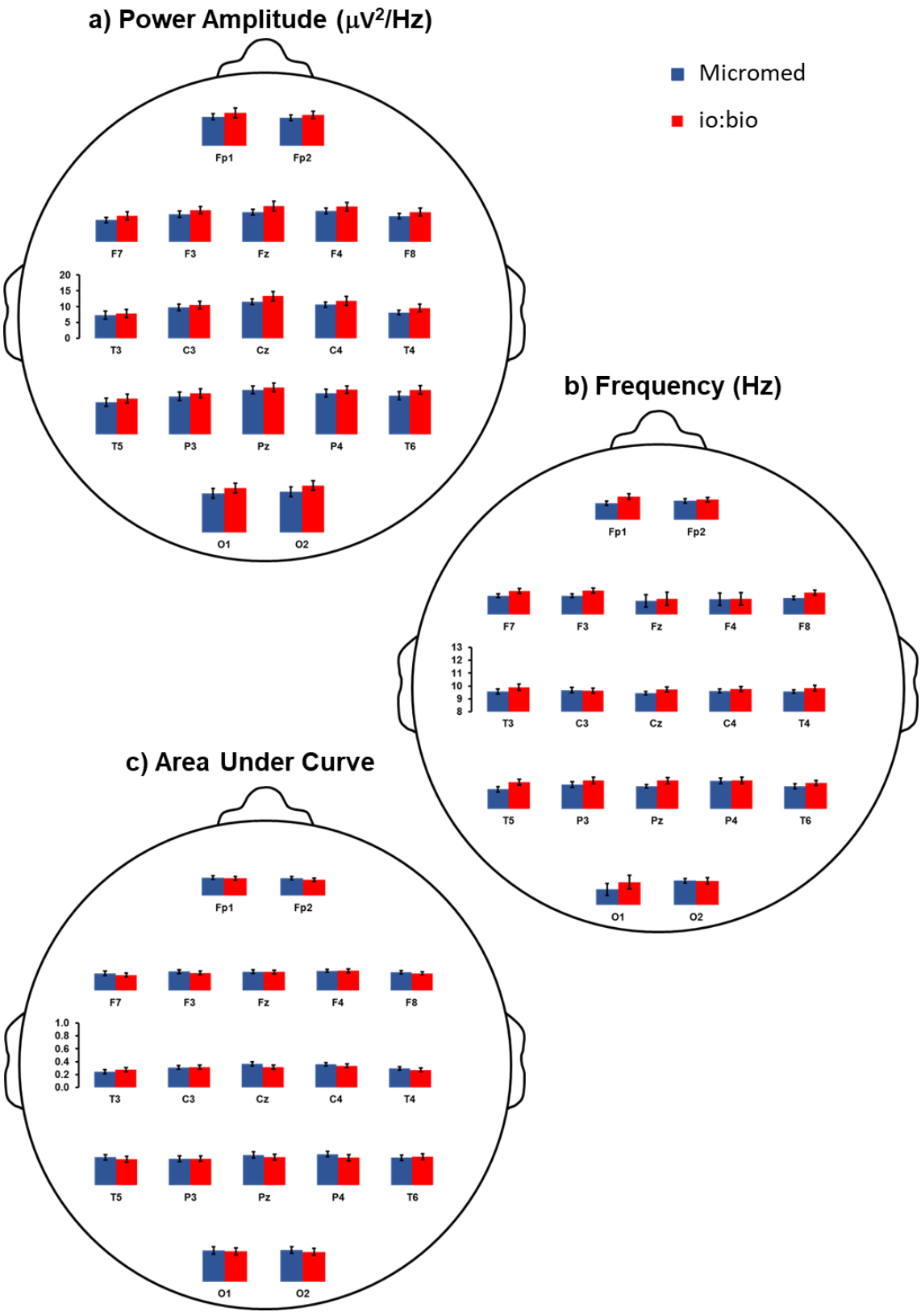

Figure 4.8 Comparison of Micromed (blue) and io:bio systems (red) during period 2 of eyes closed for alpha band **a)** peak power amplitude, **b)** peak frequency, and **c)** area under the curve (normalised). Data are presented as mean ± SEM, n=16-21. No significance was found (p>0.00263).

Table 4.2 shows the resultant statistical p values from a two tailed, paired t-test between periods 1 and 2 for the Micromed and the io:bio systems for all 19 channels. Table 4.3 shows the resultant P values from a two tailed, paired t-test between Micromed and io:bio systems for period 1 and 2 and all channels. Both tables show that across all comparisons made significance has not been reached at the p>0.00263 level.

Table 4.2 P values for intra-system comparison (period 1 vs period 2) for Micromed and io:bio systems. Alpha parameters used for comparison were obtained during participants lying down with eyes closed (n=16-21).

	Micromed			io:bio		
EEG Channel	**Peak Amplitude**	**Peak Frequency**	**AUC**	**Peak Amplitude**	**Peak Frequency**	**AUC**
FP1	0.82	0.12	0.71	0.53	0.51	0.22
FP2	0.98	0.74	0.95	0.32	0.96	0.7
F7	0.39	0.3	0.93	0.66	0.35	0.79
F3	0.4	0.09	0.77	0.64	0.28	0.75
FZ	0.78	0.7	0.68	0.37	0.74	0.4
F4	0.79	0.65	0.62	0.5	0.11	0.17
F8	0.34	0.1	0.48	0.83	0.77	0.33
T3	0.56	0.21	0.72	0.65	0.97	0.3
C3	0.85	0.03	0.96	0.13	0.05	0.62
CZ	0.54	0.01	0.41	0.11	0.49	0.87
C4	0.63	0.22	0.32	0.06	0.55	0.32
T4	0.6	0.26	0.11	0.87	0.24	0.52
T5	0.96	0.04	0.1	0.43	0.09	0.43
P3	0.65	0.12	0.82	0.71	0.44	0.39
PZ	0.51	0.04	0.27	0.23	0.22	0.36
P4	0.78	0.92	0.19	1	0.59	0.51
T6	0.74	0.38	0.59	0.19	0.06	0.75
O1	0.94	0.05	0.43	0.92	0.54	0.99
O2	0.68	0.37	0.5	0.85	0.06	0.85

Table 4.3 P values for inter-system comparison (Micromed system vs io:bio system) for period 1 and period 2 of participants lying down with eyes closed (n=16-21).

	Period 1			Period 2		
EEG Channel	**Peak Amplitude**	**Peak Frequency**	**AUC**	**Peak Amplitude**	**Peak Frequency**	**AUC**
FP1	0.15	0.03	0.75	0.28	0.82	0.66
FP2	0.26	0.69	0.36	0.69	1.00	0.42
F7	0.13	0.75	0.23	0.31	0.84	0.44
F3	0.12	0.07	0.26	0.28	0.46	0.58
FZ	0.16	0.35	0.36	0.16	0.89	0.42
F4	0.15	0.87	0.97	0.52	0.64	0.79
F8	0.19	0.10	0.56	0.55	1.00	0.65
T3	0.33	0.13	0.25	0.85	0.97	0.91
C3	0.33	0.90	0.64	0.70	0.72	0.55
CZ	0.09	0.17	0.14	0.80	1.00	0.35
C4	0.31	0.42	0.36	0.66	0.71	0.44
T4	0.09	0.33	0.19	0.22	0.27	0.85
T5	0.20	0.01	0.37	0.51	0.05	0.91
P3	0.32	0.31	0.99	0.19	0.69	0.47
PZ	0.43	0.11	0.34	0.61	0.27	0.42
P4	0.16	0.89	0.16	0.26	0.56	0.32
T6	0.02	0.33	0.60	0.62	0.15	0.57
O1	0.16	0.06	0.52	0.19	1.00	0.94
O2	0.08	0.96	0.50	0.23	0.33	0.99

4.3.4 Bland-Altman plots

The Bland-Altman plots have been presented in an order organised firstly by participant posture (lying down and sitting etc.), secondly by the metrics used for comparison (amplitude, frequency and AUC of alpha peak), and finally by mode of comparison (intra-system and inter-system). It is important to consider intra-system agreement before inter-system agreement as a system that does not give repeatable results would provide meaningless results for inter-system comparison.

4.3.4.1 Participants lying down with eyes closed

In this section Bland-Altman plots were generated from data recorded while participants were lying down. Channels O1 and O2 were selected as it is the posterior brain area where the alpha peak is dominant with eyes closed.

4.3.4.1.1 Intra-system agreement of alpha peak amplitude

Bland-Altman plots were constructed for intra-system agreement between period 1 and period 2 of participants lying down with eyes closed using the Micromed (Figure 4.9a), and io:bio systems (Figure 4.9b). Bland-Altman plots for the Micromed system (Figure 4.9a) have limits of agreement ranging from -5.83 to 5.73 $\mu V^2/Hz$ (95% CI -8.22 to -3.44 and 3.34 to 8.12) for channel O1, and -6.73 to 6.14 $\mu V^2/Hz$ (95% CI -9.32 to -4.14 and 3.34 to 8.12) for channel O2. Since it was decided *a priori* that the limits of agreement obtained from the intra-system agreement of the Micromed would be used as the acceptable limits for the intra-system agreement of the io:bio system, these limits will be referred to when considering the io:bio system. Although the mean bias for each channel is close to the zero line, O1 bias = -0.05 µV (95% CI -1.43 to 1.33) and O2 bias = -0.29 µV (95% CI -1.79 to 1.20), there is no systematic bias to either period as observed differences exist either side of zero.

The corresponding Bland-Altman plots for the io:bio system (Figure 4.9b) have limits of agreement ranging from -4.61 to 4.50 μV^2/Hz (95% CI -6.49 to -2.72 and 2.62 to 6.39) for channel O1, and -4.27 to 4.46 μV^2/Hz (95% CI -9.32 to -4.14 and 3.55 to 8.72) for channel O2. These are within the limits of agreement obtained for the Micromed system and therefore satisfy the *a priori* criteria for intra-system agreement. The mean bias's for O1 are -0.05 μV^2/Hz (95% CI -1.14 to 1.04), and for O2 0.09 μV^2/Hz (95% CI -0.92 to 1.11), indicate that there is no systematic bias to either period as observed differences exist either side of zero for both plots.

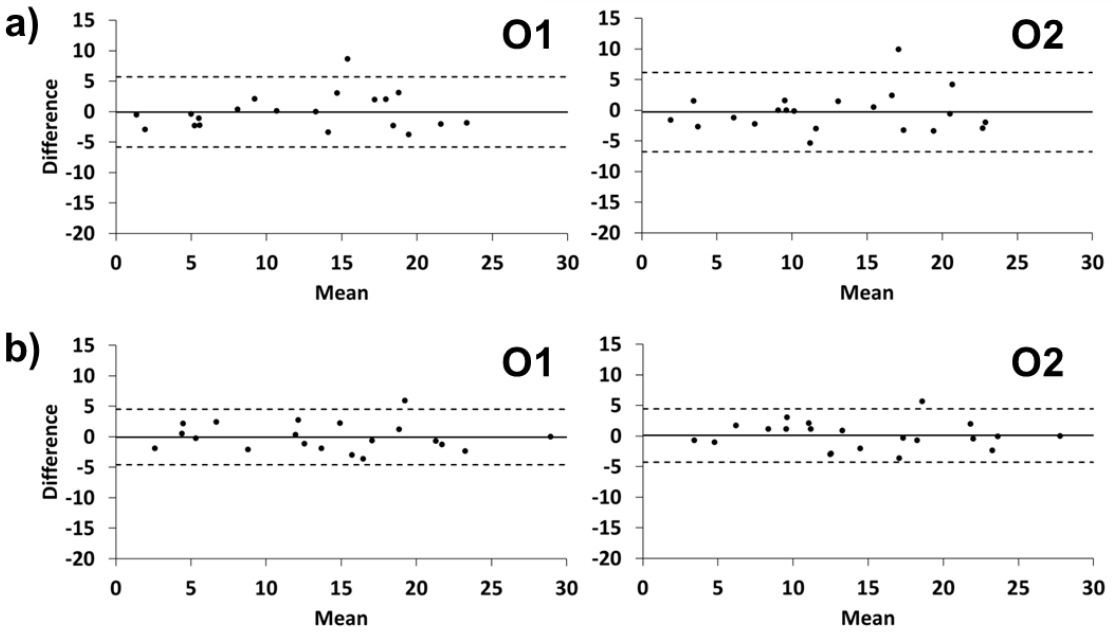

Figure 4.9 Bland-Altman plots for alpha peak amplitude comparison between period 1 and period 2, recorded during participants lying down with eyes closed using a) Micromed and b) io:bio systems. n=20 for channel O1, n=21 for channel O2. The x-axis represents the mean alpha peak amplitude ((period 1+period 2)/2), across the range 0 to 30 μV^2/Hz. The y-axis represents the difference (period 1-period 2) in the measured alpha peak amplitude across a range of -20 to 15 μV^2/Hz.

4.3.4.1.2 Inter-system agreement of alpha peak amplitude

Bland-Altman plots were constructed for inter-system agreement between the Micromed and io:bio systems. Bland-Altman plots comparing the two systems for agreement for periods 1 (Figure 4.10a) have limits of agreement ranging from -11.54 to 8.21 μV^2/Hz (95% CI -15.62 to -7.46 and 4.12 to 12.29) for channel O1, and -11.51 to 7.61 μV^2/Hz for channel O2 (95% CI -15.36 to -7.66 and 3.77 to 11.46). The limits of agreement for Period 2 (Figure 4.10b) range from -12.56 to 9.21 μV^2/Hz (95% CI -17.06 to -8.05 and 4.71 to 13.71) for channels O1, and from -12.85 to 9.74 μV^2/Hz (95% CI -17.39 to -8.31 and 5.20 to 14.29) for channel O2. The limits of agreement are wider in relation to those obtained in the intra-system comparisons, but are within the limits decided *a priori* (twice that of intra-system limits). A bias towards the io:bio system has been recorded for period 1, with channel O1 bias = -1.67 μV^2/Hz (95% CI -4.03 to 0.69) and O2 bias = -1.95 μV^2/Hz (95% CI -4.17 to 0.27). A bias towards the io:bio system has also been recorded for period 2 with O1 bias = -1.67 μV^2/Hz (95% CI -4.27 to 0.93) and O2 bias = -1.55 μV^2/Hz (95% CI -4.18 to 1.07). However, none of these biases is significant as the line of equality resides inside the CIs of the bias.

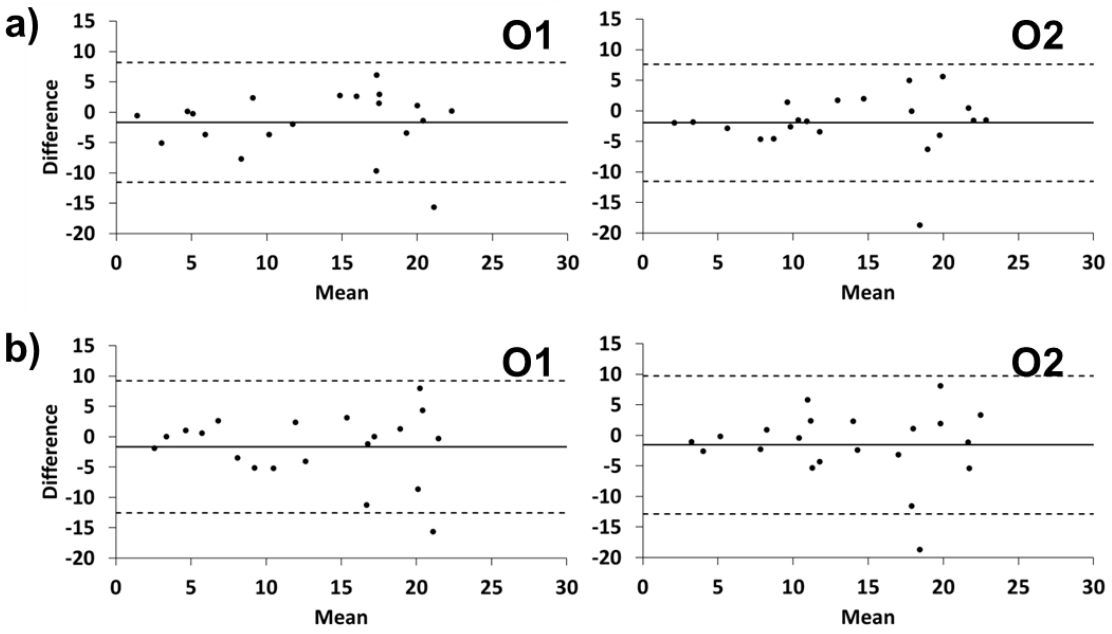

Figure 4.10 Bland-Altman plots for alpha peak amplitude comparison between recordings made using Micromed and io:bio systems, recorded during participants lying down with eyes closed during a) period 1, and b) period 2. n=20 for channel O1, n=21 for channel O2. The x-axis represents the mean alpha peak amplitude ((Micromed + io:bio)/2). The y-axis represents the difference (Micromed - io:bio) in the measured alpha peak amplitude across a range of -20 μV^2/Hz to 15 μV^2/Hz.

4.3.4.1.3 Intra-system agreement of alpha peak frequency

Bland-Altman plots were constructed for intra-system agreement between period 1 and period 2 of participants lying down with eyes closed using the Micromed (Figure 4.11a), and io:bio systems (Figure 4.11b). Bland-Altman plots for Micromed system (Figure 4.11a) have limits of agreement ranging from -2.55 to 1.58 Hz (95% CI -3.38 to -1.72 and 0.75 to 2.41) for channels O1, and -2.37 to 1.92 Hz (95% CI -3.23 to -1.50 and 1.06 to 2.79) for channel O2. Although the mean bias for each channel is negative, O1 bias = -0.49 Hz (95% CI -1.43 to 1.33) and O2 bias = -0.22 Hz (95% CI -1.43 to 1.33) no systematic bias to either period exists as observed differences exist either side of zero.

The corresponding Bland-Altman plots for the io:bio system (Figure 4.11b) have limits of agreement ranging from -1.60 to 1.84 Hz (95% CI -2.29 to -0.91 and 1.15 to 2.53) for channel O1, and -2.73 to 1.76 Hz (95% CI -3.64 to -1.83 and 0.85 to 2.66) for channel O2. These are within the limits of agreement obtained for the Micromed system and therefore satisfy the *a priori* criteria for intra-system agreement. The mean bias for O1 was 0.12 Hz (95% CI -0.06 to 0.06) and for O2 -0.49 Hz (95% CI -0.08 to 0.07), indicating that there is no bias to either period as the line of equality lies with the CIs of the bias.

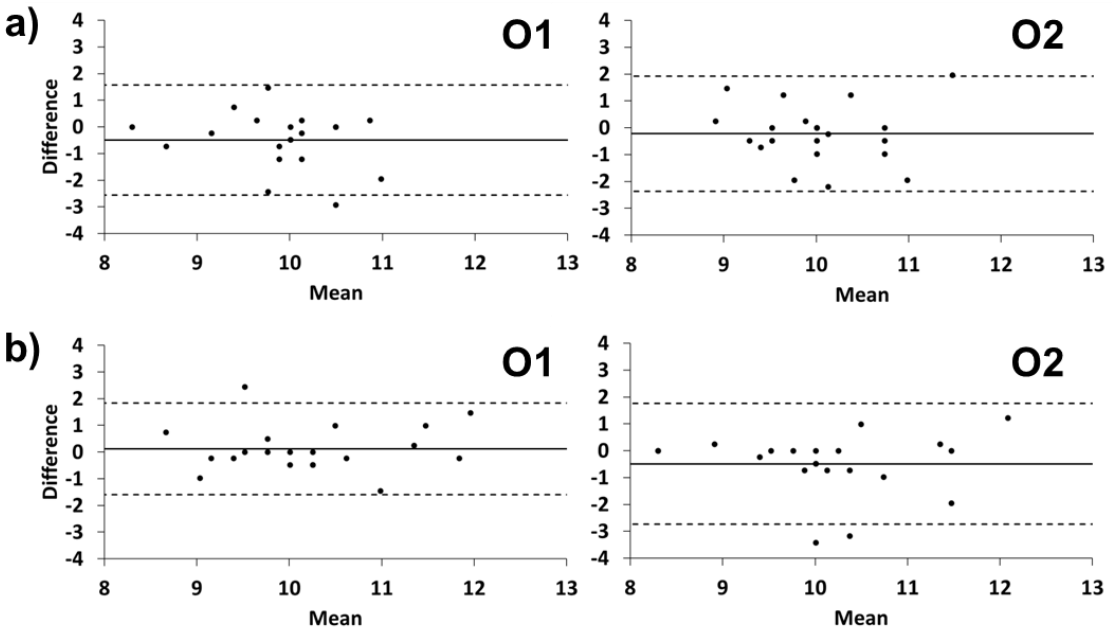

Figure 4.11 Bland-Altman plots for alpha peak frequency comparison between period 1 and period 2, recorded during participants lying down with eyes closed using a) Micromed system b) io:bio system. n=21 for both channels. The x-axis represents the mean ((period1 + period2)/2), alpha peak frequency across the range 8 to 13Hz. The y-axis represents the difference (period1 - period2) in the measured alpha peak amplitude across a range of -4 to 4Hz.

4.3.4.1.4 Inter-system agreement of alpha peak frequency

Bland-Altman plots comparing the two systems for agreement for periods 1 (Figure 4.12a) have limits of agreement ranging from -3.32 to 2.10 Hz (95% CI -4.42 to -2.23 and 1.01 to 3.19) for channel O1, and -1.91 to 1.93 Hz for channel O2 (95% CI -2.67 to -1.13 and 1.16 to 2.70). The limits of agreement for period 2 (Figure 4.12b) range from -1.93 to 1.93 Hz (95% CI -2.71 to -1.16 and 1.16 to 2.71) for channel O1 and from -2.54 to 2.03 Hz (95% CI -3.45 to -1.62 and 1.11 to 2.94) for channel O2. The limits of agreement have now increased in value in relation to those obtained in intra-system comparisons but not significantly as the CIs of the limits of agreement overlap in all cases. All inter-system results for alpha peak frequency are within the *a priori* defined limits except for O1 for period 1. However, when the bias is considered along with the confidence intervals, this range is acceptable. The biases recorded during period 1 are O1 = -0.61 Hz (95% CI -1.24 to 0.02) and O2 = 0.01 Hz (95% CI -0.43 to 0.46). Those recorded during period 2 are O1 = 0 Hz (95% CI -0.45 to 0.45) and O2 = -0.26 Hz (95% CI -0.79 to 0.27). These show for both periods and both channels show that no significant or systematic bias exists.

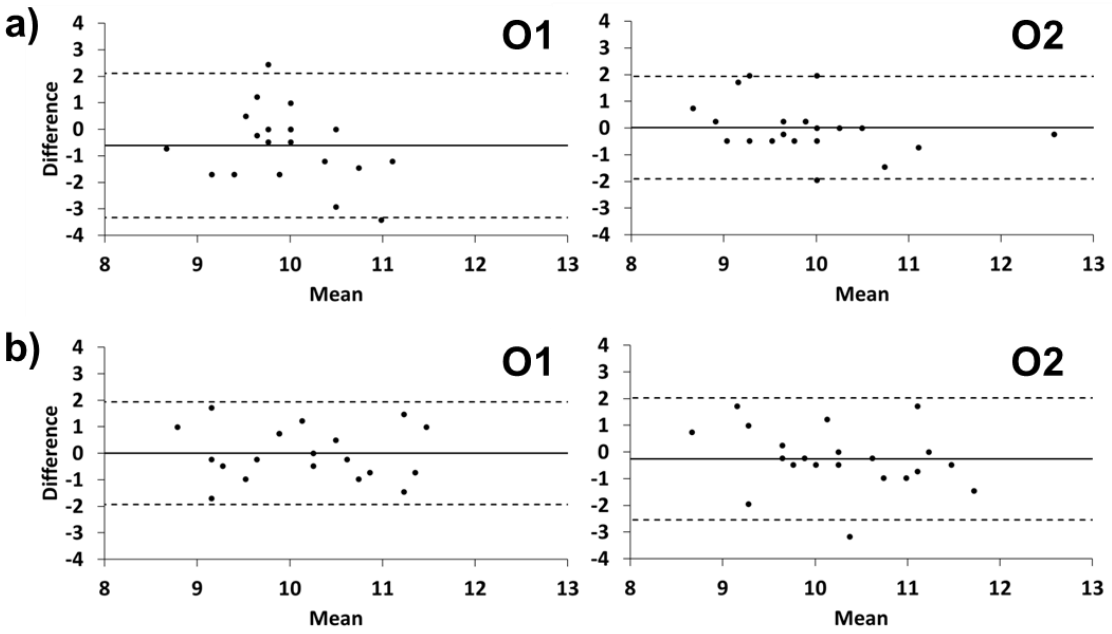

Figure 4.12 Bland-Altman plots for alpha peak frequency comparison between recordings made using Micromed and io:bio systems, recorded during participants lying down with eyes closed during a) period 1 b) period 2. n=21 for both channels. The x-axis represents the mean ((Micromed + io:bio)/2), alpha peak frequency across the range 8 to 13Hz. The y-axis represents the difference (Micromed - io:bio) in the measured alpha peak amplitude across a range of -4 to 4Hz.

4.3.4.1.5 Intra-system agreement of alpha AUC

The Bland-Altman plots comparing AUC of the alpha band for the two periods of participants lying down with eyes closed, recorded using the Micromed system (Figure 4.13a) have limits of agreement ranging from -0.25 to 0.31 (95% CI -0.36 to -0.13 and 0.19 to 0.43) for channel O1, and -0.26 to 0.30 (95% CI -0.37 to -0.15 and 0.19 to 0.41) for channel O2. The mean bias for channel O1 = 0.03 (95% CI -0.04 to 0.10) and for channel O2 = 0.02 (95% -0.04 to 0.09). The equivalent Bland-Altman plots for the io:bio system (Figure 4.13b) have limits of agreement ranging from -0.26 to 0.26 (95% CI -0.36 to -0.15 and 0.15 to 0.36) for channel O1, and -0.33 to 0.32 (95% CI -0.36 to -0.15 and 0.15 to 0.36) for channel O2. They do not differ significantly from those of the Micromed system as the CIs for the limits of agreement intersect one another in all

cases. The mean bias for channel O1 = -0.00 (95% -0.06 to 0.06) and for channel O2 = -0.01 (95% -0.08 to 0.07) and are not significantly different from each other.

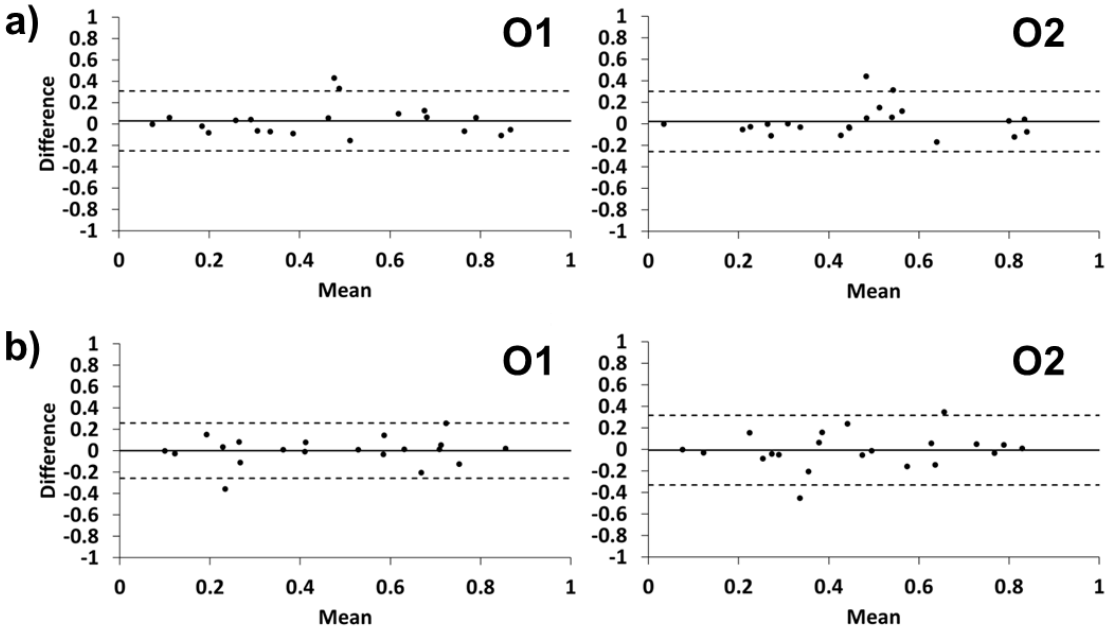

Figure 4.13 Bland-Altman plots for alpha band AUC comparison between period 1 and period 2, recorded during participants lying down with eyes closed using a) Micromed system b) io:bio system. n=20 for channel O1, n=21 for channel O2. The x-axis represents the mean ((period1 + period2)/2), alpha AUC across the range 0 to 1. The y-axis represents the difference (period1 - period2) in the measured alpha AUC across a range of -1 to 1.

4.3.4.1.6 Inter-system agreement of alpha AUC

Bland-Altman plots comparing the two systems for agreement for period 1 (Figure 4.14a) have limits of agreement ranging from 0.41 to -0.38 (95% CI -0.54 to -0.22 and 0.24 to 0.57) for channel O1, and 0.40 to -0.35 (95% CI -0.50 to -0.20 and 0.25 to 0.55) for channel O2. The limits of agreement for Period 2 (Figure 4.14b) range from -0.48 to 0.45 (95% CI -0.67 to -0.29 and 0.26 to 0.64) for channel O1 and from -0.46 to 0.46 (95% CI -0.65 to -0.28 and 0.28 to 0.65) for channel O2. The limits of agreement have

increased in value in relation to those obtained in intra-system comparisons. All inter-system results for the AUC are within the *a priori* defined limits. The biases recorded during period 1 are O1 bias = 0.01 (95% CI -0.08 to 0.11) and O2 bias = 0.03 (95% CI -0.06 to 0.12). The biases recorded during period 2 are O1 bias = -0.02 (95% CI -0.13 to 0.10) and O2 bias = 0.00 (95% CI -0.11 to 0.11). The biases recorded for both periods and both channels show no significant bias exists (the CIs for the limits of agreement intersect one another). No systematic bias exists.

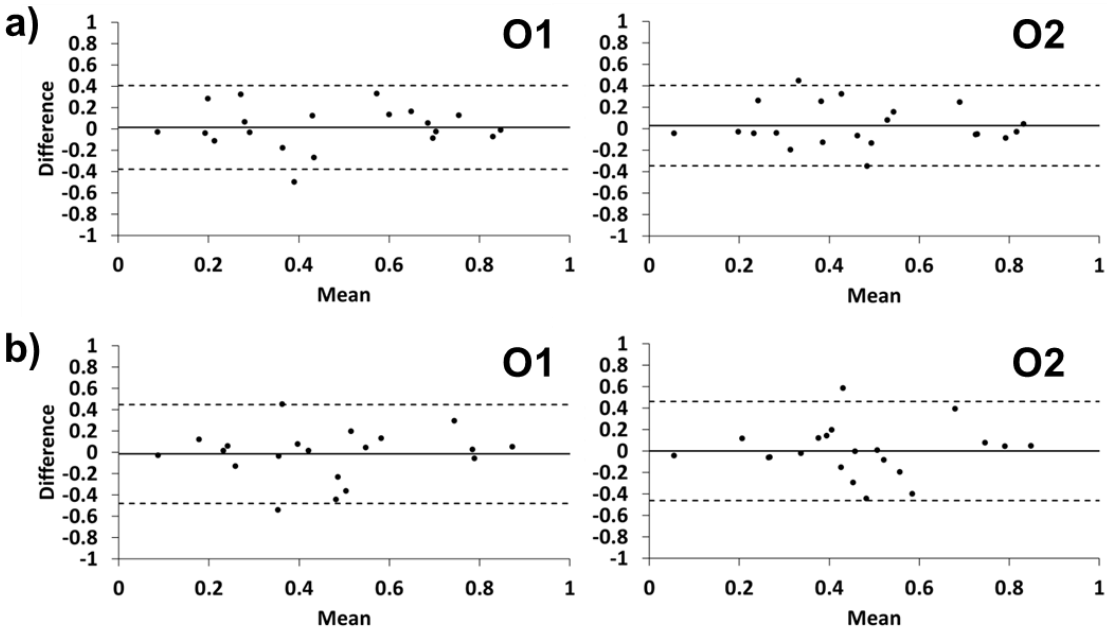

Figure 4.14 Bland-Altman plots for alpha band AUC comparison between recordings made using Micromed system and io:bio system, recorded during participants lying down with eyes closed during a) period 1 b) period 2. n=20 for channel O1, n=21 for channel O2. The x-axis represents the mean ((Micromed + io:bio) / 2), alpha AUC across the range 0 to 1. The y-axis represents the difference (Micromed - io:bio) in the measured alpha AUC across a range of -1 to 1.

4.3.4.2 Participants sitting, standing and standing with arms raised

Figure 4.15 presents example 10s EEG time series traces with participants lying down (for comparison), sitting, standing and standing with arms raised. Bland-Altman plots were generated from data recorded during these activities.

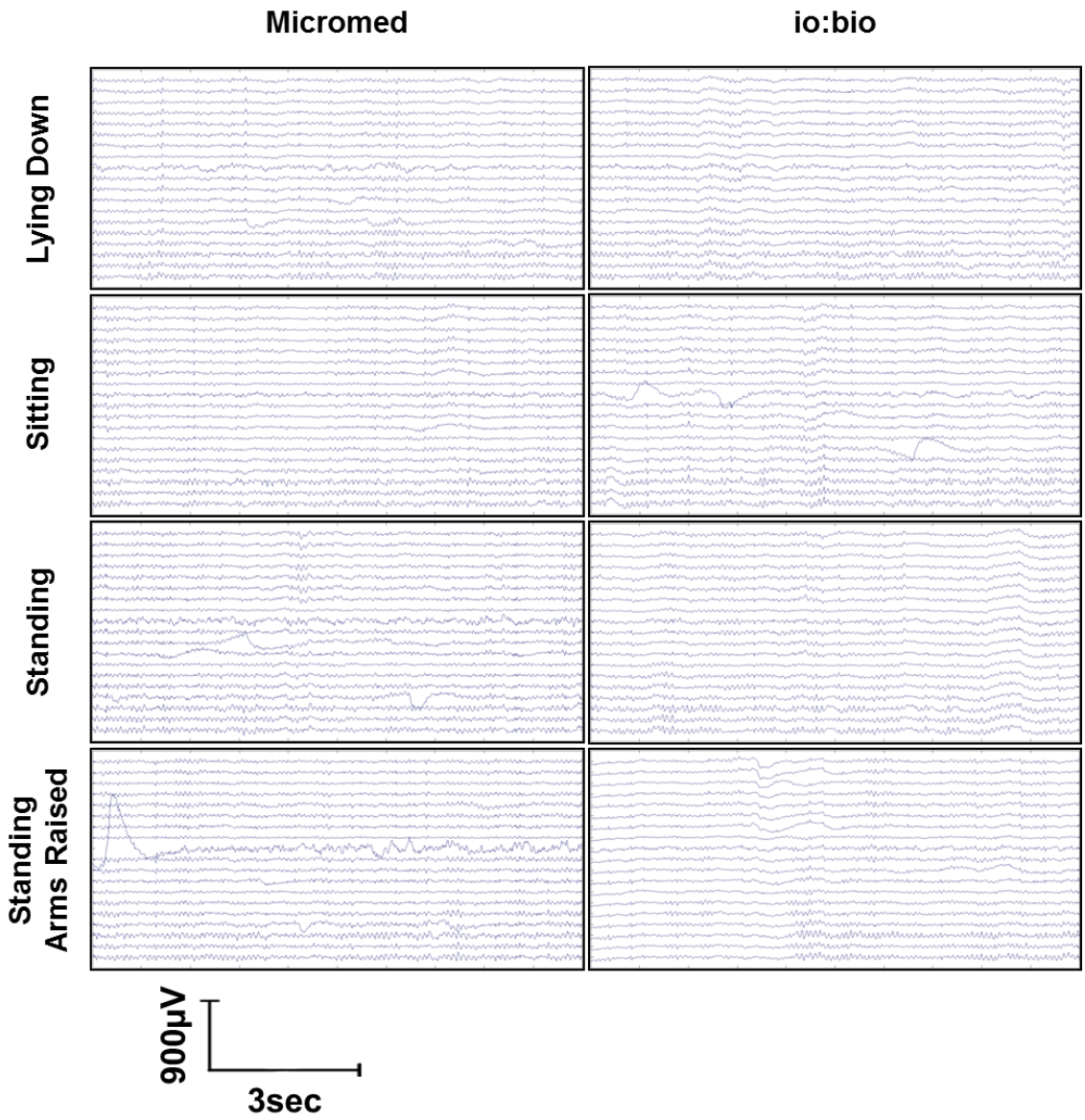

Figure 4.15 10s of EEG time series (19 channels) from data recorded using Micromed (left column) and io:bio (right column) from a single participant lying down, sitting, standing and standing arms raised with eyes closed. Channel labels as in Figure 3.12.

4.3.4.2.1 Inter-system agreement of alpha peak amplitude

The Bland-Altman plots comparing the two systems for agreement during participants sitting down, standing and standing with arms raised have been generated for the alpha peak amplitude (Figure 4.16). Limits of agreement for the various postures covered the following ranges: Sitting posture ranged -15.89 (95% CI -21.95 to -9.84) to 12.52 µV (95% CI 6.47 to 18.57) for channel O1 and -15.34 (95% CI -21.47 to -9.21) to 13.43 µV (95% CI 7.30 to 19.56) for channel O2. Standing posture ranged -12.93 (95% CI -18.10 to -7.76) to 10.59 µV (95% CI 5.42 to 15.76) for channel O1 and -15.02 (95% CI -20.43 to -9.60) to 10.41 µV (95% CI 5.00 to 15.83) for channel O2. Standing with arms raised posture ranged -14 (95% CI -19.57 to -8.42) to 12.19 µV (95% CI 6.62 to 17.77) for channel O1 and -15.01 (95% CI -20.61 to -9.40) to 11.31 µV (95% CI 5.71 to 16.92) for channel O2.

A bias towards the io:bio system has been recorded for sitting, with channel O1 bias = -1.69 $\mu V^2/Hz$ (95% CI 1.81 to -5.18) and O2 bias = -0.96 $\mu V^2/Hz$ (95% CI 2.58 to -4.49). A bias towards the io:bio system has also been recorded for standing with O1 bias = -1.17 $\mu V^2/Hz$ (95% CI 1.81 to -4.15) and O2 bias = -2.31 $\mu V^2/Hz$ (95% CI 0.82 to -5.43). A bias towards the io:bio system has also been recorded for standing with arms raised with O1 bias = -0.9 $\mu V^2/Hz$ (95% CI 2.32 to -4.12) and O2 bias = -1.85 $\mu V^2/Hz$ (95% CI 1.39 to -5.08). However, none of these biases is significant as the line of equality resides inside the CIs of the bias.

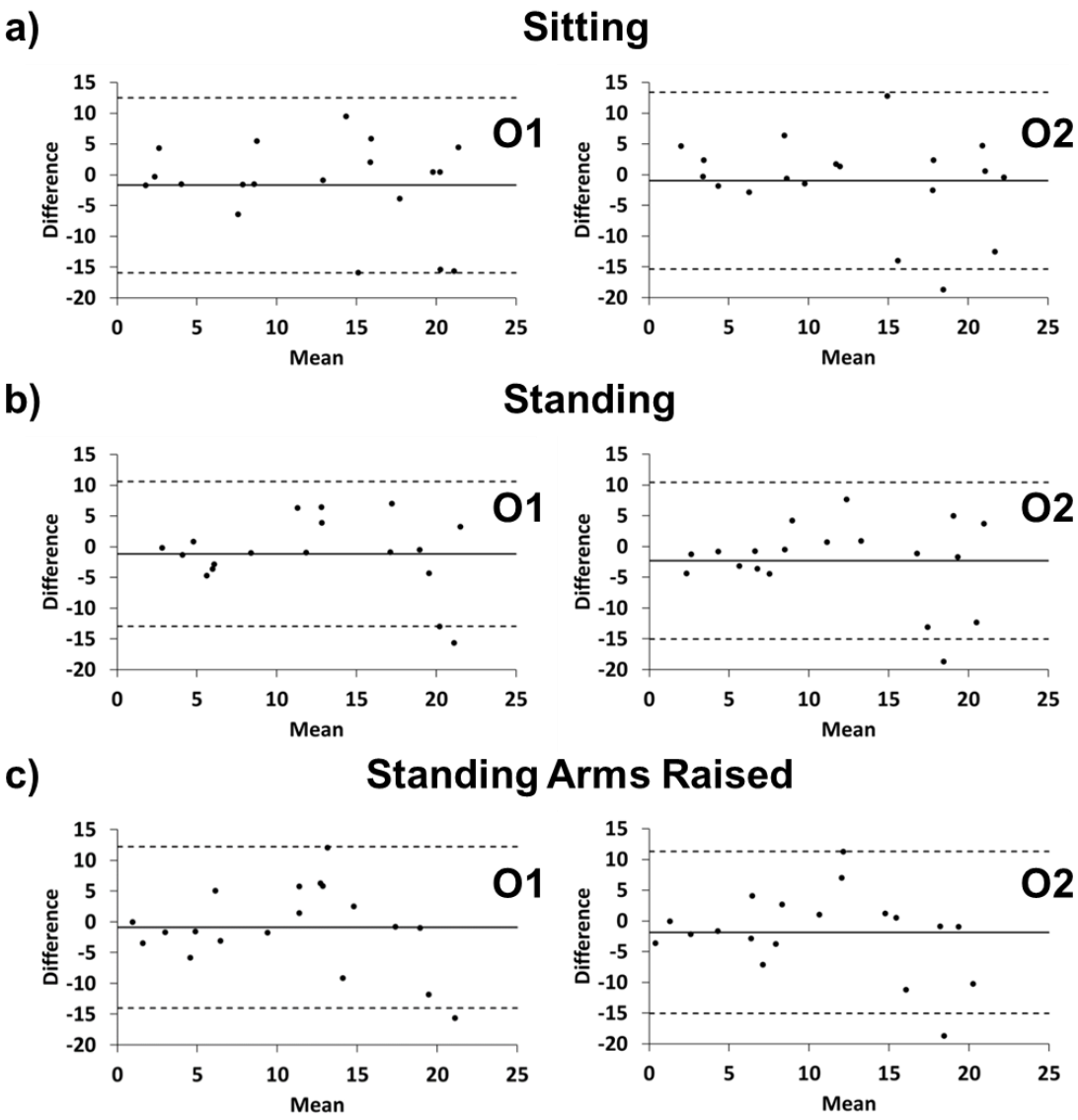

Figure 4.16 Bland-Altman plots for alpha peak amplitude comparison between recordings made using Micromed and io:bio systems, recorded with eyes closed during participants **a)** sitting (n=19) **b)** standing (n=18 for channel O1, n=19 for channel O2) and **c)** standing with arms raised (n=19).

4.3.4.2.2 Bland-Altman plots for inter-system agreement of alpha peak frequency

The Bland-Altman plots comparing the two systems for agreement during participants sitting down, standing and standing with arms raised have been generated for the alpha peak frequency (Figure 4.17). Limits of agreement for the various postures covered the following ranges: Sitting posture ranged -2.45 (95% CI -3.42 to -1.47) to 2.14 Hz (95% CI 1.16 to 3.11) for channel O1, and -2.49 (95% CI -3.47 to -1.51) to 2.11 Hz (95% CI 1.13 to 3.08) for channel O2. Standing posture ranged -3 (95% CI -4.28 to -1.72) to 3 Hz (95% CI 1.72 to 4.28) for channel O1, and -2.09 (95% CI -3.01 to -1.16) to 2.27 Hz (95% CI 1.34 to 3.19) for channel O2. Standing with arms raised posture ranged -2.82 (95% CI -3.77 to -1.86) to 1.69 Hz (95% CI 0.73 to 2.64) for channel O1 and -2.61 (95% CI -3.65 to -1.56) to 2.3 Hz (95% CI 1.25 to 3.34) for channel O2.

The biases recorded during sitting are O1 = -0.16 Hz (95% CI 0.41 to -0.72) and O2 = -0.20 Hz (95% CI 0.37 to -0.76). Those recorded during standing are O1 = 0 Hz (95% CI 0.74 to -0.74) and O2 = 0.09 Hz (95% CI 0.63 to -0.45), and those recorded during standing with arms raised are O1 = -0.56 Hz (95% CI 0.01 to -1.12) and O2 = -0.16 Hz (95% CI 0.45 to -0.76). These show for both periods and both channels show that no significant or systematic bias exists.

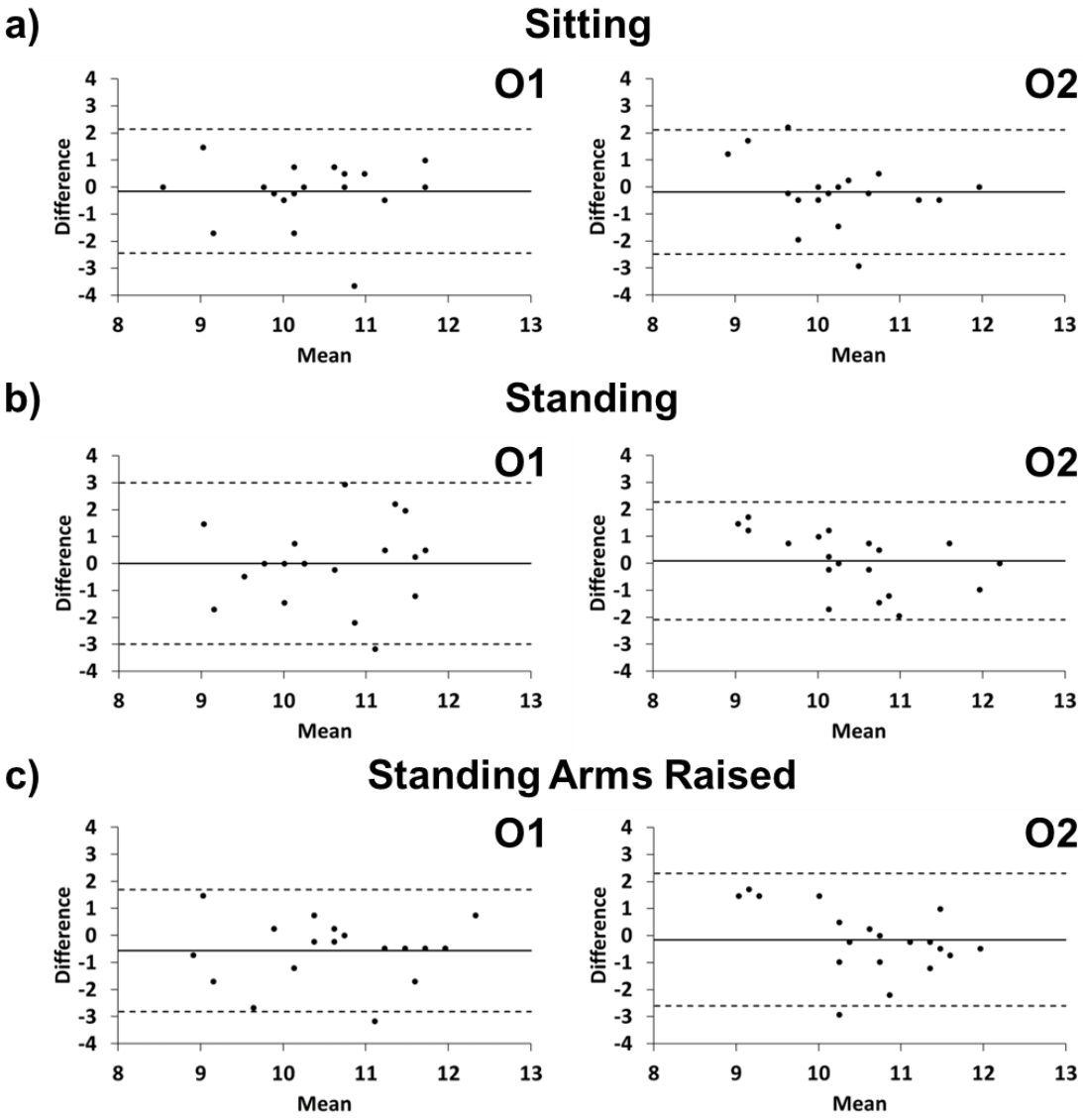

Figure 4.17 Bland-Altman plots for alpha peak frequency comparison between recordings made using Micromed and io:bio systems, recorded with eyes closed during participants **a)** sitting (n=19) **b)** standing (n=19) and **c)** standing with arms raised (n=19).

4.3.4.2.3 Bland-Altman plots for inter-system agreement of alpha AUC

The Bland-Altman plots comparing the two systems for agreement during participants sitting down, standing and standing with arms raised have been generated for alpha band AUC (Figure 4.18). Limits of agreement for the various postures covered the following ranges: Sitting posture ranged -0.33 (95% CI -0.49 to -0.16) to 0.44 (95% CI 0.28 to 0.61) for channel O1, and -0.32 (95% CI -0.48 to -0.15) to 0.48 (95% CI 0.31 to 0.65) for channel O2. Standing posture ranged -0.44 (95% CI -0.64 to -0.24) to 0.5 (95% CI 0.30 to 0.70) for channel O1, and -0.45 (95% CI -0.64 to -0.25) to 0.47 (95% CI 0.28 to 0.67) for channel O2. Standing with arms raised posture ranged -0.33(95% CI -0.50 to -0.16) to 0.47 (95% CI 0.30 to 0.64) for channel O1, and O2 -0.33 (95% CI -0.49 to -0.17) to 0.43 (95% CI 0.27 to 0.59) for channel O2.

The biases recorded during sitting are O1 bias = 0.06 (95% CI 0.15 to -0.04) and O2 bias = 0.08 (95% CI 0.18 to -0.02). The biases recorded during standing are O1 bias = 0.04 (95% CI 0.15 to -0.08) and O2 bias = 0.02 (95% CI 0.13 to -0.10). The biases recorded during standing with arms raised are O1 bias = 0.07 (95% CI 0.17 to -0.03) and O2 bias = 0.05 (95% CI 0.14 to -0.04). The biases recorded for all three postures and both channels show no systematic bias exists.

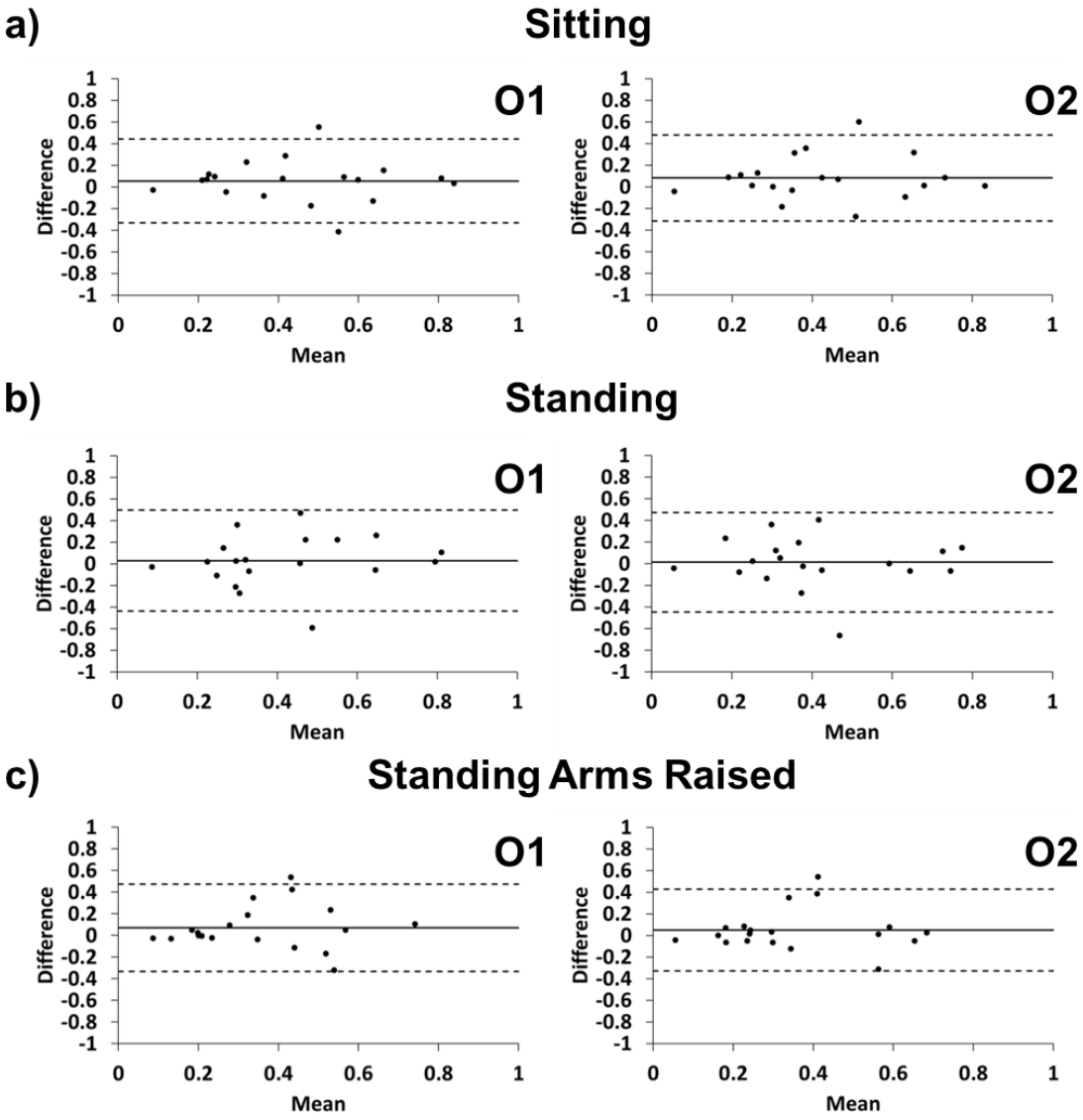

Figure 4.18 Bland-Altman plots for alpha band Area Under the Curve(AUC) comparison between recordings made using Micromed system and io:bio system, recorded with eyes closed during participants **a)** sitting (n=19) **b)** standing (n=19) and **c)** standing with arms raised (n=19).

4.3.5 Participant walking

Example time series plots are shown in Figure 4.19 for a single participant lying down and walking recorded with the io:bio and the Micromed mobile EEG system. Both systems exhibit an increase in noise during participant walking, but it is unclear from the time series if this noise occurs only at specific frequencies or across the band of interest (0 to 30 Hz). In consideration of ascertaining the noise frequency content the first 15 seconds of data captured during participant walking was analysed for PSD. The resulting plots taken from eight selected channels (Fp1, Fp2, Fz, Pz, T3, T4 O1, O2) are shown in Figure 4.20. This subset of channels was used as all other channels were too noisy for analysis. For each channel, 15 seconds of data captured during participants lying down with eyes open was plotted alongside participant walking. Data recorded across all of the plots for the eight channels during participant lying down with eyes open are very similar across both systems. During participant walking, the power across the spectrum has increased notably for both systems across the frequency band of interest. The level of power increase is higher for the io:bio system in comparison to the Micromed system.

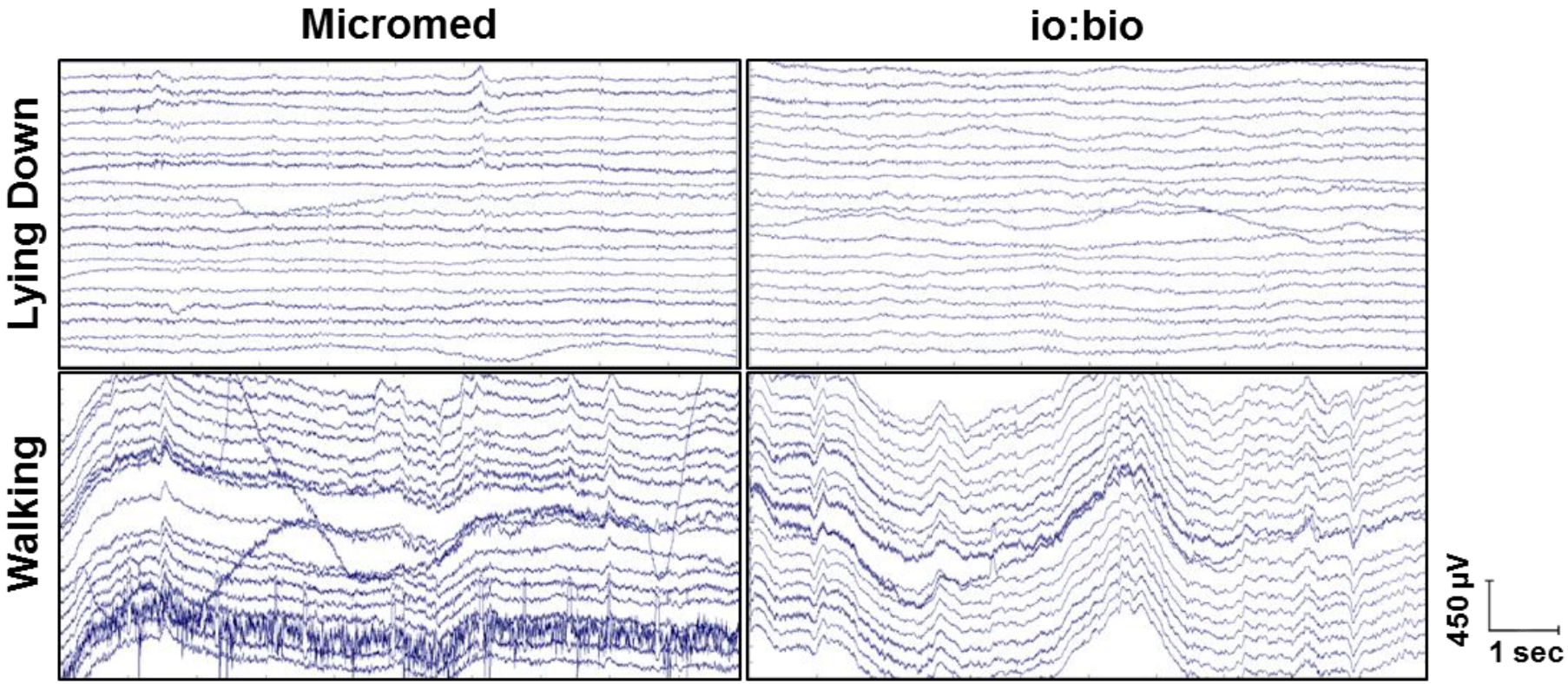

Figure 4.19 EEG time series plots (19 channels) from data recorded using Micromed (left) and io:bio systems (right) from a single participant lying down with eyes open (top) and walking with eyes open (bottom). Data band pass filtered (0.5 to 40 Hz).Channel labels as in Figure 3.12.

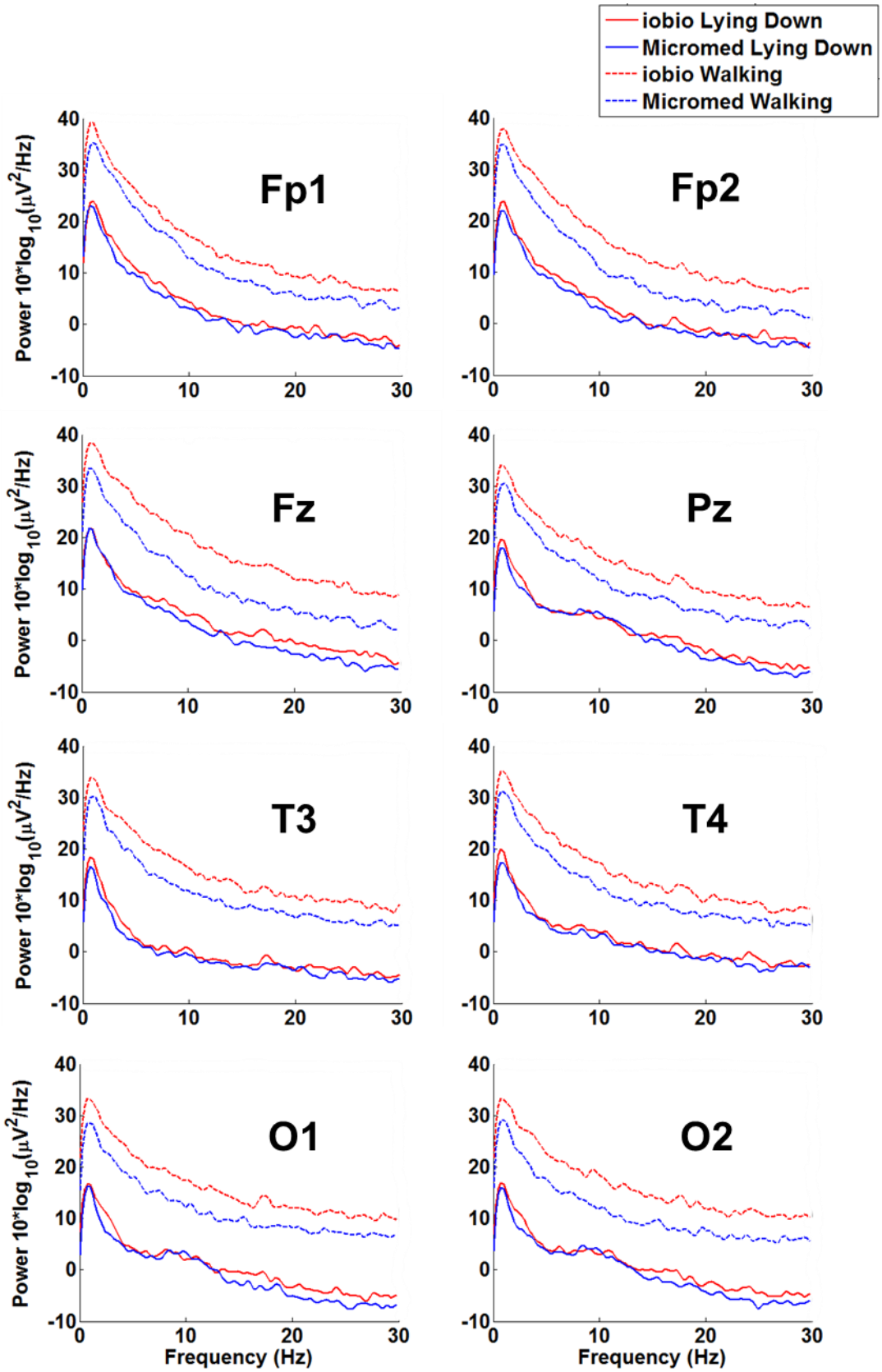

Figure 4.20 Power spectrum density plots from data recorded using Micromed system (blue) and io:bio system (red) with participants lying down with eyes open (solid) and walking with eyes open (dashed), n=16 participants.

4.4 Discussion

This chapter demonstrates that the io:bio system, via its smartphone app, can acquire and record EEG data that has a high concordance with data recorded using a FDA approved commercial system. The validation tests performed showed the two systems to be comparable. The use of the io:bio system paired with a smartphone rather than a PC for EEG recordings enables an increase in the degree of participant mobility without compromising data quality or integrity.

Initial statistical validation of the io:bio EEG system against the commercial system was performed using a paired t-test (with Bonferroni correction for multiple comparisons) on values for alpha peak frequency, amplitude and area under the curve for the alpha band in participants with eyes closed. No significant differences were found between the values obtained from the two systems in either intra-system or inter-system comparisons. However, when using a t-test information of individual measurement differences are not considered, and although a test of significance identifies when two systems used to record EEG data are related, it does not quantify agreement between them [126]. Moreover, the application of a Bonferroni correction within the current context increases the likelihood of the null hypothesis being rejected (i.e. that a significant difference between measures exists). However, if an uncorrected p value of 0.05 is selected (p value is actually more conservative in this context) there is still no significant difference in the vast majority of channels for the intra-system or inter-system comparisons for alpha peak amplitude, frequency of AUC (see Tables 4.2 and 4.3). This supports the conclusion that the Micromed and io:bio systems produce recordings that are similar.

Alpha peak frequency, peak amplitude and area under the curve for the alpha band were compared for both EEG systems using a Bland-Altman plot approach to assess individual differences that are not assessed when performing a comparison of means. *A priori* decisions for limits of agreement of ± 2.5 Hz for intra-system alpha peak

frequency comparisons and ± 3 Hz for inter-system alpha peak frequency comparisons were defined to allow for biological variation. The intra-system alpha peak frequency variability, as demonstrated in the Bland-Altman plots (Figure 4.9), have narrower limits of agreement in comparison to the inter-system equivalent plots (Figure 4.10). This is to be expected as not only are the two periods (period 1 and period 2) of recorded data taken using the same system, they are also taken very close together in time, thus limiting the variation in brain activity over time. Since it would be reasonable to assume that the commercial FDA approved mobile EEG (Micromed) has good repeatability, and the finding that the limits of agreement for both systems have overlapping confidence intervals, it is also reasonable to regard the io:bio mobile EEG system as having good repeatability. This is an important finding since if either system had poor repeatability then the agreement between the two systems is also bound to be affected [126]. The intra-system repeatability is critical within clinical and research settings [127], and since the io:bio has within system repeatability it can be used in these settings.

When the Bland-Altman plots for inter-system variability are visually considered in comparison to their intra-system counterparts it becomes evident that the limits of agreement widen in all cases (amplitude, frequency and AUC). This is not only accounted for by the differences between the two systems but probably by the greater time between the two recordings, where there may alterations in the variation level of brain activity. Napflin *et al.*, suggest that the reproducibility of spectral EEG observations for inter-individual variation of EEG spectra is large even for the same task [121]. When this is considered alongside the findings of Haegens *et al*., where alpha peak frequency increases with cognitive demands and task engagement [145], it indicates the variability of brain activity in study participants. The results obtained in the current study for inter-system variability are within the limits defined *a priori*, and therefore the io:bio mobile EEG system can be used interchangeably with the Micromed mobile EEG system. One potential criticism of the Bland and Altman approach taken is that the *a priori* limits may have been set too liberally although the various *a priori* parameters set were not simply subjective but were justified (see Section 4.2.5).

The Bland-Altman plots generated for sitting, standing, and standing with arms raised while participants had their eyes closed are similar to those for participants lying down with eyes closed, for both systems. The limits of agreement were also similar across the range of postures. This indicates that the various postures were unlikely to impact upon the parameters derived from the EEG recordings made with both systems. This is encouraging, and indicates that participants can deviate from the sitting posture without artifacts negatively impacting upon the EEG recordings. Work by Price *et al*., also included EEG recordings with participants in different postures as part of a study into mild traumatic brain injury (MTBI) but was constrained to just three seated postures (leaning, upright and reclining) [146]. The study was not interested in the effects of the postures on the EEG recordings *per se*, and excluded data from some participants due to the presence of a large number of movement related artifacts. This highlights that movement artifacts are present in some cases even though the posture range was limited to only varying types of sitting. A study by Slobounov *et al*., combined EEG with a balance study in an attempt to document the efficacy in the assessment of MTBI patient recovery [147]. This study used sitting, standing and standing on a balance board as patient postures. What is perhaps surprising is that no comment was made about participant data exclusion due to movement artifacts beyond stating that epochs were rejected that contained eye blinks, movement or heartbeats. Since each of the postures only occur once in the participant experiment protocol it was not possible to perform intra-system comparisons. Furthermore, it is not possible to say if the limits of agreement are acceptable or not since they were only defined for the lying down posture and in that case they had to be within a limit of twice that of intra-system limits of agreement. A future study which involves a repeat protocol design is needed to make intra-system comparisons possible.

The first 15 seconds of data captured during participant walking were analysed for power spectral density (participants lying down with eyes open was used by way of comparison), and the resulting plots taken from eight example channels (Fp1, Fp2, Fz, Pz, T3, T4, O1, O2) showed that the power increased for both systems across the 0 to

30 Hz frequency band. The time series traces showed evidence of movement-related noise and it is reasonable to conclude that both the time series noise and the increase in associated power amplitude are likely due to electrode displacement during participant walking. The level of power increase in each case was higher for the io:bio system in comparison to the Micromed system. This suggests that the io:bio system may have a greater sensitivity to impedance changes and could result from the lack of filtering circuitry on the channel inputs that may operate in the Micromed system (no filtering circuitry was used prior to ADS1299 IC in the io:bio system). The EEG data recorded using either system has shown that participant walking has a negative influence upon data quality. Specifically, the noise level (unwanted signal) increases across the 0 to 30 Hz EEG frequency band during participant walking.

Since both EEG systems were waist-mounted they scored 2D for device mobility, with an overall CoME score of (2D,3P,12S) for unconstrained participant walking. When the CoME scheme was developed the rational for scoring a waist-mounted mobile EEG system 2D (when no additional equipment is required) was due to several reasons. Firstly, the reduced likelihood of movement-related artifacts due to electrode displacement when using this mounting position [36,74]. Secondly, the concern that electrode leads cannot be fastened to the participant sufficiently well to completely remove electrode wire movement as this will then cause restricted head movement [75]. Thirdly, that the length of electrode wires can result in increased electromagnetic interference [36,76].

In the methodological protocol by Badcock *et al.,* [129] an electrode cap was used with the system for comparison (EPOC, Emotiv, U.S.A.) being fitted on top of the electrode cap of the gold standard system (Neuroscan Synamps). Slits were made in the electrode cap to allow the comparison system electrodes access to the scalp surface. Although a similar approach could have been taken in this thesis it was not suitable as all electrode sites were required to be located in the exact same scalp locations for both EEG systems. If they did not coincide, it would have led to critical questions being raised about differing electrode sites used in the validation process. Jackson *et al*., [128]

and Omurtag *et al*., [130] used an approach where both EEG systems were connected to an electrode cap in parallel using a signal splitter arrangement. This has the advantage of being able to record simultaneously from the same electrode positions. However, there was no discussion as to how they were able to ensure that no system interaction occurred while the two systems were connected simultaneously. It would have been interesting to show how the two systems would have performed in the same experimental conditions when connected separately as was undertaken in the current study using the io:bio and Micromed systems. A sequential recording approach was adopted in this thesis to prevent problems with different electrode placings or potential issues with signal splitting and cumbersome double electrode lead wiring arrangements on participants in the various postures and walking. However, since recordings were not taken at the same time, biological variations were likely to be introduced. Repeat periods of eyes closed were added to the protocol in an attempt to minimise variations in brain activity.

The io:bio system was developed into a waist-mounted device since this matched the mounting modality of the Micromed gold standard and allowed easy connection and disconnection of the EEG electrode cap during the current experiment. However, published research suggests that the waist is not the optimal location for a mobile EEG device, and that fully head-mounted systems should provide recordings with lower electrode displacement-related artifacts [36,74]. A head-mounted configuration is further considered in this thesis in Chapter 6.

The overall purpose of the io:bio mobile EEG system is to enable the potential for novel research studies in mobile EEG. Now that the validation of the prototype against a commercial EEG system has been accomplished, this overall purpose has been realised. Further development could seek to focus upon system facets such as: mounting position, app functionality and app platform (smartphone, PC, gaming engine, VR environment). Each of these attributes allow for variations in approaches to mobile EEG studies that could provide new knowledge in the field. In the next chapter the validated io:bio waist-mounted system is further advanced by making utility of the smartphone to develop and test mobile ERP capability of the system.

4.5 Conclusions

The io:bio mobile EEG system was validated against a commercial FDA approved system in human participants. Using recordings of alpha waves, no significant differences were found in results for intra-systems or inter-system comparisons. Bland-Altman plots showed that the differences between the values obtained from each system were within the *a priori* defined acceptable limits of agreement, and that the two systems can be used interchangeably.

Chapter 5: Recording event-related potentials (ERPs) using the io:bio smartphone-based waist-mounted mobile EEG system

5.1 Introduction

Event related potentials (ERPs) [148] are brain responses to time-locked stimuli presented to participants. Event-related potentials have been recorded in sensory modalities including visual [10,149,150], and auditory [151-153]. Auditory ERPs have been used in BCI applications [51,53,88,154-156] and have been recorded in clinical conditions including Parkinsons [157], dementia [158], Alzheimers [8,159], schizophrenia [160-162], and coma [3]. With such studies in mind there are clear benefits to be attained in terms of research potential if the smartphone-based io:bio system was developed beyond the research presented in the previous chapter to include an auditory ERP capability of the system.

The ERP waveforms components recorded as a result of presenting stimuli are described according to latency (with respect to the stimulus presentation at time zero) and amplitude (positive or negative polarity) [148]. Therefore, ERPs require the EEG data to be marked, or time-stamped, when each of the stimuli is presented. This then enables the averaging process to be undertaken post-recording by taking a known number of milliseconds prior to the event (pre-stimulus stimuli presentation), along with a number of milliseconds after the event, for each stimulus. The time period taken prior to the event provides a baseline for comparison to the post-stimulus period and a value of around 200 ms duration is used [163]. The time taken after the event largely depends upon the type of stimuli being presented, and the latency of the expected response, but is around 800 ms [36].

To extend the research capabilities of the io:bio EEG system, it is desirable to add an ERP capability to its functionality. Adding this capability would complement the system's ability to record on-going brain activity and allow many more research experiment possibilities. To achieve this aim the presentation of stimuli is required to be performed by the smartphone and the recorded EEG data marked so that the analysis of ERP responses to the events can be post-processed. In Chapter 3, the io:bio system was developed which connects wirelessly to a smartphone with a dedicated

app developed to control the function of the io:bio box and record acquired EEG data. By additional coding of the app to include an ERP option, and exploiting the smartphone to play sounds, this would enable the undertaken of auditory ERP experiments using the io:bio system.

Auditory-based stimuli can readily be presented to participants by a smartphone via commercially available headphones, and a range of tones played. This would provide the added benefit of being safe to use with participants in mobile settings. A specific paradigm for the auditory ERP experiment requires defining to be able to plan the specifics of the app developments and their implementation. A well-established paradigm provides the benefit of having numerous published results sets to compare. The Micromed mobile system used as a comparator system in Chapter 3 and 4 could not be used as it does not have an ERP capability.

The auditory 'oddball paradigm' is an established method to conveniently elicit auditory ERP components. This paradigm was first described by Ritter and Vaughan [164] as a signal detection paradigm, and involves the presentation of a sequence of repetitive stimuli that are infrequently interrupted by a deviant, or oddball, stimulus such as a sound at a distinctly different tone. The key components of interest are the N100, N200 and P300. Each of these components will be introduced, and the function they are thought to be involved with.

The N100 component is a prominent frontocentral negative peak with a latency of approximately 80 to 120 ms in response to auditory stimulation [162]. It occurs as a response to unexpected stimulus, and has the largest magnitude typically at the Cz electrode [165]. The next ERP component is the N200 since it is the earliest ERP component to differentiate target from non-target consistently in an oddball task [159]. It occurs 200 to 350 ms after the stimulus is applied but only when the stimulus is of interest, as in the case with an auditory oddball paradigm when the deviant stimulus is detected. It is found primarily over anterior scalp electrode sites [166]. The P300 was first

described by Sutton *et al.* [167] in 1965, and since then there has been an abundance of research on this component [42,43,51-53,78,88,154,168-176]. When produced in response to auditory stimuli, the P300 has a latency in the region of 250-400 ms for most adults in the range 20 to 70 years old [148]. It is understood to be a response to low probability task-relevant stimuli in auditory, visual and somatosensory modalities. Its amplitude is sensitive to stimulus probability [177], and task relevance of the eliciting stimulus, and its latency reflects stimulus evaluation time [178].

In this chapter, the io:bio mobile EEG systems functionality is extended by adding ERP capability. This will make use of the smartphone and be achieved as an incorporation into the existing app. The app will make use of the smartphones capability to deliver sounds via headphones in an auditory oddball paradigm. Analysis of the EEG responses to the auditory stimuli is to be enabled by adding a marker channel. This marker channel will indicate at what time point a sound has been presented and which sound has being played. Participants will perform the paradigm while sitting and when walking in an attempt to utilise the mobile aspects of the io:bio systems developments.

5.2 Methods

In this section, a description of how the ERP part of the smartphone app was developed, coded and tested is presented, followed by the participant experimental procedures undertaken.

5.2.1 Adding ERP capability to the smartphone app

The addition of ERP functionality will mean that a whole new series of analysis techniques, relating to events rather than steady state responses, will be made available. A smartphone can be used to supply the stimuli by adding a scripted sequence of auditory stimuli presentation to the app functionality. The smartphone can then sychronise the presentation of individual stimuli to the EEG data recordings with the use of a marker channel. Both the stimuli presentation and the data marking that are required to perform an auditory oddball paradigm based experiment can all be achieved through the smartphone app.

The app has been modified to provide an ERP option from the main menu (Figure 5.1a). Upon selection the user is presented with a dialogue box for a participant reference (alphanumeric string) and an accept button(see Figure 5.1b). The user's input is used as part of the file name to enable identification of anonymised participant data, from the capture stage through to analysis. Whatever is inputted as a participant reference, has 'ERP' addended to distinguish from non-ERP data files. After the filename has been accepted the user is presented with a byte count, time count and a start button (see Figure 5.1c). When the start button is pressed, the byte count and time count increment accordingly to indicate the passage of time, that the app has not crashed, and that data is being received.

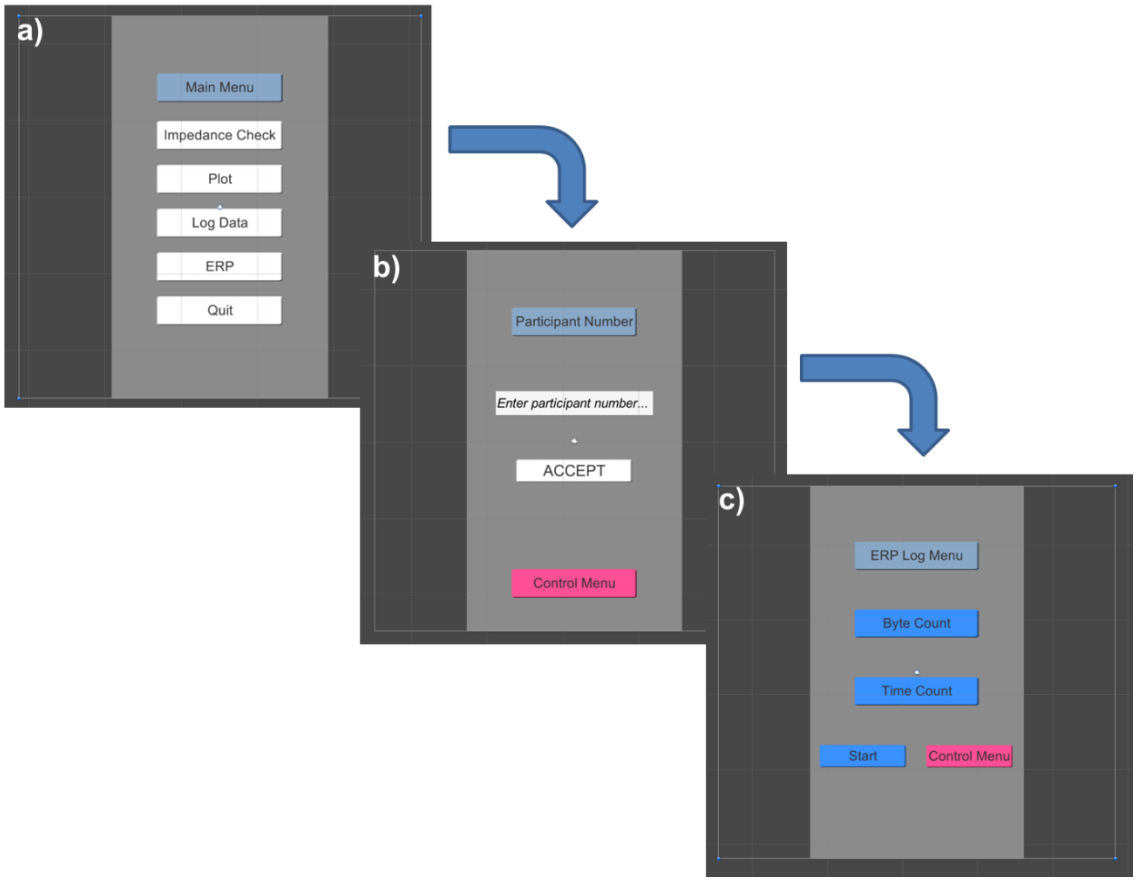

Figure 5.1 Smartphone app transitional screens showing **a)** main menu **b)** dialogue box for a participant reference and **c)** byte count, time count and a start button for the ERP experiment.

The frequency and duration of the tones used in the smartphone app had to be selected to best achieve the expected responses of the auditory oddball paradigm. The two frequencies to be presented to participants had to be both in the human hearing range and clearly distinguishable from each other. Audacity software was used to create the two pure tones of 600 and 1200 Hz, each with a duration of 62 ms. The beginning and end of both tones were modified to create a 10 ms rise and fall time (see Figure 5.2). This was performed to avoid clicking sounds being produced by potential discontinuity as this would change the nature of the auditory stimuli and thereby the recorded ERP responses. The tones were then saved as WAV files in an uncompressed audio file format. The audio files were added to the app in Unity in uncompressed format to remove the overhead of uncompressing the file at playback. Since the timing of stimuli application and associated data marking are required to be synchronised, any unnecessary processing that could impact upon this was minimised.

It should be noted that since the presentation of the stimuli were coded into the existing app, the duration and number of stimuli presented could only be changed by editing the underlying code and recompiling the app. The tone to be presented at any one time (600 or 1200 Hz) was coded to be pseudo-random with a ratio of 5 to 1.

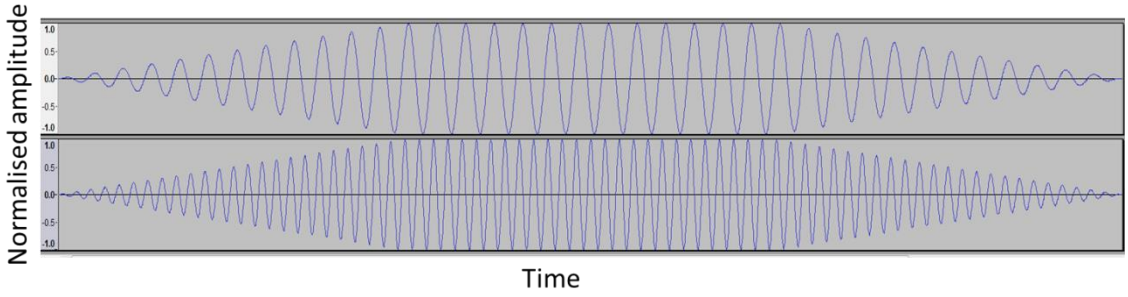

Figure 5.2 Pure tones of a) 600 and b) 1200 Hz created in Audacity and saved as WAV files. The duration was 62 ms with 10 ms rise and fall.

5.2.1.1 Creating ERP data markers

The incoming EEG data, containing stimuli responses and received via Wi-Fi on the smartphone, was marked according to the tone presented to the participant (common or uncommon tone). Therefore, the markers were numbered according to the tone they related to. Measurement timing errors relating to stimuli presentation and the corresponding EEG data marking is of concern when performing ERP experiments even when using well established hardware and software combinations [179,180]. There is the potential for timing errors to become even more problematic when the EEG data is streamed wirelessly over a Wi-Fi connection to a smartphone. Initial testing took place to measure and reduce timing errors. A set up using a microphone was used to provide a data recording on a differential channel of the io:bio system. As the auditory stimuli was presented via headphones linked to the smartphone and the responses recorded by placing the microphone into one of the headphone ear buds. This provided a sampled response waveform to assist in aligning the marker temporally with the

stimulus event. The app functionality was also tested by analysing the sampled sound inputs as though they were ERPs, and thereby averaging the response. Figure 5.3 shows the response timing from initial testing where there is a delay of around 350 ms between the marker and the onset of the sound. A 350 ms correction timing delay was inserted between the instruction to play the sound and the subsequent marking of the data. The plot in red colour shows the resultant response and increased timing accuracy (Figure 5.3). It should be noted that the marker was aligned as shown in Figure 5.3 as this was deemed the earliest point when the signal could be distinguished from the baseline noise. It was assumed that this realignment became necessary as the audio file is processed separately by the audio processing subsystem of the smartphone and the 'handing over' of the data to that subsystem takes time.

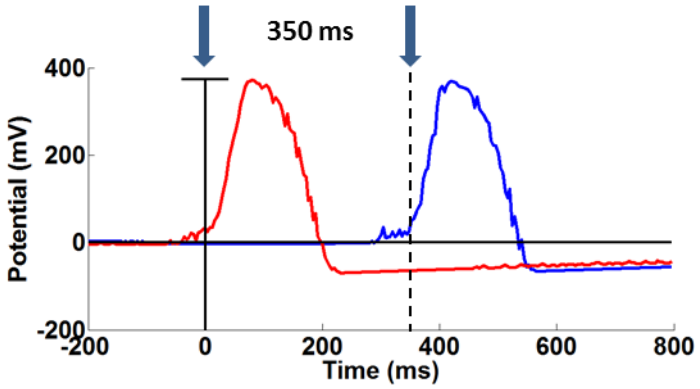

Figure 5.3 Microphone response timing tests: before latency modification in blue colour, and after latency modification in red. The solid vertical line/downward arrow represents the onset of the stimulus onset. The dashed vertical line/downward arrow represents the onset of the response before correction.

5.2.1.2 EEGLAB plug-in for data importing

A plug-in for EEGLAB was also developed to facilitate the importing of data from the io:bio mobile EEG system. The plug-in incorporated an additional 8 bit marker channel required for ERP analysis, and capable of providing markers for 255 different events (0 = no marker, 1 to 255 = individual event markers). Since the approach to loading in the EEG data was not restricted by the EDF+ format, it enabled analysis at a 24 bit rate. In the previous chapters (see Chapters 3 and 4), EEG data was limited to the restrictions of the EDF+ file format, and thereby 16 bit data.

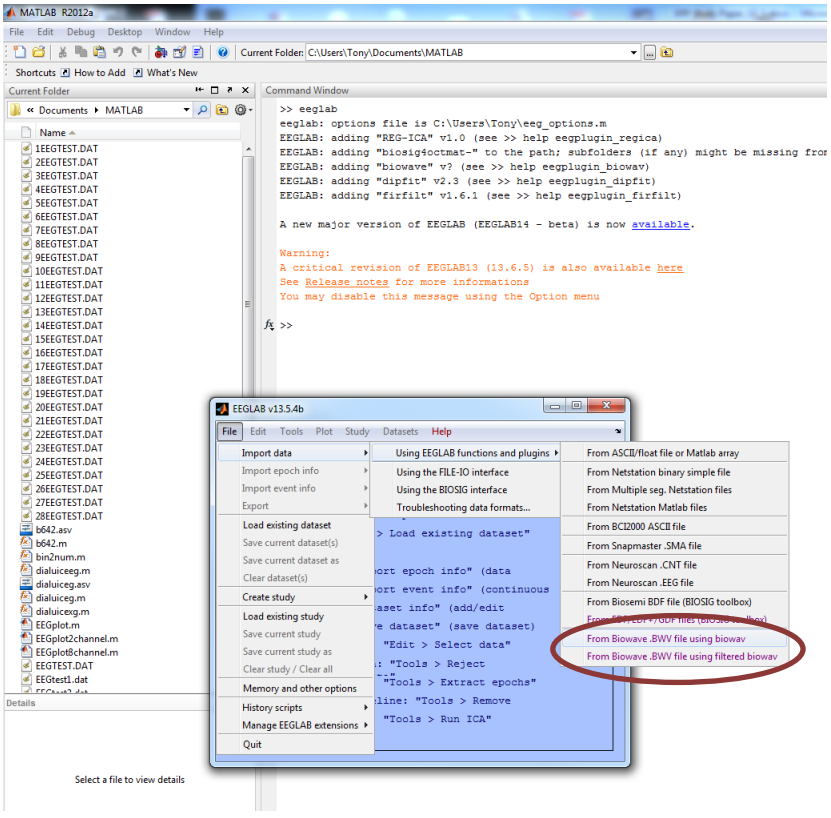

Figure 5.4 EEGLAB plug-in enabling io:bio recorded data to be loaded with or without filtering (high pass 0.15 Hz).

Since the experiment used a 19 electrode EEG cap conforming to the international 10/20 system of distribution, a corresponding spherical head model (4-shell dipfit) was used in EEGLAB. It should be noted that the head shape of individual participants was not captured and while the spherical head file provides spatial information of the electrodes in the form of three dimensional co-ordinates that deviate from the exact individual head shapes this approach should not produce significant errors [181]. This spatial information is needed when certain types of analysis are used within EEGLAB, such as topographic maps or independent component analysis.

5.2.2 Experimental Procedure

5.2.2.1 Participants

Twenty-eight participants were recruited (18 to 24 years, mean ± SEM age 19.7 ± 0.33, 18 males and 10 females), and all completed health questionnaires and consent forms prior to participation. All participants were healthy with no self-reported history of neurological disorders. The Hull York Medical School Ethics Committee provided ethical scrutiny and approval for the study.

5.2.2.2 Participant Protocol

The participants were set up with the EEG system and smartphone (Asus Zenfone 2) as illustrated in Figure 5.5. The electrode wells were filled with conductive gel and the impedance checked to be below 5kΩ to maintain signal quality. All scalp electrodes were referenced to the right ear. Data recordings were imported directly into EEGLAB [109] using the coded plug-in. The sequence in which the auditory ERP tasks (sitting and walking) were tested was alternated for each participant so as to prevent ordering effects.

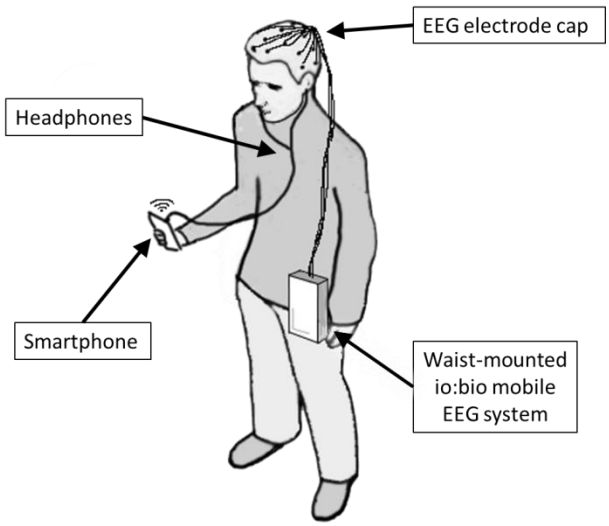

Figure 5.5 Overview of participant setup detailing the EEG system mounting position.

Two pure tones were presented binaurally with consumer in-ear headphones (Samsung EO-EG920BW). The volume was set at a comfortable level for each individual participant. Before the experiment was started, participants were presented with a brief practice run to both establish a comfortable volume and to clarify the distinction between the two tones. Standard (600 Hz) and deviant (1200 Hz) audio tones were presented in randomized order (ratio of 5 to 1) at a fixed inter-stimulus interval of 1000 ms and a duration of 62 ms. A total of 417 trials were recorded for each participant. To maintain attention, participants were asked to silently count the deviant tones and provide a verbal total at the end of the recording. The two tasks that participants were asked to perform were either: sitting or walking around a large table, while performing the auditory oddball task. The participants were asked to focus upon a fixation cross while performing the sitting version of the task.

5.2.3 Analysis Methodology

Major artifacts were first excluded by visual inspection, and EEG in each channel bandpass filtered from 0.1 to 20 Hz by implementing a zero-phase Hamming-windowed sinc FIR filter in EEGLAB. Trial epochs were extracted (-200 to 800 ms) and baseline corrected (-200 to 0 ms). After epoching, trials containing voltage changes in excess of 100 μV in any channel were removed from the analysis. Participants with more than 75% of epochs removed were completely removed from the analysis. Accepted epochs were averaged together to create a standard and deviant ERP waveform for both sitting and walking conditions, at each scalp site. The deviant ERP waveforms in both sitting and walking conditions were used to measure the N100, N200, and P300 peak amplitudes. ERP peaks and components were defined in line with Luck, by their polarity and latency [182]. More specifically, the components were defined as occurring post-stimulus onset in the following latency windows: N100 being a negative going peak between 52 - 152 ms, N200 being a negative going peak between 152 - 252 ms, and P300 being a positive going peak between 252 - 348 ms.

5.3 Results

Figure 5.6 shows an example section of data recorded from a single participant showing nineteen EEG channels. The recorded data channels are shown along with the two markers that relate to the two tones being played.

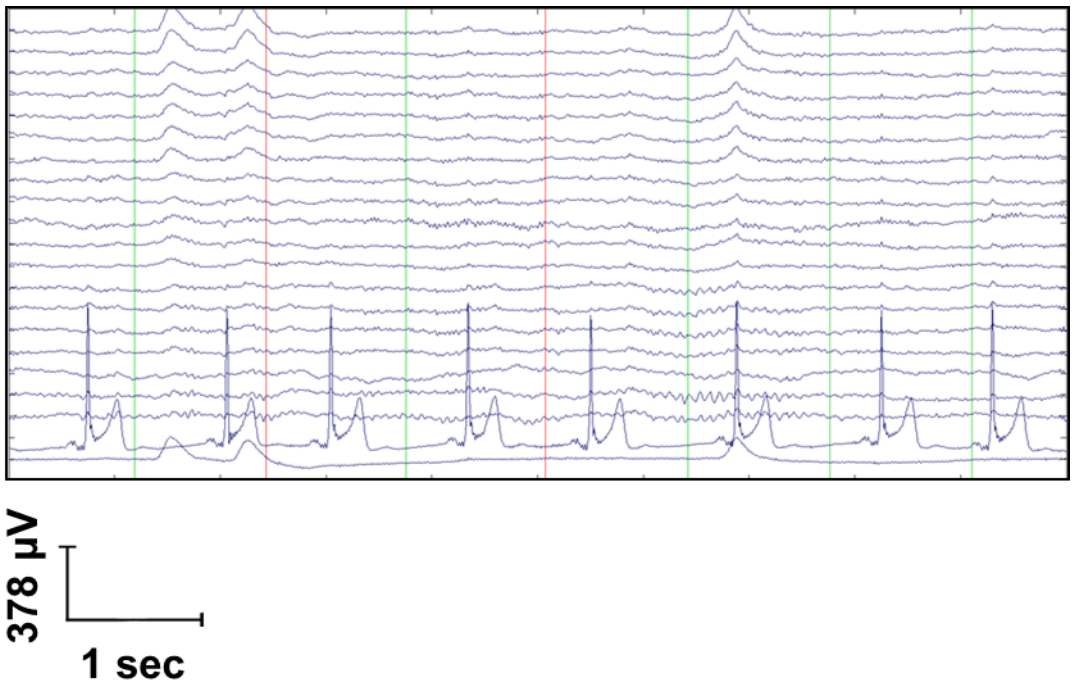

Figure 5.6 An example of seated participant time series data plotted using EEGLAB showing 19 EEG channels, ECG channel and EOG channel (bottom channels), and event markers (red colour=deviant and green=standard tones). Channels are organised with EEG from FP1 at the top to O2 (as in Figure 3.12) followed by an ECG and an EOG channel at the bottom.

5.3.1 Auditory ERPs during sitting

ERP plots for the grand mean responses to both tones during sitting, for all 19 EEG channels, are shown in Figure 5.7. Responses that differ for standard and deviant tones, have successfully been acquired using the io:bio system. The N100 deviant response is most dominant at the Fz electrode with an amplitude of -7.3 ± 0.7 μV. The N200 response is most dominant at electrodes Fp1 and Fp2. The amplitude at Fz (-3.9 ± 1.0 μV) was negative whereas at Cz (0.4 ± 0.9 μV) and Pz (0.6 ± 0.9 μV) was positive. Deviant ERPs evoked a P300 that was most prominent in the centroparietal region. P300 peaks occurred most prominently in channels Cz, Pz, P3, P4, O1, and O2. The amplitudes and latencies are presented for all three components at electrodes Fz, Cz and Pz in Table 5.1.

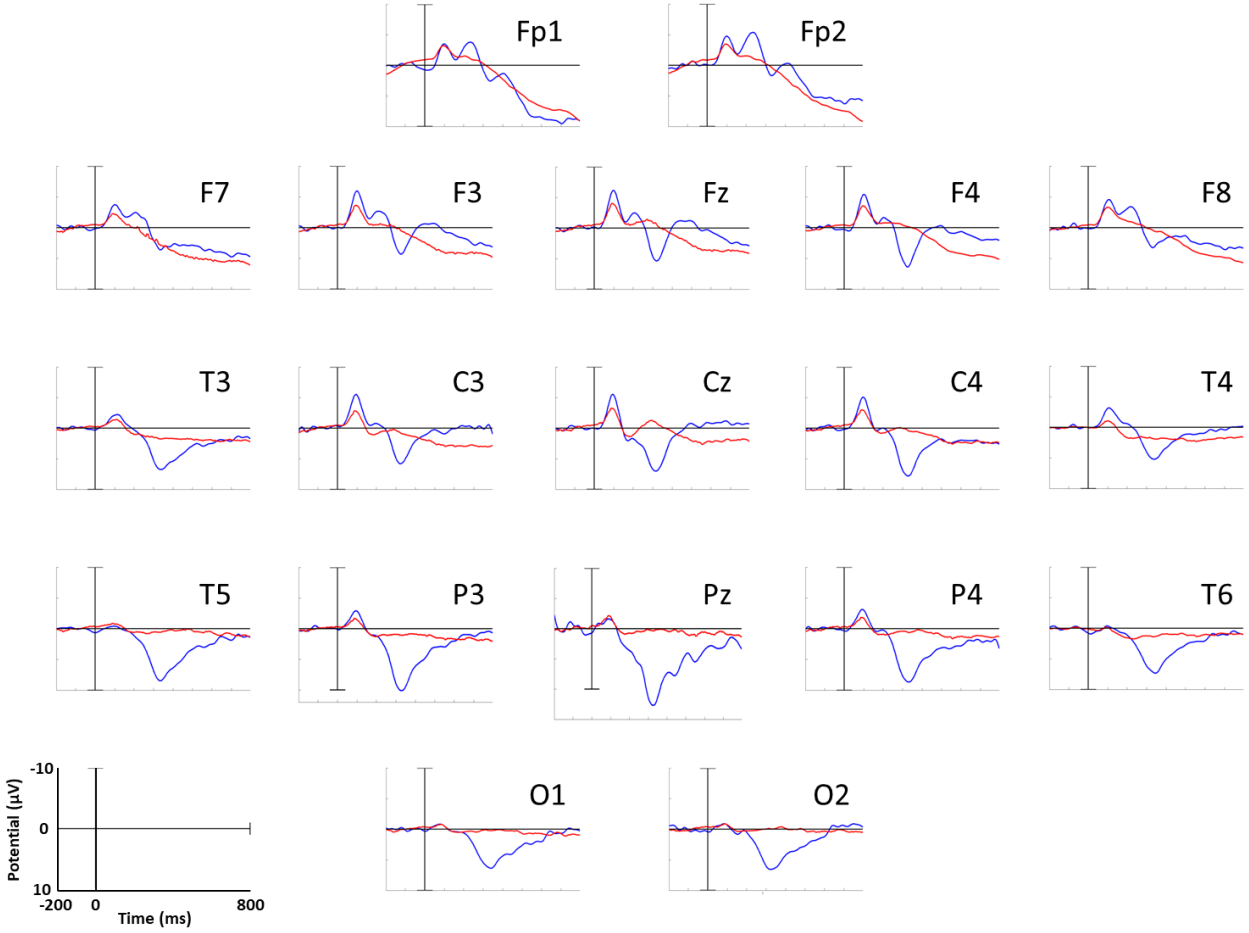

Figure 5.7 Grand mean ERPs at 19 electrode sites recorded during participant sitting using the developed io:bio ERP system. Plots show responses to the standard tone (red colour) and the deviant tone (blue). Negative voltage is plotted upwards. n=20-27.

Table 5.1 Grand mean latencies and amplitudes of N100, N200, and P300 components obtained for deviant tones at channels Fz, Cz and Pz during sitting.

	N100		N200		P300	
Channel	**Latency (ms)**	**Amplitude (μV)**	**Latency (ms)**	**Amplitude (μV)**	**Latency (ms)**	**Amplitude (μV)**
Fz (n=26)	99.7 ± 3.1	-7.3 ± 0.7	224.3 ± 5.4	-3.9 ± 1.0	323.9 ± 5.1	7.0 ± 1.7
Cz (n=23)	95.8 ± 3.4	-5.2 ± 1.0	221.1 ± 5.8	0.4 ± 0.9	318.3 ± 5.8	9.2 ± 1.6
Pz (n=23)	93.9 ± 4.3	-3.9 ± 0.5	206.6 ± 6.1	0.6 ± 0.9	320.7 ± 5.9	11.2 ± 1.5

5.3.2 Auditory ERPs during walking

An example of time series EEG data recorded during walking is shown in Figure 5.8b, and exhibits artifacts and much higher peak-to-peak amplitudes than those obtain during the sitting condition (Figure 5.8a). ERP plots for the grand mean responses to both tones during walking, for all 19 EEG channels, are shown in Figure 5.9. Visual inspection shows that the responses for standard and deviant tones during walking differ from those obtained during sitting. The N100, N200 and P300 components are still in evidence: they differ in both latency and amplitude magnitudes as well as profile. However, it was not possible to extract the latencies and amplitudes of components from the majority of the walking datasets at the level of each individual participant. Figure 5.10a,b shows the mean individual plots from two example participants versus the grand mean plots for all participants at electrode Fz (Figure 5.10c). Note that the two example walking condition individual participant's show differing ERP profiles, latencies and amplitudes, both from each other, and their sitting condition counterparts. In contrast, the grand mean plots for walking at most electrode locations show N100, N200 and P300 components (Figure 5.9). Since the N100, N200 and P300 components could not be discerned at the level of each individual participant, it was not possible to calculate means ± SEM values for the associated ERP amplitudes and latencies during walking.

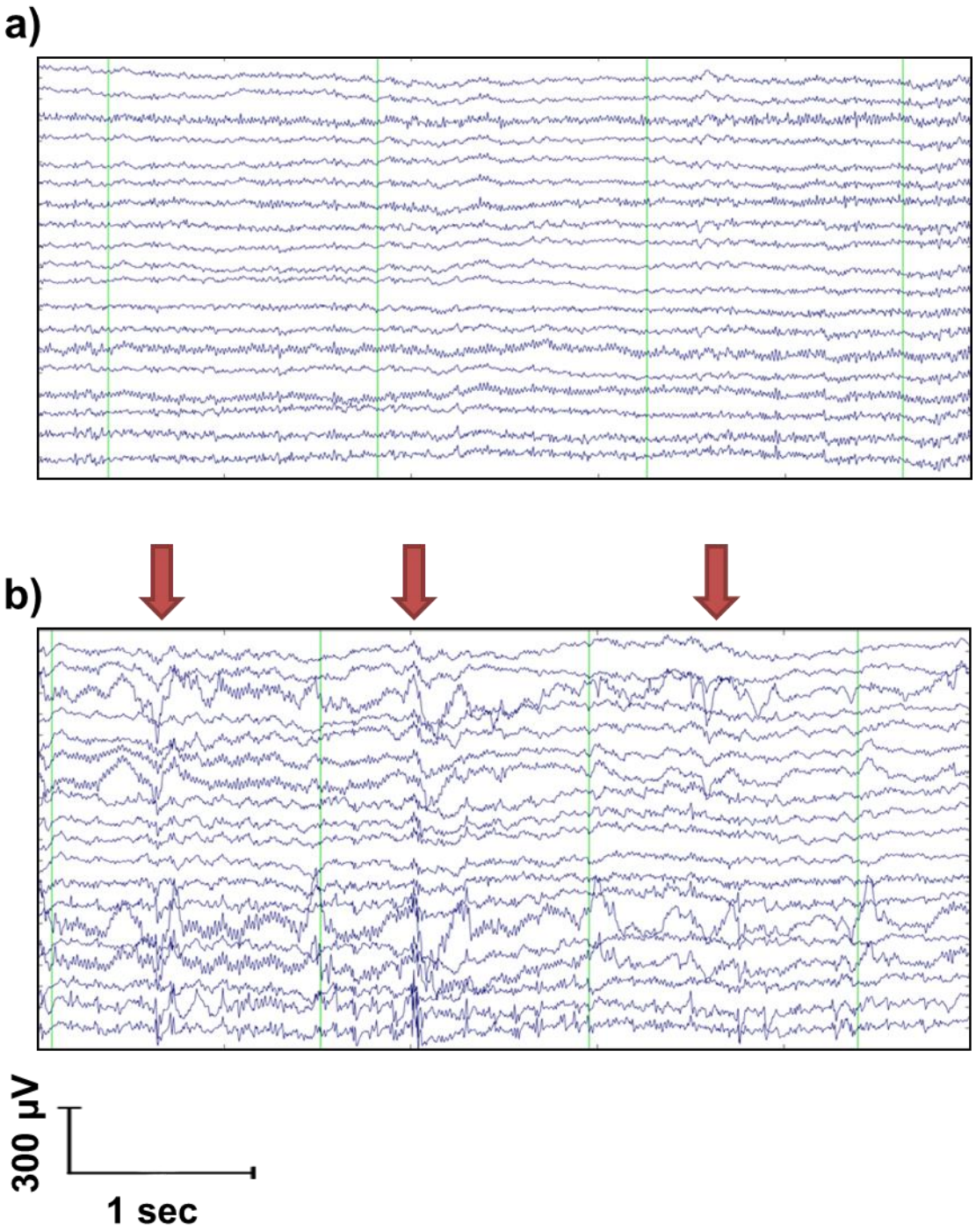

Figure 5.8 Example of a single participant time series EEG data recorded during **a)** sitting and **b)** walking. Note the presence of artifacts, some of which are highlighted by red downward arrows. Channel labels as in Figure 3.12.

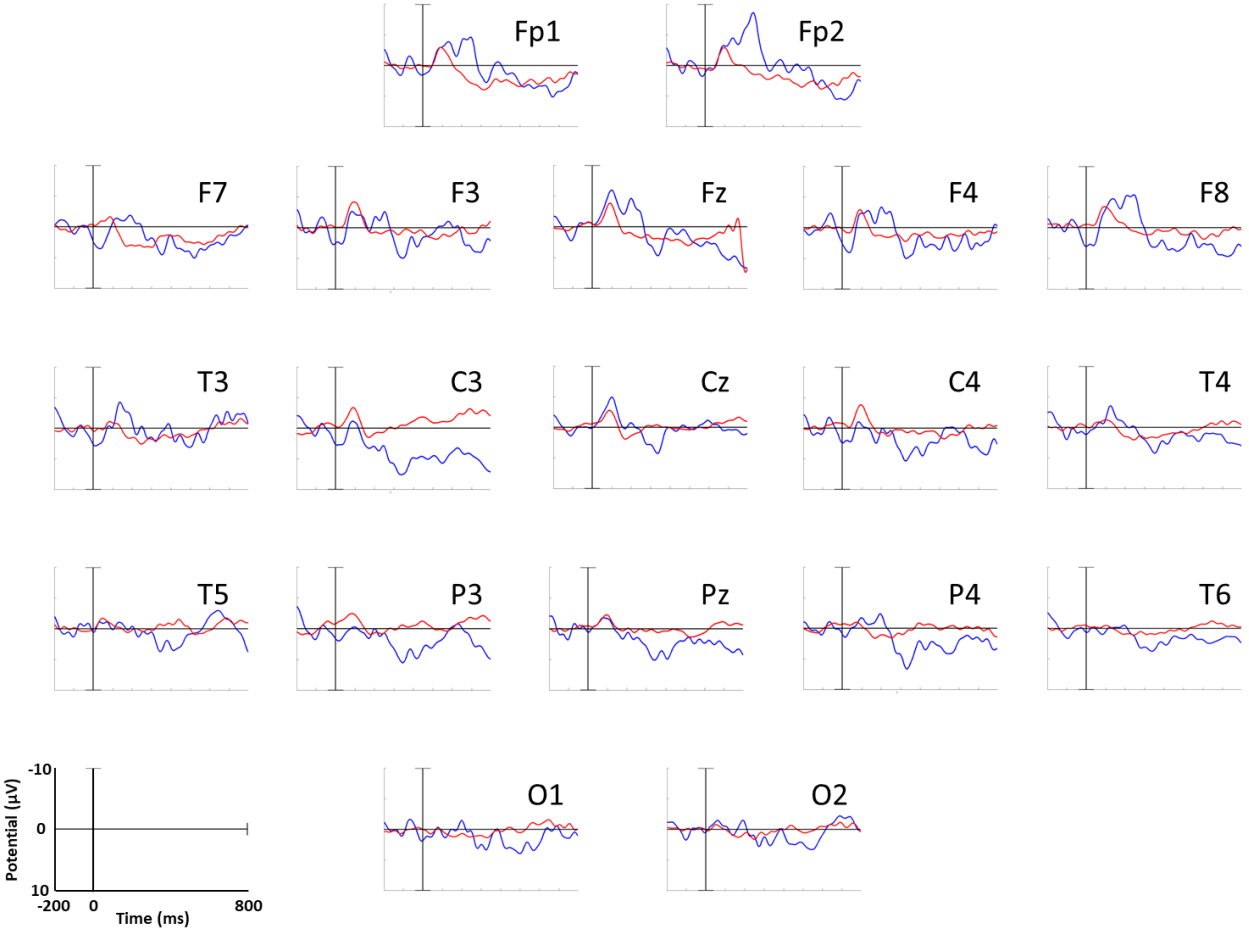

Figure 5.9 Grand mean ERPs at 19 electrode sites recorded during participant walking. Plots show responses to the standard tone (red colour) and the deviant tone (blue) with negative voltage plotted upwards. n=17-23.

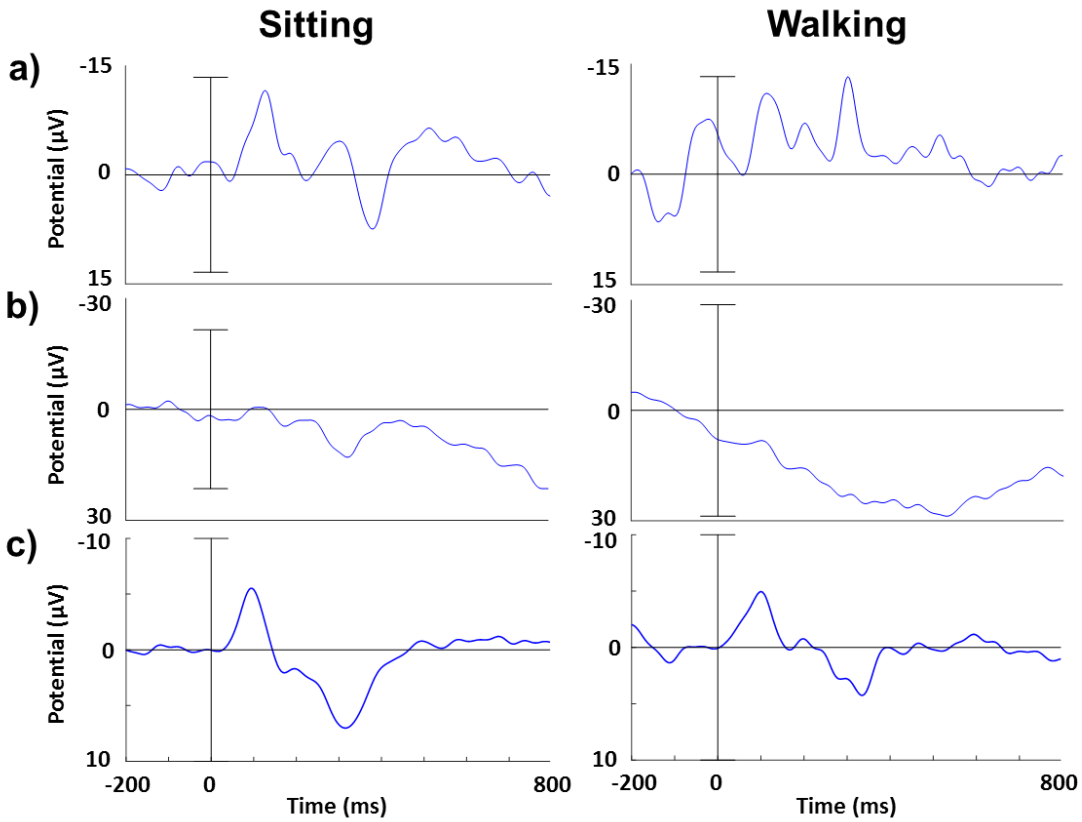

Figure 5.10 ERP plots of **a)**, **b)** two individual participant's mean responses to deviant tones in sitting and walking conditions recorded at electrode Fz, and **c)** grand mean responses to deviant tones at Fz for all (sitting n=26, walking n=20) participants. Note the differing scales on the potential axis.

5.4 Discussion

The current chapter has shown that ERP responses are able to be recorded using the io:bio mobile EEG system. The smartphone played a crucial role in this process by presenting the auditory stimuli via headphones, and recording of the received EEG data to the smartphones SD card. This development, although currently restricted to auditory stimuli, enabled ERPs to be recorded during sitting and walking conditions. EEG data was recorded successfully with stimuli presentation times marked accordingly in a separate marker channel. This data was then loaded into EEGLAB for analysis via a new coded plug-in to enable analysis of the ERP data to take place at a 24-bit resolution. The ERP results obtained when participants were seated are discussed first followed by those for walking.

With participants in a seated position three distinct deflections of the ERP waveforms were revealed from the data, with the first being the N100. The N100 component was found to be a prominent frontocentral negative peak with a latency of between 90 and 200 ms in response to auditory stimulation [148]. There is evidence to suggest that it is generated by sources in the primary auditory cortex within the temporal lobe [183]. Since it occurs as a response to an unexpected stimulus, it was predicted to occur in response to the rare (deviant) tone in the current investigation. The results show an N100 response for both standard and deviant tones, with the deviant tone response being greater in amplitude at most electrode sites. The results showed amplitudes, latencies and distributions that are in line with the published literature. In their systematic review of auditory oddball paradigm studies, Tome *et al*. obtained grand average amplitudes and latencies, from a total of 3934 participants, for the N100 of 7.3 µV (SD = 3.0) ranging from 2 to 15.1 µV, with a latency of 107.6 ms (SD = 15.0) ranging from 82 to 164 ms. An amplitude of 7 µV (SD = 3.2) ranging from 1.1 to 14.4 µV with a latency of 118.2 ms (SD = 31.5) (88.9 to 260 ms) was recorded at Fz. These values are consistent with the results obtained with the io:bio ERP system for seated participants: amplitude of -5.2 µV (SD = 5.1) with a latency of 95.8 ms (SD = 17.4) at Cz, and -7.3 µV (SD = 3.5) with a latency of 99.7 ms (SD = 16.0) at Fz.

In addition to the N100, a N200 component was also recorded by the developed io:bio ERP system. The N200 component is of particular interest because it is the earliest ERP component to differentiate target from non-target in an oddball task consistently [159]. It usually occurs 200 to 350 ms after the stimulus is applied but only when the stimulus is of interest, as is the case in an auditory oddball paradigm when the deviant stimulus is detected. Tome *et al*. obtained amplitudes and latencies for the N200 of -4.9 µV (SD = 2.6) with a latency of 231.4 ms (SD = 33.9) at Cz, and -5.7 µV (SD = 3.9) with a latency of 231.8 ms (SD = 18.9) at Fz. The results obtained with the io:bio ERP system for seated participants are comparable to these values: for electrode Fz amplitude of -3.94 µV (SD = 5.0) and latency of 224.3 ms (SD = 27.4). Simson *et al.* found that auditory stimuli elicit the highest N200 amplitudes for electrodes placed over the central-parietal region, and used a nose reference electrode when collecting recordings [184]. The right ear was used as a reference electrode with the io:bio ERP system, such that the difference in the choice of reference electrode used could explain the differences in N200 distribution across the head.

A P300 was observed in response to the deviant auditory tone with the io:bio ERP system. When generated in response to auditory stimuli, the P300 has a latency in the region of 250-400 ms for most adults in the range 20 to 70 years old [148]. A systematic review by van Dinteren *et al.,* concentrated on the auditory P300 and included 75 studies with 2811 participants [170]. This study provided a mean amplitude of 10.4 µV ranging from 2.6 to 37.7 µV, a mean latency of the P300 of 316.5 ms ranging 290.0 to 447.5 ms for the Pz electrode. The results from the io:bio ERP system are in line with these reported values: an amplitude of 11.2 µV, ranging -1.8 to 27.1 µV and a latency of 320.7 ms, ranging 264 to 352 ms. It should be noted that the review by van Dinteren *et al.,* only provides ranges of values and not SD or SEM values.

Van der Stelt *et al*., [6] performed a study using auditory P300 response comparisons which included a healthy young participant group in the age range of 19 to 25 years.

This range is similar to the age range of the participants used in this thesis chapter of 18 to 24 years of age. The amplitudes obtained with the io:bio ERP system (Fz = 7.0 ± 1.7 μV, Cz = 9.2 ± 1.6 μV and Pz = 11.2 ± 1.5 μV) are in line with those obtained by Van der Stelt *et al*. (Fz = 4.9 ± 3.7 μV, Cz = 10.1 ± 4.1 μV and Pz = 13.8 ± 3.8 μV). The P300 latencies appear to be shorter in the io:bio ERP system than those recorded by Van der Stelt *et al*.: Fz = 369 ± 34 ms, Cz = 374 ± 32 ms and Pz = 368 ± 26 ms in Van der Stelt *et al*. study and Fz = 323.9 ± 5.1 ms, Cz = 318.3 ± 5.8 ms and Pz = 320.7 ± 5.9 ms with the io:bio ERP system. It is difficult to determine whether latency differences were due to system, stimulus or paradigm differences. It could also relate to participant group capability differences. Polich *et al*., suggest that a shorter P300 latency relates to higher memory ability. Since the cohort of participants in the current chapter consisted of high achieving year medical students it could be argued that they possess a higher than average memory ability for this age group, and this factor could be the reason for the apparent shorter latencies observed.

The io:bio ERP system results for participant walking displayed increased levels of noise in comparison to those obtained during sitting. The effect of the noise is clearly seen in the individual participant time series plot for walking (see Figure 5.8a,b). The noise is also apparent in the grand mean ERPs plots (see Figure 5.9). These elevated noise levels are likely to be attributable to electrode displacement during walking (movement-related artifacts). Despite the noise, there are discernible components in the grand mean ERP plot (see Figure 5.9) although the P300 component appears to be of reduced amplitude compared to those ERPs obtained with participants sitting (see Figure 5.7 and Table 5.1). This is of potential concern when undertaking future research since the P300 component is used for BCI systems where a reduction in amplitude could result in a reduced detection rate. Interestingly, Debener *et al.*, performed an auditory oddball paradigm for sitting and outdoor walking and also found smaller P300 ERP components in the walking condition [36]. They posited that one of the reasons for the P300 reduction related to differences in cognitive processing during walking.

Taken together, the results from the previous chapter and the current one show that walking causes sufficient artifacts so as to make analysis (continuous and ERP data) using the io:bio system problematic. The next chapter aims to address, in a preliminary study, the problem of artifacts during walking, where the io:bio system's electronics are mounted on the head location and auditory ERPs recorded.

5.5 Conclusions

This chapter has demonstrated that the io:bio smartphone-based waist-mounted mobile EEG system was modified to provide a capability to provide auditory stimuli and marking of the recorded data using the smartphone. Using this io:bio system, ERP components were recorded using an oddball paradigm where N100, N200 and P300 components were similar to those found in the published literature. However, the io:bio ERP system in its waist-mounted form, although inherently portable, exhibited evidence of electrode displacement when used to record ERP data during participant walking.

Chapter 6: A preliminary study using a head-mounted mobile EEG system to acquire event-related potentials (ERPs) during walking

6.1 Introduction

Head-mounted EEG systems are increasingly being used in mobile EEG research studies [36,57,65,67]. In a head-mounted EEG system, the electrode leads connecting the head cap to the EEG acquisition electronics are minimised in length which reduces problems related to electrode displacement-induced artifacts. In addition, a head-mounted configuration enables an increase in the mobility of participants [36,76,78]. In this chapter, the io:bio mobile waist-mounted EEG system is modified from a waist-mounted system to a head-mounted system. The rationale underpinning performing this modification is that a head-mounted systems should acquire higher quality EEG recordings (reduction in electrode displacement) in comparison with waist-mounted EEG systems.

In Chapter 2, the CoME scheme was developed to address the ambiguity in using the term 'mobile EEG' that is commonly used in journal publications. The CoME scheme scores device mobility dependent upon where the EEG equipment was mounted in relation to the participant (see Table 2.3). The EEG experiments included in this thesis in Chapters 3, 4 and 5), have employed a waist-mounted position on the participant for the io:bio system. It is desirable to mount the acquisition electronics of the io:bio mobile EEG system for mounting to the head location to enable greater participant mobility. The CoME scheme scores reflect the change in device mobility score when moving from a waist-mounted to a head-mounted configuration: change from 2D (all equipment is waist-mounted) to 4D (head-mounted and requires smartphone).

The aim of this chapter is to undertake a preliminary study which:

1. Develops and tests a prototype io:bio system which is head-mounted.
2. Utilises the developed head-mounted io:bio system to acquire ERP responses to an auditory oddball paradigm during participant walking.

6.2 Methods

The methods are divided into three sections. Firstly, the redesigning of the io:bio smartphone-based system from waist-mounted to head-mounted is presented. Secondly, the experimental procedure used during EEG data recording, and finally, the visual assessment of the recorded EEG data is outlined.

6.2.1 Redesigning io:bio to a head-mounted configuration

In the waist-mounted modality the io:bio system scored (2D, 2-3P, 11S, 24C) depending upon the participant mobility (constrained or unconstrained walking). By redesigning the io:bio to a head-mounted location the scores for device and participant mobility increase to (4D, 2-4P). Figure 6.1 shows the possible scores for both waist and head-mounted versions along with possible participant mobility scores.

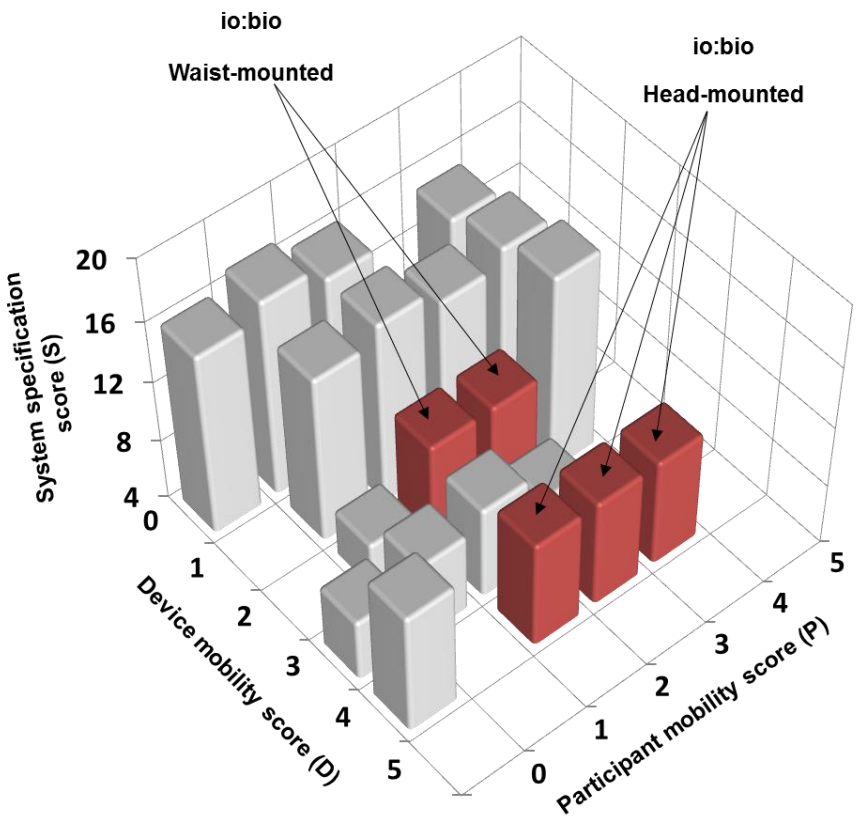

Figure 6.1 Head-mounted io:bio potential CoME scheme scores in comparison to waist-mounted io:bio system (red colour),and 15 other published studies (grey colour, see Figure 2.2 for details).

An initial approach to locating the acquisition electronics onto the head cap was made using a flexible PCB that fitted in-between the 19 electrodes and wrapped around the rear of the head (Figure 6.2). The rationale behind this was that if the design functioned and proved robust enough for use then the electronics could be moulded into the head cap design. The moulding into the cap could be achieved by coating the electronics in a non-conductive resin or polymer. However, this was not undertaken as access to the electronics during the testing of the head-mounted io:bio system was required so that modifications could be made if necessary, and any faults detected be addressed. Low-profile surface-mounted connectors were used to connect electrode leads to the acquisition electronics. The flexible PCB design was constructed, and initial testing showed it to perform similar to the waist-mounted io:bio system. Unfortunately, it only functioned on one occasion. Despite several fabrication iterations of the flexible PCB prototype over a number of months, the design proved to be too fragile. The components soldered to the surface of the flexible PCB would

become detached resulting in unpredictable behaviour of the electronics when being removed and refitted onto the head cap. Since this design was too fragile, an alternative approach to the design was sought.

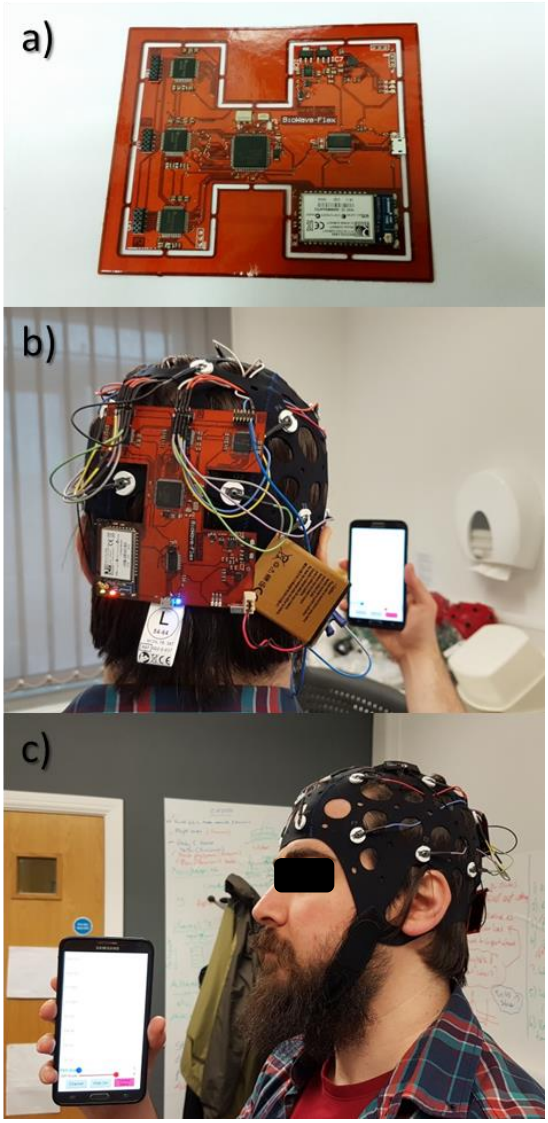

Figure 6.2 Flexible PCB design. Panel **a)** showing populated board, **b)** flexible PCB mounted on a participants head, and **c)** a side profile view of the flexible PCB.

The alternative approach resorted to using the original waist-mounted PCB design mounted on a cradle (aluminium coated in a non-conductive tape) and attached to the back of the head cap (Figure 6.3). Although this approach restricted the possible use of

the system by making it unsuitable, for example, for sleep studies it did provide a robust prototype that was used with participants during walking.

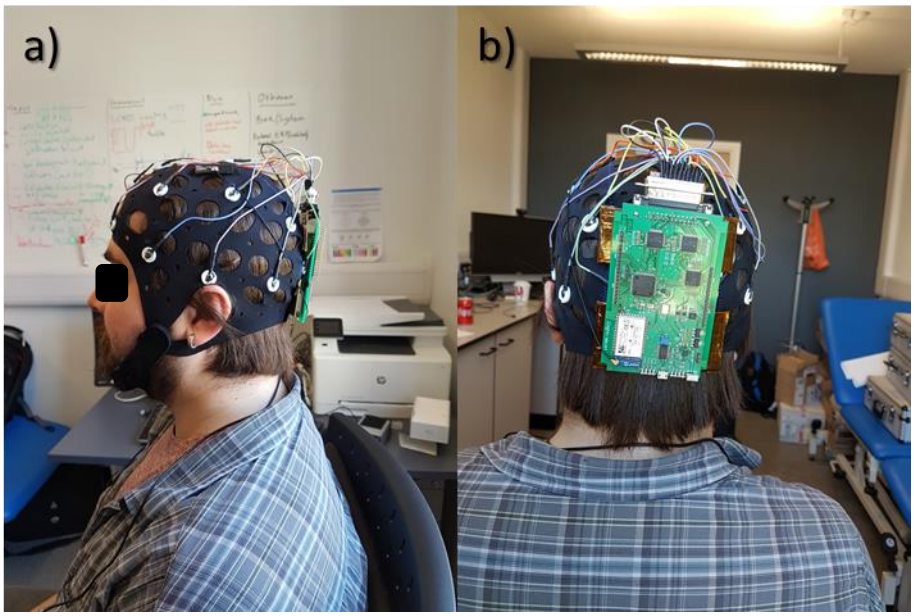

Figure 6.3 Rigid waist-mount PCB used in head-mounted modality. Panel **a)** profile view of PCB head-mounted on participant, **b)** rear view of PCB.

6.2.2 Experimental Procedure

6.2.2.1 Participants

Four participants were recruited (21 to 35 years, mean age 26.5 ± 3.2 SEM, 3 males and 1 female), and all completed health questionnaires and consent forms prior to participation. All participants were healthy with no history of neurological disorders. Hull York Medical School Ethics Committee provided ethical scrutiny and approval for the study.

6.2.2.2 Participant Protocol

The participants were setup with the EEG system and smartphone as illustrated in Figure 6.4. The electrode wells were filled with conductive gel and the impedance was below 5kΩ to maintain signal quality. All scalp electrodes were referenced to the right ear. Data recordings were imported directly into EEGLAB [109] using the written plug-in.

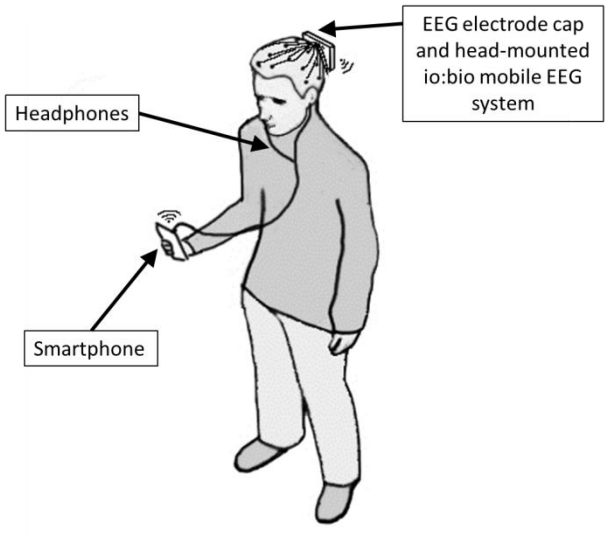

Figure 6.4 Overview of participant setup detailing equipment mounting positions.

Two pure tones were presented binaurally with consumer in-ear headphones (Samsung EO-EG920BW). The volume was set at a comfortable level for each individual participant. Before the experiment was started, participants were presented with a brief practice run to both establish a comfortable volume and clarify the distinction between the two tones. Standard (600 Hz) and deviant (1200 Hz) audio tones were presented in randomized order (ratio of 5 to 1) at a fixed inter-stimulus interval of 1000 ms and a duration of 62 ms. A total of 417 trials were recorded for each participant. Participants were asked to silently count the deviant tones and provide a verbal total at the end of the recording. The task required participants to walk around a large table, while performing the auditory oddball task.

6.2.3 Assessment of ERP data during walking

Using the head-mounted io:bio system, each channel was bandpass filtered from 0.1 to 20 Hz by implementing a zero-phase Hamming-windowed sinc FIR filter in EEGLAB. After epoching, trials containing voltage changes in excess of 100 µV in any channel were rejected from the analysis. Trial epochs were extracted (-200 to 800 ms) and baseline corrected (-200 to 0 ms). Accepted epochs were averaged together to generate standard and deviant ERP waveforms for the walking condition at each scalp site. No statistics were performed for the ERP waveform components due to the low number of participants taking part in this preliminary investigation using the developed head-mounted io:bio system. Instead, a general visual assessment was made of the artifacts, and the ERP responses during participant walking obtained using the head-mounted io:bio system was visually compared to the ERPs using the waist-mounted io:bio system during walking (see Section 5.3.2).

6.3 Results

As the flexible PCB design of the head-mounted io:bio system failed to be robust enough to be successfully utilised in a study with participants, no data results are presented. Instead, results are presented for the oddball paradigm during participant walking using the modified waist-mounted io:bio rigid PCB system which was relocated to back of the head.

6.3.1 Head-mounted io:bio system: ERPs during walking

Time series data is presented in Figure 6.5 during walking using the head-mounted io:bio system (Figure 6.5a). For comparison, time series data is included for the waist-mounted io:bio system during walking (Figure 6.5b) and sitting (Figure 6.5c).Visual assessment of the time series obtained using the head-mounted io:bio system during walking indicates relatively low levels of noise, although artifacts of relatively low amplitude are present (Figure 6.5a). In contrast, the time series obtained using the waist-mounted io:bio system during walking displayed higher levels of background noise and much higher amplitude artifacts (Figure 6.5b). Fewer artifacts and lower noise were seen in channels using the waist-mounted system during participant sitting (Figure 6.5c).

Using the head-mounted configuration of the io:bio system, grand mean ERP plots (from four participants) for the responses to both standard and deviant tones (oddball paradigm) during participant walking are shown in Figure 6.6. for 19 electrode sites. On visual inspection, the pre-stimulus (-200 to 0 ms) and post-stimulus (0 to 800 ms) periods both have a relatively lower level of noise compared to that seen using the waist-mounted io:bio system (see Figure 5.9, 5.10). The N100 and N200 components are clearly seen in fronto-central channels e.g. F3, Fz and F4 to the deviant tones (Figure 6.6). The P300 to deviant tones is evident in some channels e.g. C3, Cz, C4, P3, Pz and P4 (Figure 6.6). Figure 6.7 illustrates the individual ERP plots from the four

participants recorded to the deviant tones using the head-mounted io:bio system at electrode location Fz. Although clear N100 components at are evident in all four participants in this channel, the N200 and P300 components were not. To aid comparison, Table 6.1 tabulates the amplitudes and latencies of the N100, N200 and P300 ERP components, measured from the grand mean ERP plots, for the three different io:bio system configurations: waist-mounted sitting, waist-mounted walking and head-mounted walking.

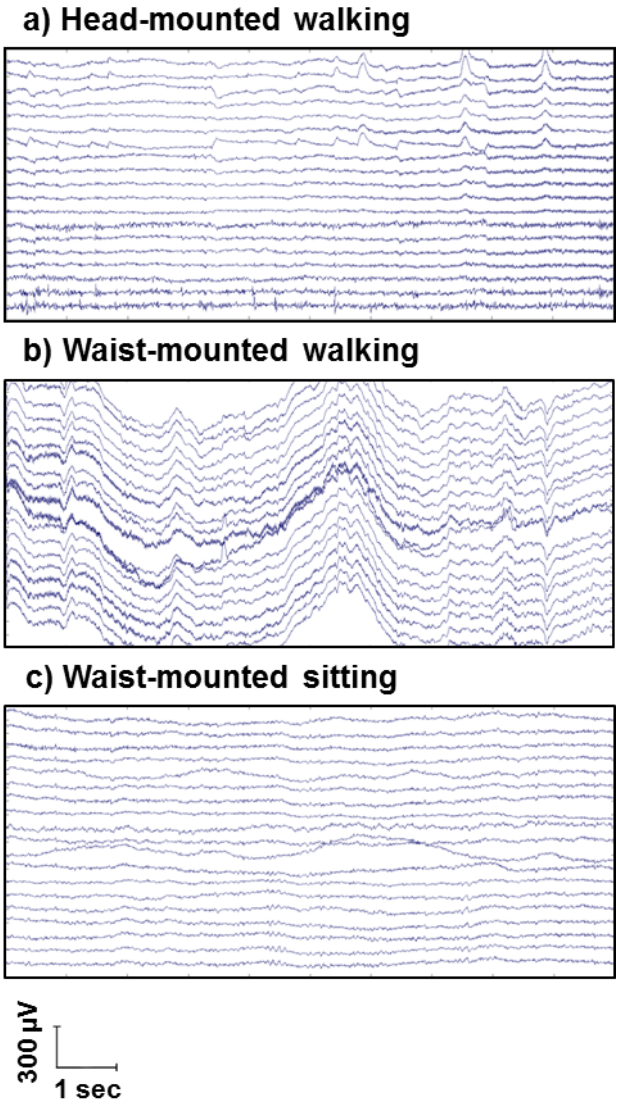

Figure 6.5 Time series plots recorded with **a)** head-mounted io:bio while walking **b)** waist-mounted io:bio while walking and **c)** waist-mounted io:bio while sitting. Filtered 0.1 to 20 Hz. Channel labels as in Figure 3.12.

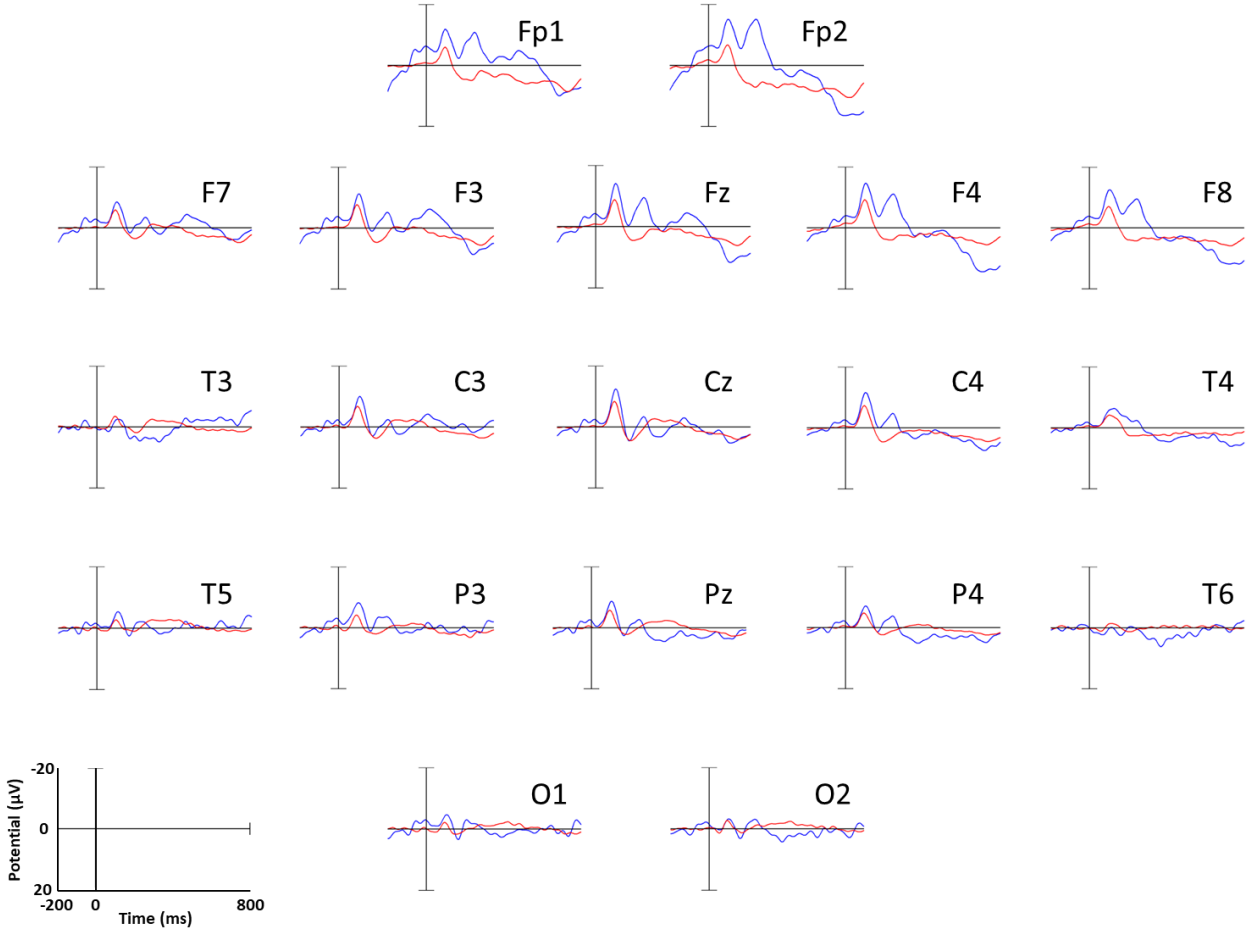

Figure 6.6 Grand mean ERP plots for all channels recorded with the head-mounted version of io:bio during participant walking. Plots show responses to the standard tone (red) and the deviant tone (blue) with negative voltage plotted upwards. Note the amplitude scale ranges from 20 to -20 µV and not 10 to -10 µV as used in the ERP plots of the previous chapter. n=4.

Table 6.1 Latencies and amplitudes of N100, N200, and P300 components taken from the grand mean ERP plots obtained for deviant tones at channels Fz, Cz and Pz during sitting (waist-mounted system) and walking (waist-mounted and head-mounted system).

			N100		N200		P300	
Channel	**Mounting**	**Activity**	**Latency (ms)**	**Amplitude (μV)**	**Latency (ms)**	**Amplitude (μV)**	**Latency (ms)**	**Amplitude (μV)**
Fz								
(n=26)	Waist	Sitting	96	-6.2	208	-2.5	320	5.4
(n=20)	Waist	Walking	100	-6.0	200	-4.6	336	4.7
(n=4)	Head	Walking	104	-14.0	248	-9.5	340	1.5
Cz								
(n=22)	Waist	Sitting	96	-5.5	196	1.7	316	12.7
(n=21)	Waist	Walking	100	-5.0	196	-0.8	336	4.3
(n=4)	Head	Walking	104	-12.4	248	-3.3	328	3.3
Pz								
(n=24)	Waist	Sitting	88	-1.6	212	3.9	328	12.7
(n=22)	Waist	Walking	80	-1.8	204	0.6	340	5.1
(n=4)	Head	Walking	104	-8.7	244	-2.7	372	4.5

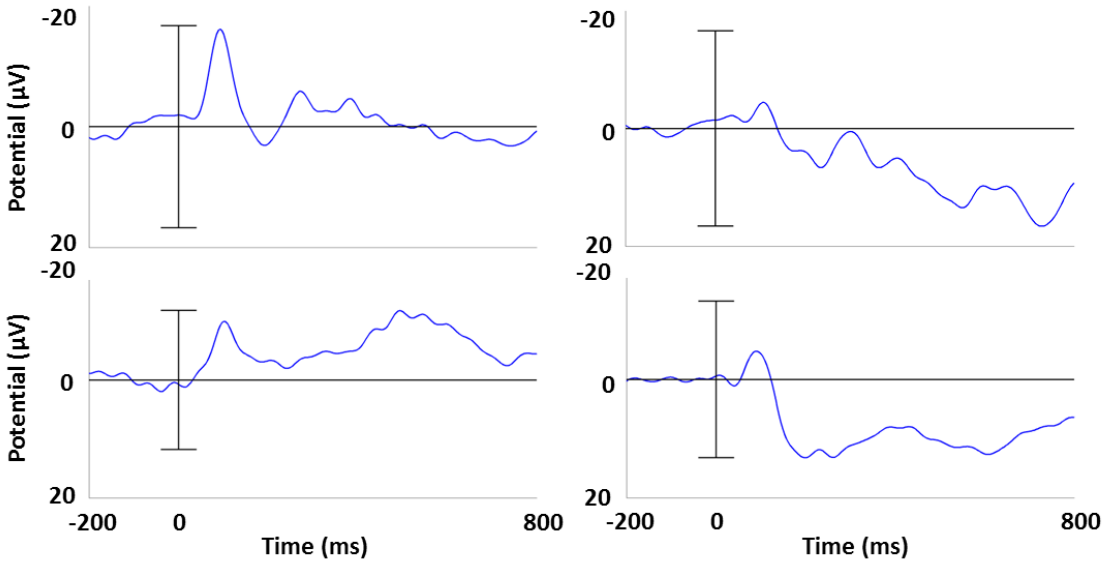

Figure 6.7 Mean ERP plots for each of the four individual participants recorded at the Fz electrode with the head-mounted io:bio system during walking.

6.4 Discussion

The initial approach taken to redesigning the io:bio mobile EEG system from a waist-mounted system to a head-mounted one used flexible PCB. This approach was selected as it would enable a low profile of the electronics architecture upon the head without protrusion from the electrode head cap. However, using this approach no EEG data could be acquired, despite concerted efforts, as the soldered connections would become detached between the individual electronic components and the flexible PCB. This also resulted in connections failing as the system was either attached to, or removed from, the head cap. It appears that there is just too much flexibility in the PCB using this design.

To enable acquisition in a head-mounted configuration, another approach was next undertaken which exploited the existing waist-mounted io:bio system, a system which has been used successfully to record ongoing EEG activity and ERP data (see Chapters 3-5). The populated rigid PCB of this system was removed from its enclosure, and a cradle located at the back of the head was used to attach it to the head cap. The cradle-rigid PCB arrangement enabled easy attachment/detachment from the head cap, and was robust enough to remain electrically intact while doing so. One limitation of this rigid populated PCB arrangement is that it could not be used for recordings in which the participants were lying down or during sleeping.

Utilising the CoME scoring scheme, the rigid PCB head-mounted io:bio system had a score of (4D,2-4P,11S,24C). The score of 4D reflects the heading mounting position of the system, and if it was able to be used without the requirement of a smartphone a score of 5D is possible. Compared to other head-mounted systems, the io:bio system had a score for device mobility of 4D which was the same as that for the SMARTING system57 (score of 4D) but higher than the scores for the studies using, the Mindwave 65 , B-Alert67 and Oldenburg Hybrid 36 (all scored 3D). The score range from 2-4P

reflects the participant mobility that the system could potentially be used for in future investigations using the system.

Using the rigid PCB head-mounted EEG configuration, time series data was able to be acquired during participant walking. There were relatively lower levels of noise in the EEG channels and lower amplitude artifacts when visually compared to walking using the waist-mounted io:bio system. It would be of value to undertake a study to determine the noise and artifact profile using the rigid PCB head-mounted EEG configuration during participant sitting to enable comparison with walking.

Notwithstanding the small number of participants (n=4), the rigid PCB head-mounted EEG configuration was successfully able to acquire ERP responses to standard and deviant auditory tones during walking. The grand mean ERPs from the four participants during walking showed relatively less noise (both pre and post-stimulus periods) when visually compared to the grand mean ERPs obtained using the waist-mounted io:bio system in sixteen participants. The ERP noise and component profiles are likely to be further improved if a larger number of participants is included in the grand ERP means using the rigid PCB head-mounted EEG system.

The grand mean ERP plots showed the presence of the N100 and N200 components especially in the fronto-central channels (F3, Fz and F4) to the deviant tones during walking with the rigid PCB head-mounted system. The P300 component was evident in some channels (C3, Cz, C4, P3, Pz and P4) but was not seen clearly in others. This was broadly similar to the grand mean ERP in the waist-mounted io:bio configuration, and when compared to participants sitting, the P300 amplitude is apparently smaller. This may be due to differences in cognitive processing [36], during walking as discussed in Chapter 5.4. An investigation could be undertaken, using a statistically-valid number of participants, which uses the head-mounted io:bio system to determine the N100, N200 and P300 profiles to walking versus sitting conditions.

The ERP's obtained using the io:bio rigid PCB electronics, mounted onto a cradle at the back of the head, were acquired without any form of electrical screening or shielding. A more robust version of this head-mounted prototype could be produced by the addition of a shielded case which would be expected to reduce electromagnetic interference. In addition, an enclosure is required for participant hygiene and cleaning. To advance the rigid head-mounted PCB system, it would be desirable to miniaturise the PCB/electronics by using smaller footprint components such as ball grid array packaged ICs [185].

6.5 Conclusion

Although an approach using a populated flexible PCB was undertaken to design the io:bio EEG system to enable a head-mounted configuration, this proved to be too fragile and no EEG data could be acquired in participants. Success was achieved in the preliminary recording of auditory ERPs during participant walking by configuring the rigid PCB waist-mounted EEG electronics onto the back of the head cap.

Chapter 7: General Discussion

7.1 Main findings and general discussion of the smartphone-based mobile EEG system

The underlying motivation for the research work in this thesis was to develop, build, validate and utilise a novel mobile smartphone-based EEG system, with the ultimate aim of enabling the acquisition of EEG data in a variety of applications and real world environments. The intention was to design a mobile smartphone-based system with the requirements of EEG researchers in mind where differences in device and participant mobility, and system specification modification are needed.

Before developing and fabricating a mobile EEG system, a review of the current literature in this area was conducted (Chapter 2). A major problem was identified in the mobile EEG literature as the term 'mobile' EEG is used in an ambiguous manner. Researchers have used it to describe a very wide range of participant and device mobility. For example, participants tethered to a treadmill, walking outdoors, or being moved on a trolley while recording EEG recordings were all termed as 'mobile EEG'. To address this definition problem in the term, 'mobile EEG', a review of thirty research papers (twenty nine using mobile EEG, and one using a static system for comparison) was undertaken. The outcome from this review was the development of a novel categorisation scheme for mobile EEG (CoME) which can more clearly define the term 'mobile EEG'. This scheme enables, for the first time, a concise and unambiguous systematic scoring for device mobility (Table 2.2), participant mobility (Table 2.3), and EEG system specification (bit resolution, sampling rate, battery life and electrode type, Table 2.6). The CoME scheme is a useful scoring system for researchers to categorise their mobile EEG studies as well as in the design and development of mobile EEG equipment. It also enables convenient comparison across research studies both retrospectively and prospectively. The results demonstrated the functionality of the CoME scheme where, interestingly, a broad range was found in the scores for device mobility, participant mobility and system specification (Figure 2.2, Table 2.8).

The limitations of the CoME scheme were discussed in Chapter 2.4.1. These include having caution when making interpretations of the combined total system specifications score versus individual scores (electrode type, bit resolution, sampling rate and battery life). Various parameters could be considered for inclusion into future revisions of the CoME scheme such as impedance, wireless connection, and parameters related to participants comfort and aesthetic form. These parameters were not included in the current CoME scheme, in part to keep the scheme researcher-use friendly, but mainly due to the problem of appropriately being able to measure and score them on a scale. It is also possible, that should the CoME scheme become adopted and established in the field of mobile EEG, it may require modification and refinement to perhaps include these or other parameters which researchers deem relevant to mobile EEG investigations. Early indications on the ResearchGate platform are that researchers are considering the CoME scheme with interest and recommendation (https://www.researchgate.net/).

The CoME scheme was utilised to aid the production of the design specification for the development of the first smartphone-based mobile EEG prototype. This was within the range found in publications of mobile EEG systems in terms of device and participant mobilities, and system specification (Figure 2.2). A waist-mounted smartphone-based mobile EEG system, known as io:bio, was successfully designed, built and initially tested using internally-generated signals. ADS1299 IC were successfully connected together in a standard-mode configuration instead of daisy-chain (Chapter 3.3.1). The CoME scheme score for the system was (2D, 3P, 11S, 24C), which was for a waist-mounted system allowing unconstrained walking with 24 recording channels (19 EEG and 5 differential) at a resolution of 24 bit and a sampling frequency of 250 Hz. A novel feature of the io:bio EEG mobile system was the exploitation of the smartphone's inherent mobility (versus a PC, for example). The smartphone was connected to the io:bio device via a Wi-Fi link (Bluetooth was not selected as it had limitations in range and energy efficiency), and an app was coded (via Unity software) for impedance checking, live plotting and data storage (SD card).

The waist-mounted smartphone-based mobile prototype system was next validated against a clinically (FDA) approved commercial (Micromed) gold standard EEG system (Chapter 4). This was achieved by recording alpha waves and analysis of power spectra (power amplitude, peak frequency and area) which were compared between the two systems in participants lying down with eyes closed. A Bland and Altman analysis was selected for statistical comparisons as this method is more appropriate than a correlation analysis or t-test approach (Chapter 4.2.5). No significant differences were found in the results for intra-system or inter-system comparisons. Bland-Altman plots showed that the differences between the values obtained from each system were within the a priori defined acceptable limits of agreement, and that the two systems could be used interchangeably. Alpha waves were also successfully acquired with various participant postures (sitting, standing, and standing with arms raised) in both the waist-mounted io:bio and Micromed systems, with Bland-Altman plots indicating that the limits of agreement were similar. In contrast, both waist-mounted EEG systems showed unacceptable levels of noise and artifacts with participant walking.

Although the waist-mounted io:bio system was validated using alpha waves, as a clear peak was observed in participants with eyes closed, it would be nonetheless useful to undertake a similar study comparing other frequency EEG bands (delta, theta, and beta) [186]. However, one difficulty could be in the identification of a clear signal of interest in these bands. Perhaps one way to address this problem would be to perform an area under the curve calculation in power spectra for both the io:bio and Micromed systems in these frequency bands.

Given the importance of acquiring brain responses to time-locked stimuli in basic and clinical research (Chapter 5.1), the functionality of the waist-mounted io:bio mobile system was extended beyond recording only continuous EEG data, to add an ERP capability. This was achieved by additional coding of the smartphone app to mark onto the EEG data recordings the time when each stimulus was presented to enable analysis via averaging of individual ERP. In addition, the capability of the smartphone to deliver sounds via headphones was exploited to provide auditory stimuli to participants. An

auditory oddball paradigm was used, where standard and deviant tones were presented binaurally to participants while seated. By taking advantage of the portability of the waist-mounted io:bio ERP system, the paradigm was also presented to participants during walking. N100, N200 and P300 ERP components were successfully acquired using the mobile io:bio ERP system and had generally larger amplitudes to the deviant tones compared to the standard ones in participants sitting. This profile was also found for walking in the grand participant mean ERP calculations, although movement-related artifacts impacted negatively upon the quality of the ERP components when plotting the mean ERPs at the level of each participant. Thus, although the waist-mounted io:bio system was able to record auditory ERPs during sitting it was much more difficult when the participant was walking, indicating that further development of the system was required to reduce movement-related artifacts.

Hemispheric lateralisation of responses to ERP components (N1, P250 and P3b) have been observed when presenting the auditory oddball task monaurally versus binaurally [187]. These findings were in line with the theory that the right hemispheric network has a greater association with stimulus evaluation and the identification of target stimuli. It would therefore be interesting to repeat the oddball task using the io:bio system with tones not only additionally presented separately in the left and right ear but while participants are sitting and walking. Using the auditory-oddball task, the amplitude of the P300 ERP component was found to be reduced in schizophrenic patients [188]. Thus, future research investigations which use the developed smartphone-based io:bio ERP system to deliver and acquire responses to various auditory stimuli should be considered in schizophrenics and other patient groups with altered auditory processing.

Given the portability of the smartphone-based io:bio auditory ERP system, studies can easily be undertaken in environments outside the laboratory such as in the home setting. In misophonia, thought to be a psychiatric condition where there is a hatred of ordinary human sounds (e.g. chewing or breathing) causing anxiety and aggression, the

amplitude of the N100 ERP to deviant tones was smaller in amplitude compared to the control group indicating an underlying deficit in auditory processing in the brain (add ref) [189]. Given the advantage of the mobility of the io:bio ERP system, this condition and others can be investigated without having the requirement of bringing such participants into the confines of a EEG laboratory but instead undertaken in an environment in which they feel more comfortable, such as their home.

In addition to auditory ERPs, the io:bio ERP system has the novel potential for the smartphone to be coded for enabling the capability for visual evoked potentials. The smartphone could be used to deliver visual stimuli such as checkerboard gratings [190,191], steady state visual evoked stimuli [64,192-194] or other visual stimuli of research interest [195]. This could be undertaken in both healthy and patient groups as has been undertaken using static EEG systems [196,197] but also developing protocols where participant mobility is required.

To address the problem of movement-related artifacts in the EEG data when using the waist-mounted io:bio system (wired connection from the waist to the head cap), the io:bio system was redesigned into a head-mounted configuration to reduce lead length. An approach taken using electronic components populated onto a flexible PCB placed onto the rear head section of the electrode cap, was not robust enough for use in participants despite several fabrication attempts. Instead, a rigid PCB form of the circuitry was taken from the io:bio waist-mounted system and mounted onto the back of the head via a cradle arrangement. Compared to the waist-mounted io:bio system, the device mobility CoME score for this smartphone-based head-mounted configuration increased from 2D (all equipment is waist-mounted) to 4D (head-mounted and requires smartphone). The head-mounted io:bio system was used in a preliminary study where the auditory oddball paradigm was undertaken, and ERP responses obtained in participants during walking. Early results indicate that artifacts were reduced using this io:bio head-mounted configuration, and N100, N200 and P300 components were clearly identifiable in some of the channels (Chapter 6).

In future work, a more robust version of the head-mounted prototype could be fabricated by the addition of a shielded case which would reduce electromagnetic interference. Perhaps, the most significant advance for the rigid head-mounted PCB system would be to substantially miniaturise the PCB/electronics to reduce component footprints. A miniaturised io:bio head-mounted system with high specification has the major potential to be used in a variety of new research investigations (using a statistically appropriate number of participants), where a high degree of participant mobility is required, such as during walking/cycling (CoME score 3D), constrained running (4D), or vigorous physical sport activities (5D). The smartphone-based head-mounted system could also be used in the study of brain signals in real world settings such as urban environments [156,198,199]. Furthermore, comparisons between responses to differing types of urban space, such as green spaces, road sides, and busy commercial districts could be performed [39,200].

The smartphone-based io:bio mobile system has advantages over commercially available mobile EEG systems as improvements and adaptations to the system and smartphone app should be relatively straight forward. For example, the current 19 channels of the io:bio system could be increased in their number by adding additional ADS1299 IC's via a standard mode configuration design, notwithstanding the increase in the electronics real estate. As technology continues to advance in the key components in the io:bio design, such as the Wi-Fi module, microcontroller, battery, and power management IC, the io:bio systems can be updated and adapted according to the research protocol required by researchers.

There is a wide range of other possible future research avenues that could be pursued using the developed smartphone-based io:bio system. For example, in the home monitoring of epilepsy [201,202], hypoglycaemia detection [203], head trauma [203], classification algorithms for EEG-based BCI systems [79,110], automated sleep stage classification [204], or integration with other imaging modalities such as fNIRS [205] and electromyography to list a number [206].

7.2 The impact of the smartphone-based io:bio mobile system in other research investigations

An unexpected major impact of developing the smartphone-based io:bio system has been the high level of interest shown by various researchers across the faculties at the University of Hull, and their desire to collaborate and use the system to address specific research hypotheses of common interest. Four examples of such non-thesis related current research collaborations and applications are as follows:

1. Research with Professor Stewart Martin (School of Education, University of Hull) is centred upon a method of obtaining more objective measures of cognitive load and in virtual reality (VR). The waist-mounted io:bio mobile system is ideal in the acquisition of EEG data during participant immersion in VR to study aspects of cognitive load including participant learning outcomes. This proposal was put forward and an interdisciplinary University of Hull cluster bid successfully awarded for three PhD student scholarships, starting in September 2018 (see http://www.stewart-martin.uk/projects/perceive.html). In addition, a Leverhulme grant research proposal is currently being written by the cluster team in a bid to provide external funding for the use of the io:bio mobile system in VR environments.

2. A fellow colleague, Dr Kevin Paulson, from the School of Engineering and Computer Science, University of Hull, has research interests in signal processing. A PhD student has been recruited to record oddball auditory ERPs using the smartphone-based io:bio ERP system during walking with the aim to determine the number of ERP repetitions required to reliably identify ERP components, and to use algorithms to help reduce movement-related walking artifacts.

3. Colleagues in the Hull University Business School (HUBS) have research interests in consumer marketing, which they typically collect completed participant-questionnaires as their methodology. There is a desire for more direct measures of the responses to the presentation of marketing-relevant images to participants. A PhD student has been recruited to determine the responses to fast moving consumer goods (FMCG) using the smart-phone-based io:bio ERP system. This research has translational application in the field of consumer neuroscience. In addition, commercial avenues are being discussed with local packaging companies via the University of Hull's commercialisation team.

4. A summer undergraduate research project was undertaken in 2018 (a HYMS medical student) using the waist-mounted io:bio mobile ERP system to record responses to the n-back task on a PC screen versus presentation in VR using a HTC Vive VR system. The waist-mounted io:bio system will also be used to teach the basics of EEG acquisition and analysis to undergraduate medical students in the spring of 2019 as part of their Scholarship and Special Interest module.

By forming external research collaborations, it is exciting to envisage that the smartphone-based io:bio mobile EEG system developed in this thesis could lead to new national and international research avenues especially those which are dependent upon portability of the device as well as mobility of the participant.

References

1. Velis D, Plouin P, Gotman J, Da Silva FL, members of the IDMCSoN. Recommendations Regarding the Requirements and Applications for Long-term Recordings in Epilepsy. Epilepsia. 48:379-384, 2007.

2. Seneviratne U, Mohamed A, Cook M, D'Souza W. The utility of ambulatory electroencephalography in routine clinical practice: A critical review. Epilepsy Research. 105:1-12, 2013.

3. Guérit J-M, Verougstraete D, de Tourtchaninoff M, Debatisse D, Witdoeckt C. ERPs obtained with the auditory oddball paradigm in coma and altered states of consciousness: clinical relationships, prognostic value, and origin of components. Clinical Neurophysiology. 110:1260-1269, 1999.

4. De Reuck JL. Stroke-related seizures and epilepsy. Neurologia i neurochirurgia polska. 41:144, 2007.

5. Wijdicks EF. The case against confirmatory tests for determining brain death in adults. Neurology. 75:77-83, 2010.

6. van der Stelt O, Lieberman JA, Belger A. Auditory P300 in high-risk, recent-onset and chronic schizophrenia. Schizophrenia Research. 77:309-320, 2005.

7. Van Dijk JG, Caekebeke JFV, Jennekens-Schinkel A, Zwinderman AH. Background EEG reactivity in auditory event-related potentials. Electroencephalography and Clinical Neurophysiology. 83:44-51, 1992.

8. Sumi N, Nan'no H, Fujimoto O, Ohta Y, Takeda M. Interpeak latency of auditory event-related potentials (P300) in senile depression and dementia of the Alzheimer type. Psychiatry and clinical neurosciences. 54:679-684, 2000.

9. Pinheiro AP, Liu T, Nestor PG, McCarley RW, Gonçalves ÓF, Niznikiewicz MA. Visual emotional information processing in male schizophrenia patients: combining ERP, clinical and behavioral evidence. Neuroscience letters. 550:75-80, 2013.

10. Gramann K, Gwin JT, Bigdely-Shamlo N, Ferris DP, Makeig S. Visual evoked responses during standing and walking. Front Hum Neurosci. 4:202, 2010.

11. Brouwer A-M, Reuderink B, Vincent J, van Gerven MA, van Erp JB. Distinguishing between target and nontarget fixations in a visual search task using fixation-related potentials. Journal of vision. 13:17, 2013.

12. Mihajlović V, Grundlehner B, Vullers R, Penders J. Wearable, wireless EEG solutions in daily life applications: what are we missing? IEEE journal of biomedical and health informatics. 19:6-21, 2015.

13. Casson AJ, Yates D, Smith S, Duncan JS, Rodriguez-Villegas E. Wearable Electroencephalography. Engineering in Medicine and Biology Magazine, IEEE. 29:44-56, 2010.

14. Gwin JT, Gramann K, Makeig S, Ferris DP. Removal of movement artifact from high-density EEG recorded during walking and running. J Neurophysiol. 103:3526-3534, 2010.

15. Borck C. Between local cultures and national styles: Units of analysis in the history of electroencephalography. Comptes Rendus Biologies. 329:450-459, 2006.

16. Collura TF. History and Evolution of Electroencephalographic Instruments and Techniques. Journal of Clinical Neurophysiology. 10:476-504, 1993.

17. Rosenblatt B, Gotman J. Computerized EEG monitoring. Seminars in Pediatric Neurology. 6:120-127, 1999.

18. Swartz BE, Goldensohn ES. Timeline of the history of EEG and associated fields. Electroencephalogr Clin Neurophysiol. 106:173-176, 1998.

19. Adrian ED, Matthews BH. The Berger rhythm: potential changes from the occipital lobes in man. Brain. 57:355-385, 1934.

20. Spironelli C, Angrilli A. EEG delta band as a marker of brain damage in aphasic patients after recovery of language. Neuropsychologia. 47:988-994, 2009.

21. Klimesch W, Doppelmayr M, Pachinger T, Ripper B. Brain oscillations and human memory: EEG correlates in the upper alpha and theta band. Neuroscience Letters. 238:9-12, 1997.

22. Klimesch W. EEG alpha and theta oscillations reflect cognitive and memory performance: a review and analysis. Brain Research Reviews. 29:169-195, 1999.

23. Gola M, Magnuski M, Szumska I, Wróbel A. EEG beta band activity is related to attention and attentional deficits in the visual performance of elderly subjects. International Journal of Psychophysiology. 89:334-341, 2013.

24. Başar E, Başar-Eroglu C, Karakaş S, Schürmann M. Gamma, alpha, delta, and theta oscillations govern cognitive processes. International journal of psychophysiology. 39:241-248, 2001.

25. Ahn M, Ahn S, Hong JH, et al. Gamma band activity associated with BCI performance – Simultaneous MEG/EEG study. Frontiers in Human Neuroscience. 7:2013.

26. Nunez PL, Cutillo BA. *Neocortical dynamics and human EEG rhythms.* Oxford University Press, USA; 1995.

27. Homan RW, Herman J, Purdy P. Cerebral location of international 10–20 system electrode placement. Electroencephalography and Clinical Neurophysiology. 66:376-382, 1987.

28. User Tutorial:EEG Measurement Setup. 2018; https://www.bci2000.org/mediawiki/index.php/User_Tutorial:EEG_Measurement_Setup.

29. Mahajan R, Morshed BI. Unsupervised eye blink artifact denoising of EEG data with modified multiscale sample entropy, kurtosis, and Wavelet-ICA. IEEE journal of Biomedical and Health Informatics. 19:158-165, 2015.

30. Iwasaki M, Kellinghaus C, Alexopoulos AV, et al. Effects of eyelid closure, blinks, and eye movements on the electroencephalogram. Clinical Neurophysiology. 116:878-885, 2005.

31. Flemons WW, Douglas NJ, Kuna ST, Rodenstein DO, Wheatley J. Access to diagnosis and treatment of patients with suspected sleep apnea. American journal of respiratory and critical care medicine. 169:668-672, 2004.

32. Leutheuser H, Gabsteiger F, Hebenstreit F, Reis P, Lochmann M, Eskofier B. Comparison of the AMICA and the InfoMax algorithm for the reduction of electromyogenic artifacts in EEG data. Paper presented at: Engineering in Medicine and Biology Society (EMBC), 2013 35th Annual International Conference of the IEEE; 3-7 July 2013, 2013.

33. Oh SS, Han Y, Lee J, et al. A pulse artifact removal method considering artifact variations in the simultaneous recording of EEG and fMRI. Neuroscience Research. 81–82:42-50, 2014.

34. Thompson T, Steffert T, Ros T, Leach J, Gruzelier J. EEG applications for sport and performance. Methods. 45:279-288, 2008.

35. Britz J, Van De Ville D, Michel CM. BOLD correlates of EEG topography reveal rapid resting-state network dynamics. Neuroimage. 52:1162-1170, 2010.

36. Debener S, Minow F, Emkes R, Gandras K, de Vos M. How about taking a low-cost, small, and wireless EEG for a walk? Psychophysiology. 49:1449-1453, 2012.

37. Delorme A, Sejnowski T, Makeig S. Enhanced detection of artifacts in EEG data using higher-order statistics and independent component analysis. NeuroImage. 34:1443-1449, 2007.

38. Fouad MM, Amin KM, El-Bendary N, Hassanien AE. Brain Computer Interface: A Review. In: Hassanien AE, Azar AT, eds. *Brain-Computer Interfaces: Current Trends and Applications*. Cham: Springer International Publishing; 2015:3-30.

39. Aspinall P, Mavros P, Coyne R, Roe J. The urban brain: analysing outdoor physical activity with mobile EEG. Br J Sports Med. 49:272-276, 2015.
40. Wascher E, Heppner H, Hoffmann S. Towards the measurement of event-related EEG activity in real-life working environments. International journal of psychophysiology : official journal of the International Organization of Psychophysiology. 91:3-9, 2014.
41. Park JL, Fairweather MM, Donaldson DI. Making the case for mobile cognition: EEG and sports performance. Neuroscience & Biobehavioral Reviews. 52:117-130, 2015.
42. Castermans T, Duvinage M, Petieau M, et al. Optimizing the performances of a P300-based brain–computer interface in ambulatory conditions. IEEE Journal on Emerging and Selected Topics in Circuits and Systems. 1:566-577, 2011.
43. Lotte F, Fujisawa J, Touyama H, et al. Towards ambulatory brain-computer interfaces: a pilot study with P300 signals. Proceedings of the International Conference on Advances in Computer Enterntainment Technology; 2009; Athens, Greece.
44. Lan T, Erdogmus D, Adami A, Mathan S, Pavel M. Channel selection and feature projection for cognitive load estimation using ambulatory EEG. Intell. Neuroscience. 2007:8-8, 2007.
45. Gwin JT, Gramann K, Makeig S, Ferris DP. Electrocortical activity is coupled to gait cycle phase during treadmill walking. NeuroImage. 54:1289-1296, 2011.
46. Ehinger BV, Fischer P, Gert AL, et al. Kinesthetic and vestibular information modulate alpha activity during spatial navigation: a mobile EEG study. Frontiers in Human Neuroscience. 8:71, 2014.
47. Johns MW. A new method for measuring daytime sleepiness: the Epworth sleepiness scale. sleep. 14:540-545, 1991.
48. Jones C. Glasgow Coma Scale. AJN The American Journal of Nursing. 79:1551-1557, 1979.
49. Hairston WD, Whitaker KW, Ries AJ, et al. Usability of four commercially-oriented EEG systems. Journal of neural engineering. 11:046018, 2014.
50. Nijboer F, van de Laar B, Gerritsen S, Nijholt A, Poel M. Usability of three electroencephalogram headsets for brain–computer interfaces: a within subject comparison. Interacting with computers. 27:500-511, 2015.
51. De Vos M, Kroesen M, Emkes R, Debener S. P300 speller BCI with a mobile EEG system: comparison to a traditional amplifier. J Neural Eng. 11:036008, 2014.
52. Duvinage M, Castermans T, Petieau M, Hoellinger T, Cheron G, Dutoit T. Performance of the Emotiv Epoc headset for P300-based applications. Biomedical engineering online. 12:56, 2013.
53. Mayaud L, Congedo M, Van Laghenhove A, et al. A comparison of recording modalities of P300 event-related potentials (ERP) for brain-computer interface (BCI) paradigm. Neurophysiologie Clinique/Clinical Neurophysiology. 43:217-227, 2013.
54. Davies PL, Gavin WJ. Validating the diagnosis of sensory processing disorders using EEG technology. The American Journal of Occupational Therapy. 61:176, 2007.
55. Askamp J, van Putten MJ. Mobile EEG in epilepsy. International journal of psychophysiology : official journal of the International Organization of Psychophysiology. 91:30-35, 2014.
56. Bulea TC, Jonghyun K, Damiano DL, Stanley CJ, Hyung-Soon P. User-driven control increases cortical activity during treadmill walking: an EEG study. Conf Proc IEEE Eng Med Biol Soc. 2014:2111-2114, 2014.
57. Debener S, Emkes R, De Vos M, Bleichner M. Unobtrusive ambulatory EEG using a smartphone and flexible printed electrodes around the ear. Scientific reports. 5:2015.
58. Doppelmayr M, Sauseng P, Doppelmayr H, Mausz I. Changes in EEG during ultralong running. Journal of Human Performance in Extreme Environments. 10:4, 2012.
59. Fitzgerald Z, Thayer Z, Mohamed A, Miller LA. Examining factors related to accelerated long-term forgetting in epilepsy using ambulatory EEG monitoring. Epilepsia. 54:819-827, 2013.

60. Gargiulo G, Bifulco P, Calvo RA, Cesarelli M, Jin C, Schaik Av. A mobile EEG system with dry electrodes. Biomedical Circuits and Systems Conference, 2008. BioCAS 2008. IEEE; 20-22 Nov. 2008, 2008.
61. Jungnickel E, Gramann K. Mobile brain/body imaging (MoBI) of physical interaction with dynamically moving objects. Frontiers in human neuroscience. 10:2016.
62. Klonovs J, Petersen CK, Olesen H, Hammershoj A. ID Proof on the Go: Development of a Mobile EEG-Based Biometric Authentication System. IEEE Vehicular Technology Magazine. 8:81-89, 2013.
63. Li Y, Zhang T, Deng L, Wang B. Acquisition technology research of EEG and related physiological signals under +Gz acceleration. Irish Journal of Medical Science. 183:187-197, 2014.
64. Lin YP, Wang Y, Wei CS, Jung TP. Assessing the quality of steady-state visual-evoked potentials for moving humans using a mobile electroencephalogram headset. Front Hum Neurosci. 8:182, 2014.
65. Liu N-H, Chiang C-Y, Hsu H-M. Improving Driver Alertness through Music Selection Using a Mobile EEG to Detect Brainwaves. Sensors. 13:8199-8221, 2013.
66. Maidhof C, Kästner T, Makkonen T. Combining EEG, MIDI, and motion capture techniques for investigating musical performance. Behavior Research Methods. 46:185-195, 2014.
67. Robertson C, Marino F. Prefrontal and motor cortex EEG responses and their relationship to ventilatory thresholds during exhaustive incremental exercise. European journal of applied physiology. 115:1939-1948, 2015.
68. Stopczynski A, Stahlhut C, Larsen JE, Petersen MK, Hansen LK. The smartphone brain scanner: a portable real-time neuroimaging system. PLoS One. 9:e86733, 2014.
69. Wagner J, Solis-Escalante T, Grieshofer P, Neuper C, Müller-Putz G, Scherer R. Level of participation in robotic-assisted treadmill walking modulates midline sensorimotor EEG rhythms in able-bodied subjects. Neuroimage. 63:1203-1211, 2012.
70. Wang Y-T, Huang K-C, Wei C-S, et al. Developing an EEG based On-line Closed-loop Lapse Detection and Mitigation System. Frontiers in Neuroscience. 8:2014.
71. Wong SWH, Chan RHM, Mak JN. Spectral modulation of frontal EEG during motor skill acquisition: A mobile EEG study. International Journal of Psychophysiology. 91:16-21, 2014.
72. Zander TO, Andreessen LM, Berg A, et al. Evaluation of a Dry EEG System for Application of Passive Brain-Computer Interfaces in Autonomous Driving. Frontiers in Human Neuroscience. 11:2017.
73. Zink R, Hunyadi B, Van Huffel S, De Vos M. Mobile EEG on the bike: disentangling attentional and physical contributions to auditory attention tasks. Journal of Neural Engineering. 13:46017-46027, 2016.
74. Kranczioch C, Zich C, Schierholz I, Sterr A. Mobile EEG and its potential to promote the theory and application of imagery-based motor rehabilitation. International journal of psychophysiology : official journal of the International Organization of Psychophysiology. 91:10-15, 2014.
75. Usakli AB. Improvement of EEG signal acquisition: An electrical aspect for state of the art of front end. Computational intelligence and neuroscience. 2010:12, 2010.
76. Makeig S, Gramann K, Jung T-P, Sejnowski TJ, Poizner H. Linking brain, mind and behavior. International Journal of Psychophysiology. 73:95-100, 2009.
77. Chi YM, Tzyy-Ping J, Cauwenberghs G. Dry-Contact and Noncontact Biopotential Electrodes: Methodological Review. Biomedical Engineering, IEEE Reviews in. 3:106-119, 2010.
78. De Vos M, Gandras K, Debener S. Towards a truly mobile auditory brain–computer interface: exploring the P300 to take away. International journal of psychophysiology. 91:46-53, 2014.

79. Lotte F, Congedo M, Lecuyer A, Lamarche F, Arnaldi B. A review of classification algorithms for EEG-based brain-computer interfaces. J Neural Eng. 4:R1-R13, 2007.
80. Yates DC, Rodriguez-Villegas E. A Key Power Trade-off in Wireless EEG Headset Design. Paper presented at: Neural Engineering, 2007. CNE '07. 3rd International IEEE/EMBS Conference on; 2-5 May 2007, 2007.
81. Dannhauer M, Lämmel E, Wolters CH, Knösche TR. Spatio-temporal regularization in linear distributed source reconstruction from EEG/MEG: a critical evaluation. Brain topography. 26:229-246, 2013.
82. Ramoser H, Muller-Gerking J, Pfurtscheller G. Optimal spatial filtering of single trial EEG during imagined hand movement. IEEE transactions on rehabilitation engineering. 8:441-446, 2000.
83. Stopczynski A, Stahlhut C, Petersen MK, et al. Smartphones as pocketable labs: Visions for mobile brain imaging and neurofeedback. International Journal of Psychophysiology. 91:54-66, 2014.
84. He B, Coleman T, Genin GM, et al. Grand challenges in mapping the human brain: NSF workshop report. IEEE transactions on Biomedical engineering. 60:2983-2992, 2013.
85. Mehta R, Parasuraman R. Neuroergonomics: a review of applications to physical and cognitive work. Frontiers in Human Neuroscience. 7:2013.
86. Wang Y-T, Wang Y, Jung T-P. A cell-phone-based brain–computer interface for communication in daily life. Journal of neural engineering. 8:025018, 2011.
87. Easycap. Easycap. 2016; http://easycap.brainproducts.com/.
88. Guger C, Krausz G, Allison B, Edlinger G. Comparison of Dry and Gel Based Electrodes for P300 Brain–Computer Interfaces. Frontiers in Neuroscience. 6:2012.
89. Jasper HH. The ten twenty electrode system of the international federation. Electroencephalography and clinical neurophysiology. 10:371-375, 1958.
90. Campbell A, Choudhury T, Hu S, et al. NeuroPhone: brain-mobile phone interface using a wireless EEG headset. Paper presented at: Proceedings of the second ACM SIGCOMM workshop on Networking, systems, and applications on mobile handhelds2010.
91. Gutierrez A, Dreslinski RG, Wenisch TF, et al. Full-system analysis and characterization of interactive smartphone applications. Paper presented at: 2011 IEEE International Symposium on Workload Characterization (IISWC); 6-8 Nov. 2011, 2011.
92. Unity Game Engine. 2015; https://unity3d.com/, 2018.
93. Unreal Game Engine. 2015.
94. Jurcak V, Tsuzuki D, Dan I. 10/20, 10/10, and 10/5 systems revisited: Their validity as relative head-surface-based positioning systems. NeuroImage. 34:1600-1611, 2007.
95. Instruments T. Low-Noise, 8-Channel, 24-Bit Analog Front-End for Biopotential Measurements ADS1299. Datasheet.
96. Nuwer MR, Comi G, Emerson R, et al. IFCN standards for digital recording of clinical EEG. Electroencephalography and clinical Neurophysiology. 106:259-261, 1998.
97. Joyce CA, Gorodnitsky IF, Kutas M. Automatic removal of eye movement and blink artifacts from EEG data using blind component separation. Psychophysiology. 41:313-325, 2004.
98. NXP. LPC1769 ARM Cortex-M3 processor. Datasheet.
99. Microchip. RN-131G & RN-131C 802.11 b/g Wireless LAN Module. 2016: http://ww1.microchip.com/downloads/en/DeviceDoc/rn-131-ds-v3.2r.pdf.
100. Microchip. MCP73871-Stand-Alone System Load Sharing and Li-Ion/Li-Polymer Battery Charge

Management Controller. 2016: http://ww1.microchip.com/downloads/en/DeviceDoc/20002090C.pdf.
101. Kernighan BW, Ritchie DM. *The C programming language.* 2006.

102. NXP. NXP Software Center. 2016; https://www.nxp.com/webapp/software-center/library.jsp#/home/query/~query~/~filter~/popularity/0, 2016.
103. Barry R. FreeRTOS reference manual. Real Time Engineers Ltd. 2011.
104. OSDN. Tera Term. 2016; https://ttssh2.osdn.jp/index.html.en, 2016.
105. Cerf VG. *ASCII format for network interchange.* 1969. 2070-1721.
106. Kemp B, Värri A, Rosa AC, Nielsen KD, Gade J. A simple format for exchange of digitized polygraphic recordings. Electroencephalography and Clinical Neurophysiology. 82:391-393, 1992.
107. Kemp B, Olivan J. European data format 'plus'(EDF+), an EDF alike standard format for the exchange of physiological data. Clinical Neurophysiology. 114:1755-1761, 2003.
108. Hejlsberg A, Wiltamuth S, Golde P. *C# language specification.* Addison-Wesley Longman Publishing Co., Inc.; 2003.
109. Delorme A, Makeig S. EEGLAB: an open source toolbox for analysis of single-trial EEG dynamics including independent component analysis. Journal of Neuroscience Methods. 134:9-21, 2004.
110. Blum S, Debener S, Emkes R, Volkening N, Fudickar S, Bleichner MG. EEG Recording and Online Signal Processing on Android: A Multiapp Framework for Brain-Computer Interfaces on Smartphone. BioMed Research International. 2017:2017.
111. Friedman R, Kogan A, Krivolapov Y. On Power and Throughput Tradeoffs of WiFi and Bluetooth in Smartphones. IEEE Transactions on Mobile Computing. 12:1363-1376, 2013.
112. Gruzelier JH, Foks M, Steffert T, Chen MJL, Ros T. Beneficial outcome from EEG-neurofeedback on creative music performance, attention and well-being in school children. Biological Psychology. 95:86-95, 2014.
113. Choo A, May A. Virtual mindfulness meditation: Virtual reality and electroencephalography for health gamification. Paper presented at: Games Media Entertainment (GEM), 2014 IEEE2014.
114. Murphy B, Aleni A, Belaoucha B, Dyer J, Nolan H. Quantifying cognitive aging and performance with at-home gamified mobile EEG. Paper presented at: 2018 International Workshop on Pattern Recognition in Neuroimaging (PRNI)2018.
115. Szegletes L, Koles M, Forstner B. Socio-cognitive gamification: general framework for educational games. Journal on Multimodal User Interfaces. 9:395-401, 2015.
116. Luu TP, He Y, Brown S, Nakagome S, Contreras-Vidal JL. Gait adaptation to visual kinematic perturbations using a real-time closed-loop brain–computer interface to a virtual reality avatar. Journal of neural engineering. 13:036006, 2016.
117. Wairagkar M, Zoulias I, Oguntosin V, Hayashi Y, Nasuto S. Movement intention based Brain Computer Interface for Virtual Reality and Soft Robotics rehabilitation using novel autocorrelation analysis of EEG. Paper presented at: Biomedical Robotics and Biomechatronics (BioRob), 2016 6th IEEE International Conference on2016.
118. Bland JM, Altman D. Statistical methods for assessing agreement between two methods of clinical measurement. The lancet. 327:307-310, 1986.
119. Mantha S, Roizen MF, Fleisher LA, Thisted R, Foss J. Comparing Methods of Clinical Measurement: Reporting Standards for Bland and Altman Analysis. Anesthesia & Analgesia. 90:593-602, 2000.
120. Wei W, Tölle M, Zidek W, van der Giet M. Validation of the mobil-O-Graph: 24 h-blood pressure measurement device. Blood pressure monitoring. 15:225-228, 2010.
121. Näpflin M, Wildi M, Sarnthein J. Test–retest reliability of resting EEG spectra validates a statistical signature of persons. Clinical Neurophysiology. 118:2519-2524, 2007.
122. Gasser T, Bächer P, Steinberg H. Test-retest reliability of spectral parameters of the EEG. Electroencephalography and Clinical Neurophysiology. 60:312-319, 1985.
123. Bazanova OM, Vernon D. Interpreting EEG alpha activity. Neuroscience & Biobehavioral Reviews. 44:94-110, 2014.

124. Goljahani A, D'Avanzo C, Schiff S, Amodio P, Bisiacchi P, Sparacino G. A novel method for the determination of the EEG individual alpha frequency. NeuroImage. 60:774-786, 2012.
125. Goldstein MR, Peterson MJ, Sanguinetti JL, Tononi G, Ferrarelli F. Topographic deficits in alpha-range resting EEG activity and steady state visual evoked responses in schizophrenia. Schizophrenia Research. 168:145-152, 2015.
126. Bland JM, Altman DG. Measuring agreement in method comparison studies. Statistical Methods in Medical Research. 8:135-160, 1999.
127. Giavarina D. Understanding Bland Altman analysis. Biochemia medica. 25:141-151, 2015.
128. Jackson G, Radhu N, Yinming S, et al. Comparative evaluation of an ambulatory EEG platform vs. clinical gold standard. Paper presented at: Engineering in Medicine and Biology Society (EMBC), 2013 35th Annual International Conference of the IEEE; 3-7 July 2013, 2013.
129. Badcock NA, Mousikou P, Mahajan Y, de Lissa P, Thie J, McArthur G. Validation of the Emotiv EPOC® EEG gaming system for measuring research quality auditory ERPs. PeerJ. 1:e38, 2013.
130. Omurtag A, Baki S, Chari G, et al. Technical and clinical analysis of microEEG: a miniature wireless EEG device designed to record high-quality EEG in the emergency department. Int J Emerg Med. 5:1-10, 2012.
131. Bland JM, Altman DG. Applying the right statistics: analyses of measurement studies. Ultrasound in obstetrics & gynecology. 22:85-93, 2003.
132. Kassab A, Le Lan J, Tremblay J, et al. Multichannel wearable fNIRS-EEG system for long-term clinical monitoring. Human brain mapping. 39:7-23, 2018.
133. Porto LGG, JUNQUEIRA J. Comparison of Time-Domain Short-Term Heart Interval Variability Analysis Using a Wrist-Worn Heart Rate Monitor and the Conventional Electrocardiogram. Pacing and Clinical Electrophysiology. 32:43-51, 2009.
134. Micromed. MORPHEUS Product Brochure. 2013; https://www.micromeduk.com/eeg. Accessed 2/12/2013, 2013.
135. Fumoto M, Oshima T, Kamiya K, et al. Ventral prefrontal cortex and serotonergic system activation during pedaling exercise induces negative mood improvement and increased alpha band in EEG. Behavioural brain research. 213:1-9, 2010.
136. Kubota Y, Sato W, Toichi M, et al. Frontal midline theta rhythm is correlated with cardiac autonomic activities during the performance of an attention demanding meditation procedure. Cognitive Brain Research. 11:281-287, 2001.
137. Helfrich Randolph F, Schneider Till R, Rach S, Trautmann-Lengsfeld Sina A, Engel Andreas K, Herrmann Christoph S. Entrainment of Brain Oscillations by Transcranial Alternating Current Stimulation. Current Biology. 24:333-339, 2014.
138. Klimesch W, Sauseng P, Hanslmayr S. EEG alpha oscillations: The inhibition–timing hypothesis. Brain Research Reviews. 53:63-88, 2007.
139. Ng SC, Raveendran P. EEG peak alpha frequency as an indicator for physical fatigue. Paper presented at: 11th Mediterranean Conference on Medical and Biomedical Engineering and Computing 20072007.
140. Mihajlovic V, Haoxuan L, Grundlehner B, Penders J, Schouten AC. Investigating the impact of force and movements on impedance magnitude and EEG. Paper presented at: Engineering in Medicine and Biology Society (EMBC), 2013 35th Annual International Conference of the IEEE; 3-7 July 2013, 2013.
141. Kappenman ES, Luck SJ. The effects of electrode impedance on data quality and statistical significance in ERP recordings. Psychophysiology. 47:888-904, 2010.
142. Ferree TC, Luu P, Russell GS, Tucker DM. Scalp electrode impedance, infection risk, and EEG data quality. Clinical Neurophysiology. 112:536-544, 2001.
143. Bunce C. Correlation, Agreement, and Bland Altman Analysis: Statistical Analysis of Method Comparison Studies. American Journal of Ophthalmology. 148:4-6, 2009.

144. Barry RJ, Clarke AR, Johnstone SJ, Magee CA, Rushby JA. EEG differences between eyes-closed and eyes-open resting conditions. Clinical Neurophysiology. 118:2765-2773, 2007.
145. Haegens S, Cousijn H, Wallis G, Harrison PJ, Nobre AC. Inter- and intra-individual variability in alpha peak frequency. NeuroImage. 92:46-55, 2014.
146. Price TF, Harmon-Jones E. Approach motivational body postures lean toward left frontal brain activity. Psychophysiology. 48:718-722, 2011.
147. Slobounov S, Sebastianelli W, Hallett M. Residual brain dysfunction observed one year post-mild traumatic brain injury: Combined EEG and balance study. Clinical Neurophysiology. 123:1755-1761, 2012.
148. Sur S, Sinha V. Event-related potential: An overview. Industrial psychiatry journal. 18:70, 2009.
149. Dietrich A, Kanso R. A review of EEG, ERP, and neuroimaging studies of creativity and insight. Psychological bulletin. 136:822, 2010.
150. Kober SE, Wood G, Kampl C, Neuper C, Ischebeck A. Electrophysiological correlates of mental navigation in blind and sighted people. Behavioural Brain Research. 273:106-115, 2014.
151. Guo M, Xu G, Wang L, Lingdi F. Functional brain network analysis during auditory oddball task. Paper presented at: 2016 Asia-Pacific International Symposium on Electromagnetic Compatibility (APEMC); 17-21 May 2016, 2016.
152. Burns CG, Fairclough SH. Use of auditory event-related potentials to measure immersion during a computer game. International Journal of Human-Computer Studies. 73:107-114, 2015.
153. Mahajan Y, Peter V, Sharma M. Effect of EEG Referencing Methods on Auditory Mismatch Negativity. Frontiers in Neuroscience. 11:560, 2017.
154. Ferracuti F, Freddi A, Iarlori S, Longhi S, Peretti P. Auditory paradigm for a P300 BCI system using spatial hearing. Paper presented at: Intelligent Robots and Systems (IROS), 2013 IEEE/RSJ International Conference on; 3-7 Nov. 2013, 2013.
155. Halder S, Rea M, Andreoni R, et al. An auditory oddball brain–computer interface for binary choices. Clinical Neurophysiology. 121:516-523, 2010.
156. Touyama H, Maeda K. EEG Measurements towards Brain Life-Log System in Outdoor Environment. In: Stephanidis C, ed. *HCI International 2011 – Posters' Extended Abstracts: International Conference, HCI International 2011, Orlando, FL, USA, July 9-14, 2011, Proceedings, Part II*. Berlin, Heidelberg: Springer Berlin Heidelberg; 2011:308-311.
157. Wright MJ, Geffen GM, Geffen LB. ERP measures of stimulus processing during an auditory oddball task in Parkinson's disease: Evidence for an early information processing deficit. Parkinsonism & Related Disorders. 2:13-21, 1996.
158. Verma NP, Nichols CD, Greiffenstein MF, Singh RP, Hurst-Gordon D. Waves earlier than P3 are more informative in putative subcortical Dementias: A study with mapping and neuropsychological techniques. Brain Topography. 1:183-191, 1989.
159. Olichney JM, Yang J-C, Taylor J, Kutas M. Cognitive Event-Related Potentials: Biomarkers of Synaptic Dysfunction Across the Stages of Alzheimer's Disease. Journal of Alzheimer's disease : JAD. 26:215-228, 2011.
160. Hegerl U, Gaebel W, Gutzman H, Ulrich G. Auditory evoked potentials as possible predictors of outcome in schizophrenic outpatients. International Journal of Psychophysiology. 6:207-214, 1988.
161. Gilmore CS, Clementz BA, Buckley PF. Stimulus sequence affects schizophrenia–normal differences in event processing during an auditory oddball task. Cognitive Brain Research. 24:215-227, 2005.
162. Rosburg T, Boutros NN, Ford JM. Reduced auditory evoked potential component N100 in schizophrenia — A critical review. Psychiatry Research. 161:259-274, 2008.

163. Woodman GF. A brief introduction to the use of event-related potentials in studies of perception and attention. Attention, Perception, & Psychophysics. 72:2031-2046, 2010.
164. Ritter W, Vaughan HG. Averaged evoked responses in vigilance and discrimination: a reassessment. Science. 164:326-328, 1969.
165. Tomé D, Barbosa F, Nowak K, Marques-Teixeira J. The development of the N1 and N2 components in auditory oddball paradigms: a systematic review with narrative analysis and suggested normative values. Journal of Neural Transmission. 122:375-391, 2015.
166. Folstein JR, Van Petten C. Influence of cognitive control and mismatch on the N2 component of the ERP: a review. Psychophysiology. 45:152-170, 2008.
167. Sutton S, Braren M, Zubin J, John E. Evoked-potential correlates of stimulus uncertainty. Science. 150:1187-1188, 1965.
168. Papadaniil CD, Kosmidou VE, Tsolaki A, Tsolaki M, Kompatsiaris IY, Hadjileontiadis LJ. Cognitive MMN and P300 in mild cognitive impairment and Alzheimer's disease: A high density EEG-3D vector field tomography approach. Brain Research. 1648:425-433, 2016.
169. Yajima H, Makino S, Rutkowski TM. P300 responses classification improvement in tactile BCI with touch-sense glove. Paper presented at: Asia-Pacific Signal and Information Processing Association, 2014 Annual Summit and Conference (APSIPA); 9-12 Dec. 2014, 2014.
170. van Dinteren R, Arns M, Jongsma ML, Kessels RP. P300 development across the lifespan: a systematic review and meta-analysis. PloS one. 9:e87347, 2014.
171. Bougrain L, Saavedra C, Ranta R. Finally, what is the best filter for P300 detection? Paper presented at: TOBI Workshop lll-Tools for Brain-Computer Interaction2012.
172. Kübler A, Furdea A, Halder S, Hammer EM, Nijboer F, Kotchoubey B. A brain–computer interface controlled auditory event-related potential (P300) spelling system for locked-in patients. Annals of the New York Academy of Sciences. 1157:90-100, 2009.
173. Hoffmann U, Vesin J-M, Ebrahimi T, Diserens K. An efficient P300-based brain–computer interface for disabled subjects. Journal of Neuroscience Methods. 167:115-125, 2008.
174. Helmy S, Al-ani T, Hamam Y, El-madbouly E. P300 based brain-computer interface using Hidden Markov Models. Paper presented at: Intelligent Sensors, Sensor Networks and Information Processing, 2008. ISSNIP 2008. International Conference on; 15-18 Dec. 2008, 2008.
175. Changxu W, Yili L, Quinn-Walsh CM. Queuing Network Modeling of a Real-Time Psychophysiological Index of Mental Workload—P300 in Event-Related Potential (ERP). Systems, Man and Cybernetics, Part A: Systems and Humans, IEEE Transactions on. 38:1068-1084, 2008.
176. Spyrou L, Sanei S, Took CC. Estimation and location tracking of the P300 subcomponents from single-trial EEG. Paper presented at: Acoustics, Speech and Signal Processing, 2007. ICASSP 2007. IEEE International Conference on2007.
177. Polich J, Margala C. P300 and probability: comparison of oddball and single-stimulus paradigms. International Journal of Psychophysiology. 25:169-176, 1997.
178. Johnson R, Donchin E. P300 and Stimulus Categorization: Two Plus One is not so Different from One Plus One. Psychophysiology. 17:167-178, 1980.
179. Garaizar P, Vadillo MA, López-de-Ipiña D, Matute H. Measuring Software Timing Errors in the Presentation of Visual Stimuli in Cognitive Neuroscience Experiments. PLoS ONE. 9:e85108, 2014.
180. Garaizar P, Vadillo MA. Accuracy and precision of visual stimulus timing in psychopy: No timing errors in standard usage. PloS one. 9:e112033, 2014.
181. Cuffin BN. Effects of head shape on EEGs and MEGs. IEEE Transactions on Biomedical Engineering. 37:44-52, 1990.
182. Luck SJ. *An introduction to the event-related potential technique.* 2014.

183. Vaughan HG, Ritter W. The sources of auditory evoked responses recorded from the human scalp. Electroencephalography and Clinical Neurophysiology. 28:360-367, 1970.
184. Simson R, Vaughan Jr HG, Ritter W. The scalp topography of potentials in auditory and visual discrimination tasks. Electroencephalography and Clinical Neurophysiology. 42:528-535, 1977.
185. Brunnbauer M, Meyer T, Ofner G, Mueller K, Hagen R. Embedded wafer level ball grid array (eWLB). Paper presented at: Electronic Manufacturing Technology Symposium (IEMT), 2008 33rd IEEE/CPMT International2008.
186. Başar E, Güntekin B. Review of delta, theta, alpha, beta, and gamma response oscillations in neuropsychiatric disorders. *Supplements to Clinical neurophysiology.* Vol 62: Elsevier; 2013:303-341.
187. Gilmore CS, Clementz BA, Berg P. Hemispheric differences in auditory oddball responses during monaural versus binaural stimulation. International Journal of Psychophysiology. 73:326-333, 2009.
188. Doege K, Bates A, White T, Das D, Boks M, Liddle P. Reduced event-related low frequency EEG activity in schizophrenia during an auditory oddball task. Psychophysiology. 46:566-577, 2009.
189. Schröder A, van Diepen R, Mazaheri A, et al. Diminished N1 Auditory Evoked Potentials to Oddball Stimuli in Misophonia Patients. Frontiers in Behavioral Neuroscience. 8:2014.
190. Zhang P, Jamison K, Engel S, He B, He S. Binocular rivalry requires visual attention. Neuron. 71:362-369, 2011.
191. Klistorner AI, Graham SL. Electroencephalogram-based scaling of multifocal visual evoked potentials: effect on intersubject amplitude variability. Investigative ophthalmology & visual science. 42:2145-2152, 2001.
192. Zhu D, Bieger J, Molina GG, Aarts RM. A survey of stimulation methods used in SSVEP-based BCIs. Computational intelligence and neuroscience. 2010:1, 2010.
193. Gernot RM-P, Reinhold S, Christian B, Gert P. Steady-state visual evoked potential (SSVEP)-based communication: impact of harmonic frequency components. Journal of Neural Engineering. 2:123, 2005.
194. Bakardjian H, Tanaka T, Cichocki A. Optimization of SSVEP brain responses with application to eight-command Brain-Computer Interface. Neurosci Lett. 469:34-38, 2010.
195. Romei V, Brodbeck V, Michel C, Amedi A, Pascual-Leone A, Thut G. Spontaneous fluctuations in posterior α-band EEG activity reflect variability in excitability of human visual areas. Cerebral cortex. 18:2010-2018, 2007.
196. Schreiter-Gasser U, Gasser T, Ziegler P. Quantitative EEG analysis in early onset Alzheimer's disease: correlations with severity, clinical characteristics, visual EEG and CCT. Clinical Neurophysiology. 90:267-272, 1994.
197. Sainio K, Stenberg D, Keskimäki I, Muuronen A, Kaste M. Visual and spectral EEG analysis in the evaluation of the outcome in patients with ischemic brain infarction. Electroencephalography and clinical neurophysiology. 56:117-124, 1983.
198. Pizzamiglio S, Naeem U, Abdalla H, Turner DL. Neural Correlates of Single- and Dual-Task Walking in the Real World. Frontiers in Human Neuroscience. 11:2017.
199. Cruz-Garza JG, Brantley JA, Nakagome S, et al. Deployment of Mobile EEG Technology in an Art Museum Setting: Evaluation of Signal Quality and Usability. Frontiers in human neuroscience. 11:527, 2017.
200. Tilley S, Neale C, Patuano A, Cinderby S. Older people's experiences of mobility and mood in an urban environment: a mixed methods approach using electroencephalography (EEG) and interviews. International journal of environmental research and public health. 14:151, 2017.
201. Kiral-Kornek I, Roy S, Nurse E, et al. Epileptic Seizure Prediction Using Big Data and Deep Learning: Toward a Mobile System. EBioMedicine. 27:103-111, 2018.

202. Polat K, Güneş S. Classification of epileptiform EEG using a hybrid system based on decision tree classifier and fast Fourier transform. Applied Mathematics and Computation. 187:1017-1026, 2007.
203. Clewett CJ, Langley P, Bateson AD, Asghar A, Wilkinson AJ. Non-invasive, home-based electroencephalography hypoglycaemia warning system for personal monitoring using skin surface electrodes: a single-case feasibility study. Healthcare technology letters. 3:2-5, 2016.
204. Fraiwan L, Lweesy K, Khasawneh N, Wenz H, Dickhaus H. Automated sleep stage identification system based on time–frequency analysis of a single EEG channel and random forest classifier. Computer Methods and Programs in Biomedicine. 108:10-19, 2012.
205. Irani F, Platek SM, Bunce S, Ruocco AC, Chute D. Functional Near Infrared Spectroscopy (fNIRS): An Emerging Neuroimaging Technology with Important Applications for the Study of Brain Disorders. The Clinical Neuropsychologist. 21:9-37, 2007.
206. Gennaro F, de Bruin ED. Assessing Brain–Muscle Connectivity in Human Locomotion through Mobile Brain/Body Imaging: Opportunities, Pitfalls, and Future Directions. Frontiers in Public Health. 6:2018.

Appendix 1 – CoME scheme form

Categorisation of Mobile EEG (CoME)

Instructions: Complete Sections 1, 2, 3 and 4 to score Device Mobility (D), Participant Mobility (P), System Specification (S), and Number of Channels respectively.

For each category, select the most appropriate descriptor for your mobile EEG study and EEG system. Circle the score next to the selected descriptor for D and P.

For the system specification (S), separately record scores for bit resolution, sampling rate, battery life and electrode type, and then total these scores to provide a total system specification score. For electrode type score the individual facets such as passive/active etc. and total to give an electrode type score of 1 to 5.

In Section 4, just report the number of channels required in the study.

In Section 5, transfer the scores from Device Mobility (D), Participant Mobility (P), System Specification (S) and Number of Channels (C) to obtain the final categorisation score.

Study Title:

EEG System:

Section 1: Device Mobility Score (D)

0	All equipment off-body mounted and participant tethered via cabling to EEG acquisition equipment.
1	Waist-mounted (or back-mounted) with additional equipment located in a rucksack.
2	All equipment is waist-mounted.
3	Head-mounted EEG system, with additional equipment located in a rucksack or off-body.
4	Head-mounted and requires smartphone/tablet.
5	Head-mounted and does not require any additional equipment.

Section 2: Participant Mobility Score (P)

0	Lying, sitting or standing still.
1	Lying, sitting or standing with localised movement.
2	Constrained walking/cycling.
3	Unconstrained walking/cycling.
4	Walking and carrying, climbing stairs, constrained running.
5	Unconstrained running, vigorous physical exercise or sport.

Section 3: System Specification Score (S)

	Bit resolution (bits)	Sampling rate (Hz)	Battery Life (Hrs)		Electrode Type			
1	14	125 or 128	Mains, USB or equivalent		Passive (0)	Active (1)		
2	16	250 or 256	1 to 8		Unshielded (0)	Shielded (1)		
3	22	500 or 512	9 to 16		Dry (1)	Wet (2)	Gel (3)	
4	24	1000 or 1024	17 to 24					
5	>24	>1000	>24		**Electrode Score**			
	+	+	+			=		**(S)**

Section 4: Number of Channels: **(C)**

Section 5: Final Categorisation Score:

(……D, ……P, ……S, ……C)